

71-9293



**TRANSNUCLEAR, INC.**

March 2, 2000

E-17906

Mr. David Tiktinsky  
Spent Fuel Project Office  
Division of Industrial and Medical Nuclear Safety  
Office of Nuclear Material Safety and Safeguards  
Nuclear Regulatory Commission  
Washington, D.C. 20555-0001

Subject: TN-68 Transport SAR Responses to RAI1  
Docket 71-9293, TAC No. L22899

Dear Mr. Tiktinsky:

Enclosed please find the responses to RAI#1 on the TN-68 Transport SAR. Also enclosed are the following revisions to the SAR which have been marked Rev. 1:

- Drawings 972-71-2 Rev. 1, 972-71-3 Rev. 3, 972-71-4 Rev. 2, 972-71-5 Rev. 1, 972-71-6 Rev. 1, 972-71-7, Rev. 2, 972-71-8, Rev. 1, 972-71-9 Rev.1, 972-71-14, Rev. 0
- Appendix 2.10.9 has been revised to incorporate the results of the drop and puncture testing. (Complete Appendix)
- Chapter 4 (Complete) to incorporate revisions requested in the RAI
- Chapter 6 (Pages 6-1 through 6-10)
- Chapter 7 (Complete) to incorporate revisions requested in the RAI
- Chapter 8 page 8-1/8-2

Please replace these pages in your copies of the SAR. The revisions to Chapter 1, 3 and 5 discussed in the RAI will be submitted after the NRC has reviewed our responses. TN will be happy to meet with you to discuss any or all of our responses.

If you have any questions or comments, please call me.

Sincerely,

Tara J. Nelder  
Vice President - Engineering

cc: 972 File

**FOUR SKYLINE DRIVE, HAWTHORNE, NEW YORK 10532**  
**Phone: 914-347-2345 ♦ Fax: 914-347-2346**

*Amssolpublic*

## Chapter 1      General Description

The regulatory basis for questions 1-1 through 1-5 related to package drawings is 10 CFR 71.33 which requires that the packaging and contents be described in sufficient detail to provide an adequate basis for its evaluation.

1-1      Revise drawing No. 972-71-2 to specify the following information:

1-1-1    Modify note 6 to specify the codes and standards for fabrication, examination, assembly, and testing.

1-1-2    Modify note 8 to identify the containment system.

1-1-3    Modify note 9 to specify the maximum allowable weight of package, maximum allowable weight of contents and secondary packaging.

These items are important to the safety of the package. Therefore, they should be specified on the drawing. A reference to the drawings will be specified as a condition of approval in a certificate of compliance for transportation.

**Response: The drawing has been modified as requested.**

1-1-4    The outside diameter of the inner containment shell and the inside diameter of the gamma shield, including tolerances, prior to shrink fit (see related RAI 2-13.)

The inner containment shell and the gamma shield are joined by an interference fit. The radial interference between these shells determines the hoop stress in the inner containment shell. The tolerance could adversely impact the integrity of the inner shell.

**Response: See response to 2-13 below.**

1-2      Revise drawing no. 972-71-3 to include the boron-10 content of the neutron absorber material and poison plates.

**Response: The boron-10 content is now specified on the drawings.**

1-3      Revise drawing no. 972-71-6 to provide details of the shear key (Part No. 40) and its attachment to the containment shell wall.

Structural details of the shear key and an attachment detail to the containment vessel are not provided on the package certification drawings. Since the shear key may affect the integrity of the containment boundary (see structural question No. 2-6) during side impact, this information should be provided on the package certification drawings.

**Response: The details of the shear key have been added to drawing 972-71-6.**

- 1-4 Clarify whether the transport frame shown on drawing No. 972-71-8 is a structural part of the package.

If the transport frame is a structural part of the package, then it should be included in the package and tiedown analysis and details should be provided on the drawings (e.g., dimensions, materials of construction, etc.). If the transport frame is not a structural part of the TN-68 packaging, then it should not be included as part of the package certification drawings and the drawing should be modified to state that it is for information purposes only or deleted.

**Response: The transport frame is not a structural part of the package, Transnuclear drawing no. 972-71-8 has been revised to show the transport frame in phantom.**

- 1-5 Clarify whether or not a tarp will be used during transport.

Section 1.2.1 of the SAR indicates that a tarp will be placed around the entire TN-68 transport package (including the impact limiters) during transport; however, this item is not included in the package certification drawings. Neither were the effects of a tarp evaluated for the normal conditions of transport (see related thermal RAI 3-1).

**Response: A tarp will not be placed around the transport package. Section 1.2.1 of the SAR will be revised accordingly.**

- 1-6 Provide a description of the allowable contents of the packaging in chapter 1.2.3 of the SAR, that is consistent with those analyzed in chapters 5 and 6. The contents should be revised to include the following:

- 1-6-1 The description of allowable contents states that fuel with a minimum 10 year decay time can be loaded and shipped. However, the design basis fuel used in the shielding analysis (SAR section 5) is for 20 year cooled fuel (see related RAI 5-1) and therefore is not consistent with SAR chapter 1.2.3. This discrepancy should be resolved.

**Response: Shielding analyses have been performed in response to question 5-1 for a loading configuration with 44 design basis fuel assemblies (10 year cooled) surrounded by 24, "colder" fuel assemblies. The results of the analysis shows that the 10CFR71 dose rate limits are meet. Additional analyses have been performed to show that a cask loaded with 68 design basis fuel assemblies, cooled 16 years, also meets the 10CFR71 dose rate limits. The thermal analyses, structural (temperature dependent), and containment analyses provided in the SAR utilize the design basis fuel with 10 year cooling. Therefore, a fuel assembly with a maximum burnup of**

**40,000 MWD/MTU and a minimum cooling time of 10 years is the bounding fuel assembly for transport in the TN-68. From the thermal, structural, and containment analyses, the cask could contain 68 of the bounding assemblies; however, shielding analyses limit this number to less than the maximum, 68. The number of bounding assemblies (40,000 MWD/MTU, 10 year cooled) that can be transported in the TN-68 cask is dependent on the location in which they are placed within the cask and the “source parameters” of the other assemblies that are loaded. The allowable contents for the TN-68 cask is a BWR fuel assembly with no more than 40,000 MWD/MTU burnup and cooled for at least 10 years. The quantity of this bounding fuel assembly or for that matter any other non-bounding fuel assembly is determined by compliance with the 10CFR71 dose rate limits which is accomplished by measuring the dose rates around the cask prior to shipment.**

**The proposed revised Section 1.2-3 is provided below:**

The contents of the TN-68 packaging are limited to the following.

- Fuel parameters
  - Fuel is limited to 68 unconsolidated intact GE BWR fuel assemblies with zircalloy cladding. An intact fuel assembly is a spent nuclear fuel assembly without known or suspected cladding defects greater than pinhole leaks or hairline cracks and which can be handled by normal means. Partial fuel assemblies, that is spent fuel assemblies from which fuel rods are missing, shall not be classified as intact fuel assemblies unless dummy fuel rods are used to displace an amount of water equal to that displaced by the original fuel rod(s).
  - Fuel may be transported with or without channels. Nominal channel thicknesses of up to 0.120 inches thick are acceptable for transport.
  - Permissible fuel assembly types are listed below (fuel designs may be C, D, or S lattice)

<u>GE Type</u>	<u>Designation</u>	<u># of Fueled Rods</u>	<u>Uranium Content (MTU/assembly)</u>
7x7	2A	49	0.1977
7x7	2, 2B	49	0.1977
7x7	3, 3A, 3B	49	0.1896
8x8	4, 4A, 4B	63	0.1880
8x8	5, 6, 6B, 7, 7B	62	0.1876
8x8	8, 8B	62	0.1885
8x8	8, 8B, 9, 9B, 10	60	0.1824
9x9	11,13	74	0.1757
10x10	12	92	0.1857

**Fuel characteristics of each assembly type are provided in Table 6.2-1.**

- Provided all the requirements listed in this section are met, the bounding fuel characteristics are:

<u>Characteristic</u>	<u>Parameter</u>
Maximum Initial lattice-average enrichment	3.7%
Minimum Initial bundle average enrichment	3.3%
Maximum assembly average burnup	40,000 MWD/MTU
Minimum cooling time	<b>10 years (Note 1)</b>

**Note 1: Fuel cooled for a minimum time of 10 years may be transported in the TN-68 cask. The quantity of 10 year cooled fuel that may be transported is dependent on the number, location and parameters of the other fuel assemblies loaded in the cask and is determined by meeting the external dose rate requirements of 10CFR71.47.**

- The maximum contents weight shall not exceed 75.6 kips. The total weight of the BWR fuel assemblies shall not exceed 47.9 kips.
- The total decay heat of the cavity contents shall not exceed 21.2 kW (**0.312 kW/assembly**).
- Measured external radiation levels shall not exceed the requirements of 10 CFR 71.47. Measured surface contamination levels shall not exceed the requirements of 10 CFR 71.87(i).
- Table 1-1 provides the minimum cooling time required for various combinations of minimum initial enrichment and maximum burnup.

Table 1-1  
Cooling Time as a Function of Maximum Burnup and Minimum Initial Enrichment

REQUIRED BWR COOLING TIMES (YEARS)

Initial Enrichment (bundle ave %w)	Burnup (GWd/MTU)											
	15	20	30	32	33	34	35	36	37	38	39	40
1.0	10	10										
1.1	10	<b>10</b>										
1.2	10	10										
1.3	10	10										
1.4	10	10										
1.5	10	10	<b>10</b>	10	<b>11</b>	11	<b>11</b>					
1.6	10	10	10	10	10	11	11	11				
1.7	10	10	10	10	<b>10</b>	11	11	11	<b>12</b>			
1.8	10	10	10	10	10	11	11	11	<b>11</b>	<b>12</b>		
1.9	10	10	10	10	10	11	11	11	11	12		
2.0	10	10	10	10	10	<b>10</b>	11	11	<b>11</b>	12	<b>12</b>	
2.1	10	10	10	10	10	10	11	11	11	12	12	<b>12</b>
2.2	10	10	10	10	10	10	11	11	11	12	12	12
2.3	10	10	10	10	10	10	11	11	11	<b>11</b>	12	12
2.4	10	10	10	10	10	10	<b>10</b>	11	11	11	12	12
2.5	10	10	10	10	10	10	10	11	11	11	12	12
2.6	10	10	10	10	10	10	10	11	11	11	12	12
2.7	10	10	10	10	10	10	10	<b>10</b>	11	11	<b>11</b>	12
2.8	10	10	10	10	10	10	10	10	10	11	11	12
2.9	10	10	10	10	10	10	10	10	10	11	11	12
3.0	10	10	10	10	10	10	10	10	<b>10</b>	10	11	12
3.1	10	10	10	10	10	10	10	10	10	10	11	12
3.2	10	10	10	10	10	10	10	10	10	10	<b>10</b>	<b>11</b>
3.3	10	10	10	10	10	10	10	10	10	10	10	10
3.4	10	10	10	10	10	10	10	10	10	10	10	10
3.5	10	10	10	10	10	10	10	10	10	10	10	10
3.6	10	10	10	10	10	10	10	10	10	10	10	10
3.7	10	10	10	10	10	10	10	10	10	10	10	10

■ - not evaluated

Notes:

1. Total dose from gamma and neutron considered.
2. Cooling Times entered in bold and italics are cases actually run. Other values interpolated.

1-6-2 Maximum rod pitch.

**Response:** The fuel parameters are given in Table 6.2-1, with the maximum rod pitch shown as 0.738 in. Each of the designated GE fuel types identified in Section 1.2.3 is associated with a nominal rod pitch. A reference to Table 6.2-1 will be provided in Section 1.2.3.

1-6-3 Minimum rod outside diameter.

**Response:** The fuel parameters are given in Table 6.2-1, with the minimum rod outside diameter shown as 0.510 in. Reference to this table will be provided in Section 1.2.3.

1-6-4 Fuel channel thickness should be limited to the value stated in chapter 6.1 (0.065 to 0.120 inches).

**Response:** The criticality analyses were performed with no fuel channel in place, as shown in Table 6.4-1. This analysis bounds channels smaller than 0.065 inches. A limit on the upper bound thickness is provided in Section 1.2.3.

1-6-5 Maximum heat load per assembly (see related RAI 3-3.)

**Response:** The maximum heat load per assembly for a 40,000 MWD/MTU, 3.3%wt ave. enrichment, 10 year cooled assembly is 0.312 kW. This limit will be added to Section 1.2.3.

1-6-6 Resolve or explain discrepancies between the fuel parameters for the TN-68 during storage and transport. For example, the parameters for storage allow for fuel with enrichments of less than 3.3% to be stored but the application for transport does not include enrichments below 3.3%. In addition, dummy fuel pins are authorized in fuel bundles for storage but are not contained in the SAR for transport.

The SAR must identify, with respect to the contents of the package, the maximum radioactive constituents. (10 CFR 71.33(b)).

The package must be evaluated to demonstrate compliance with the requirements specified in 10 CFR Part 71, Subpart E, under the conditions and tests of Subpart F (10 CFR 71.35(a), and 10 CFR 71.41(a)).

**Response:** Table 2.1-4 in the TN-68 storage SAR is also applicable for transport since the basis for this table is the design basis fuel assembly with 40,000 MWD/MTU burnup, 3.3%wt ave. enrichment, and 10 year cooling time. Table 1-1

**which is a duplicate of Table 2.1-4 of the storage SAR will be added to Chapter 1. The thermal source, releasable activity source and dose source of the assemblies in this table are bounded by the design basis fuel.**

**As in the TN-68 storage SAR, fuel assemblies with missing pins are not allowed. Missing fuel pins must be replaced with pins that have an equivalent fuel pin OD, (dummy fuel pin). A definition of an intact fuel assembly will be added to the contents description which will allow the use of dummy fuel pins.**

**Section 1.2.3 will be updated to incorporate these comments. A rewrite of this section is provided in response to RAI 1-6-1.**

Chapter 2 Structural

2-1 With respect to hydrogen generation in the package.

2-1-1 Provide the calculations leading to the estimates of the total surface areas of the aluminum/steel interface at the basket perimeter and neutron absorber to compartment wall interface in SAR Section 2.4.4.4, p. 2-16.

**Response: Aluminum/low alloy steel interface: height of basket\* perimeter aluminum Deduct the portion of the basket perimeter that has stainless steel rails:  
~4\*13.7 inches [69.5π - 4(13.7)]\*164 = 26821 in<sup>2</sup> = 186 ft<sup>2</sup>**

**Neutron absorber plate/compartment wall interface:  
compartment perimeter\*number of compartments\*height of basket  
(the entire height of neutron absorber plates is actually less than the basket height)  
4(6.38)\*68\*164 = 284,599 in<sup>2</sup> = 1976 ft<sup>2</sup>**

2-1-2 Provide a justification for not including other potential sources of hydrogen gas generation, such as radiolytic decomposition of water, in the calculations shown on page 2-16.

**Response: The TN-68 is vented during operations that occur while the cask is filled with water and there is no source of ignition during TN-68 cask operations. (There is no welding). Ignoring radiolytic hydrogen generation is justified by the use of compensating conservative assumptions in the calculation:**

- **The hydrogen generation rate is constant, that is, no credit is taken for the fact that less surface area is submerged as draining proceeds**
- **All generated hydrogen is released instantly to the plenum between the water and the lid, that is, no dissolved hydrogen is pumped out with the water, no released hydrogen escapes through the open vent port, and no recombination of oxygen and hydrogen occurs.**

The package must be made of materials and construction which assure that there will be no significant chemical, galvanic, or other reactions among the packaging components, among package contents, or between the packaging components and the package contents, including possible reaction resulting from in-leakage of water, to the maximum credible extent. The effects of radiation on the materials of construction must also be considered (10 CFR 71.43(d)).

The regulatory requirements of 10 CFR 71.45 related to lifting and tiedown standards for all packaging are applicable to RAI's 2-2 and 2-3.

2-2 Describe the methods used to assure that the trunnions and impact limiter lifting lugs will be used only for the intended purpose.

Sections 1.2.1.3, 1.2.1.4, and 2.5 of the SAR indicate that there are two lifting lugs on each impact limiter, two front trunnions for lifting, and two rear trunnions for tie-down. To prevent impact limiter lifting lugs or the two front trunnions being used for package tie-down, they should be rendered inoperable for tie-down. Conversely, the rear trunnions should be rendered inoperable for lifting.

**Response:** A 1¼ inch diameter bolt and nut will be installed in all impact limiter lifting lug holes in order to prevent them from accidentally being used to lift the package.

In the transport configuration (see TN drawing 972-71-8), the regulatory tie down loads [10CFR71.45 (b)(1)] are shared by the two rear trunnions and the outer surface of the cask at the front end which contacts a two foot wide saddle of the transport frame. The transport frame pedestals capture the two rear trunnion shoulders, which makes it impossible to lift the package with the rear trunnions. The rear trunnions are designed to take the 10G longitudinal tie-down load. Therefore they will not exceed the allowable stresses if inadvertently subjected to the 6G lifting load.

The two front trunnions are used to lift the cask and are designed to meet the requirements of ANSI N14.6<sup>(1)</sup>. They are analyzed with a safety factor of 6 against yield strength and 10 against ultimate strength with a 1.15 dynamic load factor. In the transport configuration, it is possible that the front trunnions could accidentally be used as tie-down devices. The following calculation evaluates the condition in which the front and rear trunnions share equally the tie-down load without taking structural credit for the front support saddle.

#### Front Trunnion Loads

Total Tie-Down Load	2G Vertical	5G Lateral	10G Longitudinal
Front Trunnion Load	0.5G Each Trunnion	2.5G Each Trunnion	2.5G Each Trunnion

Figure 2-3 of the TN-68 SAR shows the basic dimensions of the front trunnions. The package weight used in this calculation is W = 271,950 pounds.

- **Material**

Front Trunnion: SA-182 Gr. F6NM Yield Strength : 85.55 ksi  
 Trunnion Bolt: SA-320 Gr. L43 Yield Strength : 95.7 ksi

- **Loading and Geometry**

0.5G Vertical Load = 0.5 (271,950) = 135,975 lbs  
2.5G Lateral Load = 2.5 (271,950) = 679,875 lbs  
2.5G Longitudinal Load = 2.5 (271,950) = 679,875 lbs

The vertical and longitudinal loads are combined to form a resultant transverse load:

$$R = (0.5^2 + 2.5^2)^{1/2} = 2.55G$$
$$\text{Resultant Force} = 2.55 (271,950) = 693,473 \text{ lbs}$$

Cross - Section Area and Moment of Inertia (See Figure 2-3 of the TN-68 SAR)

At Section A-A (shoulder):

$$A_{A-A} = \pi/4 (9.75^2 - 7.6^2) = 29.30 \text{ in}^2$$
$$I_{A-A} = \pi/64 (9.75^4 - 7.6^4) = 279.83 \text{ in}^4$$
$$M = 693,473 (2.06) = 1,428,554 \text{ in-lb}$$

• Stress Calculations

At Section A-A (shoulder):

$$\text{Shear Stress} = 693,473/29.3 = 23,668 \text{ psi}$$
$$\text{Bending stress} = (1,428,554/279.83) (9.75/2) = 24,887 \text{ psi}$$
$$\text{Tension stress} = 679,875/29.3 = 23,204 \text{ psi}$$
$$\text{Maximum Stress Intensity} = [(24,887 + 23,204)^2 + 4(23,668)^2]^{1/2}$$
$$= 67.48 \text{ ksi} < S_y = 85.55 \text{ ksi}$$

At Trunnion Bolt:

The bending moment at the flange interface due to 2.55G is equal to 693,473 x 7.51 = 5,207,982 in-lbs. From Reference 2, Case 3, (for bolt patterns symmetrical about the vertical axis and flange rotating about the bottom bolt) the maximum bolt force due to bending moment M is:

$$F_{\max} = [4/(3RN)]M$$

where

$$R = \text{Bolt circle radius} = 6.875 \text{ in.}$$

$$N = \text{No. of bolts} = 12$$

$$F_{\max} = 4(5,207,982)/(3 \times 6.875 \times 12) = 84,169 \text{ lbs.}$$

$$\text{The bolt stress area} = 1.492 \text{ in}^2$$

**Max. tensile stress =  $84,169/1.492 = 56,414$  psi = 56.42 ksi**

**The bolt allowable yield stress =  $S_y = 95.7$  ksi > 56.42 ksi**

**Based on the above calculations, even if the front trunnions were accidentally used as tie-down devices, the trunnions could withstand the tie-down loads and would not exceed the allowable stresses.**

- 2-3 Provide the margins of safety for the trunnion design components due to lifting or tie-down loads.

The application states that the minimum margin of safety occurs at the trunnions' shoulders. However, no quantitative information is provided, nor is it clear as to what part of the trunnion design (e.g., trunnion welds, trunnion bolts, etc.), the margins of safety of the trunnions' shoulders are compared to. The regulations require that the ability of the package to meet the other requirements of 10 CFR Subpart E should not be impaired by the failure of either lifting devices or tie-down devices.

**Response:** The front trunnions are SA-182 Grade F6NM alloy forgings and are attached to the cask body with bolted (twelve 1.5-8UN-2A, SA-320 Gr. L43) flange connections. The two front trunnions are used for lifting the cask and are designed to the requirements of ANSI N14.6. They are analyzed with a safety factor of 6 against yield strength and 10 against ultimate strength with 1.15 dynamic load factor. Table 2-13 of the TN-68 SAR presents the summary of the front trunnion stresses. The trunnion bolt stresses are calculated in Section 2.5.1.2 of the TN-68 SAR. The local stresses at front trunnion/containment vessel interface are listed in Table 2.10.1-57 of TN-68 SAR. These calculated stresses (based on 6G load) and their margins of safety are summarized in the following table.

Component	Maximum Calculated Stress (ksi)	Allowable Stress (ksi)	Margin of Safety
Trunnion Shoulder	63.9	85.55	0.34
Trunnion Bolt	67.4	95.7	0.42
Stress at Containment Vessel	19.7	35.4	0.80

Based on the above calculation, the minimum margin of safety occurs at the trunnion shoulder. Therefore, an excessive load would damage the trunnion, but the cask would not lose its structural integrity and the design meet the requirements of the 10CFR71.45(a).

The rear trunnions are SA-105 carbon steel forgings, and are welded to the cask body. The rear trunnions serve as the packaging tie-down devices and are designed to withstand 2/5/10 tie-down loads. Table 2-15 of the TN-68 SAR presents the summary of the rear trunnion stresses at both the trunnion shoulders (see Section

A-A, Figure 2-3 of TN-68 SAR) and trunnion weld (Section B-B). The local stresses at rear trunnion/containment vessel interface are listed in Table 2.10.1-55 of TN-68 SAR. These maximum calculated stresses and their margins of safety are summarized in the following table.

Component	Maximum Calculated Stress (ksi)	Allowable Stress (ksi)	Margin of Safety
Trunnion Shoulder (Section A-A)	30.67	32.35 (SA-105)	0.05
Trunnion Weld to Gamma Shield (Section B-B)	27.75	31.45 (SA-266 Class 2)	0.13
Stress at Containment Vessel	23.44	35.4 (SA-203 Gr. E)	0.51

Based on the above calculation, the minimum margin of safety occurs at the trunnion shoulder. Therefore, under excessive load the trunnion shoulder would fail before the trunnion welds or stress allowables in the gamma shield or containment vessel are exceeded. The design meets the requirements of the 10CFR71.45 (b) (3).

The Regulatory requirements of 10 CFR 71.73 related to hypothetical accident conditions are applicable to questions 2-4 through 2-11.

- 2-4 Evaluate the effects of the ancillary shield ring on the attachment of the impact limiter during the 30-foot drop tests.

Section 5.3.1.1 of the SAR indicates that the ancillary shield ring may be used to lower the dose rates of the TN-68 transportation package. However, it is not clear from Drawing No. 972-71-7 whether the ancillary shield ring is attached to the cask body. Although two set screws are shown on the ancillary shield ring, no description or analysis of the ancillary shield ring attachment (if any) is provided in the structural chapter of the SAR. If the ancillary shield ring is not attached to the cask body, it could impact other components of the cask (e.g., top impact limiter) or the cask surroundings during the 30-foot drop tests.

**Response:** TN Drawing No. 972-71-7 has been revised to include following attachments to secure the ancillary shield ring to the top two trunnions:

**Attachment straps:** (2) 1" thick × 2" width with 1 ¼ diameter hole at each end

**Attachment bolts and nuts:** (4) 1" – 8UNC bolts with nuts

**Attachment brackets:** (4) 1" thick bracket with 1 ¼ diameter hole at each end

**The material and properties are as follows:**

Component	Material	S <sub>u</sub> (ksi)	S <sub>y</sub> (ksi)	S <sub>m</sub> (ksi)
Attachment Straps	SA-516-70	70.0	38.0	23.3
Attachment brackets	SA-516-70	70.0	38.0	23.3
Attachment bolts	SA-193-B7	100.0	75.0	25.0

The accident allowable stresses are calculated as follows:

Component	Shear Stress (ksi)	Tensile Stress (ksi)
Attachment Straps	0.42 S <sub>u</sub> = 29.4	0.7 S <sub>u</sub> = 49.0 ksi
Attachment brackets	0.42 S <sub>u</sub> = 29.4	0.7 S <sub>u</sub> = 49.0 ksi
Attachment bolts	Lesser of 0.4 S <sub>u</sub> (40.0) or 0.6 S <sub>y</sub> (45.0) = 40.0	N/A
Welds	0.42 S <sub>u</sub> = 29.4	N/A

**Analysis:**

**Weight of ancillary shield ring = 1.0 kips**

**Maximum axial acceleration = 80 Gs**

**Tensile area of 1" bolt = 0.606 in<sup>2</sup>**

**Attachment bolts**

**Shear stress at bolt =  $1.0 \times 80 / (4 \times 0.606) = 33.0 \text{ ksi} < 40.0 \text{ ksi}$**

**Attachment Straps**

**Shear stress through the strap hole =  $1.0 \times 80 / (4 \times 1 \times 2 \times 2) = 5.0 \text{ ksi} < 29.4 \text{ ksi}$**

**Tensile stress through the strap hole =  $1.0 \times 80 / [4 \times 1 \times (2 - 1.25)] = 26.7 \text{ ksi} < 49.0 \text{ ksi}$**

**Attachment brackets**

**Bending moment =  $1.0 \times 80 \times 5.03/4 = 100.6 \text{ in-kips}$**

**Moment of inertia =  $bh^3/12 = 1 \times 4^3/12 = 5.33 \text{ in}^4$**

**Bending stress =  $Mc/I = 100.6 \times 2/5.33 = 37.7 \text{ ksi} < 49.0 \text{ ksi}$**

**Shear stress through the bracket hole =  $1.0 \times 80 / [4 \times 1 \times 2 \times (2 - 1.25)] = 13.3 \text{ ksi} < 49.0 \text{ ksi}$**

**Attachment bracket welds**

**Shear stress at bracket welds =  $1.0 \times 80 / (4 \times 0.5 \times 0.707 \times 10) = 5.7 \text{ ksi} < 29.4 \text{ ksi}$**

**Based on the above calculations, all the calculated stresses are less than the allowable stresses. Therefore, during the lid end drop the shield ring will remain attached to the trunnions and will not impact the impact limiter. During a bottom end drop, the shield ring will be supported by the trunnions. The top two trunnions are designed to lift the cask and can support a load equal to 6 times the weight of the loaded cask (240.0 kips) without exceeding the minimum yield strength of the material. Therefore, the trunnion can support the shield ring with a large margin of safety.**

**During the side drop case, the shield ring will be supported by the surrounding gamma shield. The outside diameter of the cask is 84.5 in. Assume a contact surface area spans an arc of 45°. The corresponding contact area is calculated as follows:**

$$A = \pi \times 84.5 \times 12.31 \times 45/360 = 408.5 \text{ in}^2$$

**The maximum stress due to an 80G side impact is  $1.0 \times 80/408.5 = 0.2 \text{ ksi}$ . The gamma shield allowable stress ( $P_m + P_b$ ) for accident loads is  $S_u$  (73.5 ksi). Therefore, the gamma shield can withstand the shield ring side impact with a large margin of safety (up to 29,400G).**

- 2-5 Evaluate buckling of the inner containment due to the 30-foot end and corner/oblique drops in accordance with ASME Section III, Code Case N-284.

In order to adequately evaluate the containment system performance resulting from the hypothetical accident tests as specified in 10 CFR § 71.73, the potential buckling of the inner containment must be addressed.

**Response:** The containment boundary consists of the inner shell (both cylinder and bottom) and closure flange out to the seating surface and lid assembly outer plate. During the 30 foot end and corner/oblique drops onto the bottom end, the inner cylinder and bottom plate are completely supported by the thick gamma shield at the closure flange and buckling cannot occur. However, during a drop onto the lid end, loads will be taken by the containment boundary directly through loading of the flange. Therefore, a buckling analysis of the inner shell due to an end drop at the lid end is performed.

Based on the results from the ADOC computer analysis (Appendix 2.10.8 of the TN-68 SAR), the highest axial G load occurs during a 90° end drop. Therefore, a buckling analysis of the inner shell based on the end drop G load will bound all other drop orientations on the lid end.

**Analysis:**

Weight of bottom plate = 1,650 lbs

Weight of inner shell = 17,420 lbs

Cross section area of the inner shell =  $\pi/4 (72.5^2 - 69.5^2) = 334.58 \text{ in}^2$

End drop acceleration = 80 G

The accident compressive stress applied to the inner shell during a 30 foot lid end drop is:

$$\sigma = (1,650 + 17,420) \times 80 / 334.58 = 4,560 \text{ psi}$$

The analytical method provided in ASME Code Case N-284-1<sup>(3)</sup> is used to determine the adequacy of the inner shell with respect to buckling due to the end drop compressive load.

**Notation:**

The following notation is taken from reference 3, Section –1200.

- Subscripts  $\phi$  and  $\theta$  = axial (meridional) and circumferential directions respectively.
- $l_\phi$  = length of unsupported inner shell, 178.00 in.
- $R$  = shell radius, mean radius =  $[69.5 \text{ inner diameter} + 1.5] / 2 = 35.5 \text{ in.}$
- $t$  = shell thickness, 1.5 in.
- $\sigma_\phi$  = calculated membrane stress component due to applied load, psi
- $M_\phi = \frac{l_\phi}{\sqrt{(R)(t)}}$
- $C_\phi$  = elastic buckling coefficient.
- $\sigma_{\phi_{eL}}$  = theoretical buckling value, psi.
- $E$  = modulus of elasticity of the material at design temperature,  $26.7 \times 10^6 \text{ psi.}$   
@ 300° F.
- $\alpha_{\theta L}$  = capacity reduction factor
- $\eta_\phi$  = plastic reduction factor
- $\sigma_y$  = tabulated yield stress of material at design temperature, 35,400 psi.  
@ 300° F.

**Analysis**

**Factor of Safety (FS), Section - 1400 (c):**

From reference 3, Section 1400 (c) Factor of Safety, FS = 1.34 for accident conditions

**Capacity Reduction Factor ( $\alpha_{\theta L}$ ) – Section 1511 (a):**

From reference 3, Section –1511 (a), unstiffened cylinder shell, the Capacity Reduction Factor ( $\alpha_{\theta L}$ ) is calculated as follows:

$$\alpha_{\theta L} = 1.0 \times 10^{-5} \times \sigma_y - 0.033 = 1.0 \times 10^{-5} \times 35,400 - 0.033 = 0.321$$

**Plasticity Reduction Factor ( $\eta_\phi$ ), Section –1611 (a):**

The plasticity reduction factor is computed based on the formula provided in reference 3, Section –1611 (a) as follows.

$$\sigma_\phi \times FS / \sigma_y = 4,560 (1.34) / 35,400 = 0.17 < 0.55, \text{ therefore, } \eta_\phi = 1.0$$

**Theoretical Buckling Value ( $\sigma_{\phi eL}$ ), Section – 1712.1.1 (a):**

The theoretical buckling value is computed based on the formulae provided in Section – 1712.1.1 (a) as follows:

$$M_\phi = \frac{l_\phi}{\sqrt{(R)(t)}} = 178 / (35.5 \times 1.5)^{1/2} = 24.39 > 1.73, \text{ therefore, } C_\phi = 0.605, \text{ and the theoretical buckling value is,}$$

$$\sigma_{\phi eL} = C_\phi (E)(t) / R = 0.605 (26.7 \times 10^6)(1.5) / 35.5 \approx 682.5 \text{ ksi}$$

The following table summarizes the Code Case N-284 buckling stress calculations.

Summary of Code Case N-284 Buckling Stress Calculations

Code Case N-284 Reference Paragraphs	Stress Calculations
Compression Stress Based on 80G End Drop	4.56 ksi
Factor of Safety (Para. 1400)	1.34
	6.11 ksi
Capacity Reduction Factor (Para. 1500)	0.321
Elastic Amplified Stress	19.03 ksi
Plastic Reduction Factor (Para. 1600)	1
Plastic Amplified Stress	19.03 ksi
Theoretical Buckling Stress (Para. 1712)	682.5 ksi
Analysis Result	19.03 ksi < 682.5 ksi

It is concluded that the allowable buckling load of the inner shell is much higher than 80G end drop load and thus there is no potential of buckling of the inner shell structure.

Interaction Equations, Section – 1713:

The combination of axial compression from the 80 G end drop with the radial compression from the fabrication stress is analyzed using the interaction equation provided in Code Case N-284, Section –1713. Since the combination of 80 G end drop with fabrication stress is considered an accident condition, a Factor of Safety (F.S.) of 1.34 is used (Section –1400 (c)).

$$\sigma_{\phi s} = \frac{(\sigma_{\phi})(F.S.)}{\alpha_{\phi}} = \frac{(4,560)(1.34)}{0.321} = 19,035 \text{ psi.}$$

$$\sigma_{\theta s} = \frac{(\sigma_{\theta})(F.S.)}{\alpha_{\theta}} = \frac{(9,547)(1.34)}{0.8} = 15,991 \text{ psi.}$$

Where  $\sigma_{\phi s}$  is the amplified stress due to axial compression, and  $\sigma_{\theta s}$  is the amplified stress due to fabrication stress (see response to RAI 2-13). Since,  $\sigma_{\phi s} < 0.5\sigma_{\theta s}$ , the interaction equations in Section -1713 (a) apply.

From Section -1713 (a),

$$\sigma_{\phi s} < \sigma_{heL} \text{ (19,035 psi. < 44,900 psi.)}$$

Where  $\sigma_{heL}$  is the theoretical buckling stress due to fabrication stress (see response to RAI 2-13). Therefore no interaction check is required.

- 2-6 Evaluate the structural adequacy of the shear key (Part No. 40 on Drawing No. 972-71-6) during the 30-foot drop tests.

The purpose of the shear key is to prevent the basket assembly from rotating freely inside the cask. Structural details of the shear key and attachment details to the containment vessel are not provided on the package certification drawings (see related RAI 1-3.) During a 30-foot drop onto the side of the package, it is possible that the shear key will be loaded transversely. Depending on the attachment detail, this could adversely load the containment shell.

**Response:** The shear key is attached to the containment shell using a 0.25” partial penetration plus a 0.06” fillet weld on both sides of the 0.75” thick key. TN drawing no. 972-71-6 has been revised to show the weld details and is included with this response. The structural analysis of the shear key is provided below.

### Analysis

The computer program ANSYS<sup>(4)</sup> was used to conduct the stress analysis. A two dimensional finite element model of the shear key and containment cylinder was constructed to calculate the stresses in the key and cylindrical shell during a 30 foot side drop event.

### Finite Element Model

A two-dimensional finite element model of the shear key and containment cylinder was constructed using Plane 42, 2-D structural solid (with thickness option) elements. The mesh size in the model was determined from two basic considerations, namely, (1) proximity to the point (or line) of impact and (2) the level of stress anticipated at the location. The portion of the cylinder away from shear key intersection was modeled with a coarser mesh than that near the

intersection. The finite element model is shown in Figure 2-1 of this RAI. There are separate nodes at weld locations between the key and containment shell, the partial penetration welds are simulated by coupling the nodes (both x and y directions) at the weld locations. The fillet welds are not included in the model. This is conservative, since the fillet welds will increase the weld area and reduce stress. Figure 2-2 shows this constraint detail.

### Loading and Boundary Conditions

The load applied to the shear key for a side drop accident was taken from the basket side drop analyses as described in Appendix 2.10.5 of the TN-68 SAR. The reaction forces in basket model nodes, close to shear key, were obtained from the ANSYS result file. The loading due to a 45° side drop was considered most critical because it generates the maximum tangential force acting on the shear key. This load was distributed on 5 shear key nodes for the 80G side drop (see Figure 2-2).

The containment shell is completely enclosed by the gamma shield. Therefore, during a horizontal side drop, the bottom half of the containment shell is support by the gamma shield. The loading and boundary conditions are shown on Figure 2-3.

### Stress Results

Detailed elastic stresses, displacements, and forces in the finite element model are available in ANSYS output files for the 80G load. These results were postprocessed. The nodal stress intensities and deformed geometry are plotted in Figures 2-4. The maximum stress intensity is 1,066 psi. This stress is less than the membrane allowable stress intensity of 23,300 psi for the shear key and containment shell material (SA-203, Gr. E at 300°F).

Based on this calculation, it concluded that the accident loads will not result in any structural damage to either the shear key or the containment shell.

- 2-7 Evaluate the effects of the 40-inch puncture test considering the damage to the impact limiter during the 30-foot drop test.

10 CFR § 71.73 requires that cumulative damages (in the sequence specified) be addressed. The evaluation should consider that the 30-foot free drop tests precede the 40-inch puncture tests (e.g., the wood impact limiters may be damaged prior to the puncture test). The puncture pin would impact onto the damaged impact limiter and could potentially impact the sealing surface and containment system penetrations. Subsequently, the effects of exposed wood of the impact limiter, if any, resulting from puncture tests should also be factored into the subsequent fire test analysis (see related thermal RAI 3-8.)

**Response:** The TN-68 Impact Limiter testing program included a 40 inch drop

onto a 6 inch diameter puncture bar using a previously damaged (30 foot end drop to the unyielding surface) impact limiter. The damaged test model package was dropped in the 90° end drop orientation with the puncture bar impacting the lid end. The puncture bar was centered over the center of gravity of the test model package so that 100% of the drop energy was absorbed by the impact (please note that other drop orientation, such as 0° side drop, only 50% of the energy is needed to be absorbed by each impact limiter). During the puncture drop, the impact limiter wood was well contained, and the puncture bar penetrated only 4.0 inches into impact limiter. The puncture bar would not impact the sealing surface or penetrations, since the 4.0 inch puncture depth represents only 1/3 of the thickness of the impact limiter. A detailed discussion of the puncture drop description and results are presented in the attached Appendix 2.10.9, Rev. 1. A discussion of the effects of the post puncture drop fire accident is presented in the response to RAI 3-8.

2-8 Justify that the maximum and minimum force-deflection relationships for the impact limiters at various drop orientations are valid.

Section 2.10.8.4.1 indicates that calculated force-deflection relationships are compared with static crush test results. Describe the static crush tests that were performed (including orientations and test specimens). If the test specimens are not a scaled model of the TN-68 impact limiter design, explain why these test results are applicable. Provide plots that show and compare the calculated values and the values derived from these physical tests.

**Response:** The ADOC computer code was used to determine the orientation for which maximum damage would occur, and is used in conjunction with testing to evaluate the 30 foot drop hypothetical accidents.

The ADOC computer code and the wood mechanical properties in the TN-68 impact limiters have been validated using the following four methods.

1. Comparison of dynamic results provided by ADOC with actual measured dynamic impact testing results.
2. Comparison of ADOC output with independent analytical calculations for simple drop orientations where classical mechanics remains manageable.
3. Comparison of results obtained from analysis and testing of the TN-FSV Transport Package.
  - a) Comparison of ADOC output with other recognized computer codes, such as SCANS<sup>(5)</sup>, using the TN-FSV geometry.
  - b) Comparison of force deflection relationships computed by ADOC with force deflection relationships measured during static crush tests.

## 1. Comparison with Dynamic Testing.

The results of dynamic tests performed on a 1/3 scale model of the TN-68 transport package have been compared to the results computed by ADOC. The measured deformations, accelerations and dynamic behavior of the test model are very similar to those calculated by ADOC. The following tables compare measured and predicted deformations and accelerations for the TN-68 Impact Limiter Dynamic Testing.

Drop Orientation	Measured Deformation (in.)	Deformation Predicted by ADOC (in.)
15° Slap Down (2 <sup>nd</sup> Impact)	5.13	5.17 - 6.28
90° End Drop	2.24	2.32 - 2.95
0° Side Drop	5.87* (Top Impact Limiter) 4.43 (Bottom Impact Limiter)	4.51 - 5.27

\* Slightly higher than predicted deformation is attributed to the fact that this impact limiter was used previously for 15° slap down first impact (see Appendix 2.10.9, Rev. 1 for detail descriptions)

Drop Orientation	Measured Acceleration (gs)	Acceleration Predicted by ADOC (gs)
90° End Drop	75**	50 - 66
0° Side Drop	35	39 - 53

\*\* Higher than predicted acceleration is attributed to the fact that the bottom impact limiter was chilled to -20° F prior to the drop test. The crush strength of balsa and redwood increase as temperature decreases.

The strong agreement between the ADOC results and the dynamic testing results further demonstrate the validity of the ADOC computer program. A detailed description of the TN-68 dynamic testing program and results is provided in the attached Appendix 2.10.9, Rev. 1.

## 2. Comparison with Analytical Calculations.

The follow simple calculation is an example of the correlation between ADOC results and results obtained by other analytical means. The sample problem

provided here is for a 90°, 30 ft end drop of a package of weight,  $W = 182,000$  lb. The impact limiter is assumed to have a radius of 60 inches. The crushable material inside the impact limiters is assumed to be perfectly plastic having a crushing stress,  $\sigma_c = 1,300$  psi. If the cask falls from a height,  $h = 30$  feet, the impact velocity,  $V$ , is,

$$V = \sqrt{2gh} = \sqrt{2 \times 32.2 \times 30} = 527.5 \text{ in. s.}^{-1}$$

During an end drop the force,  $F$ , decelerating the cask is,

$$F = \sigma_c \times \text{Area} = 1,300 \text{ psi.} \times \pi 60^2 = 1.47 \times 10^7 \text{ lb.}$$

The equation of motion of the cask is,

$$\frac{W}{g} \ddot{u} = W - F = W - 1.47 \times 10^7$$

Therefore, the vertical acceleration of the cask,  $\ddot{u}$ , is,

$$\ddot{u} = 386.4 - 31,210 = 30,830 \text{ in. s.}^{-2}$$

Integrating the above equation, and using the following initial conditions,  $u_{(0)} = 0$ , and  $\dot{u}_{(0)} = 527.5$ , gives,

$$\begin{aligned} \dot{u} &= -30,830t + 527.5 \\ u &= -15,415t^2 + 527.5t \end{aligned}$$

The cask stops when  $\dot{u} = 0$ , at time,  $t = 527.5/30,830 = 0.017$  seconds. At this time the maximum cask displacement is,

$$u = -15,415 \times 0.017^2 + 527.5 \times 0.017 = 4.15 \text{ in.}$$

The deceleration is constant, and is,

$$\ddot{u} = 30,830 \text{ in. s.}^{-2}, \text{ or } 79.8 \text{ gs.}$$

The same problem was performed using the ADOC computer program. The results from ADOC are as results.

Time at which the cask stopped,  $t = 0.017$  s.  
Crush depth of the impact limiter,  $u = 4.59$  in.  
Peak acceleration,  $\ddot{u} = 80.1$  gs.

It can be seen that there is excellent agreement between the two sets of results.

**3. a) Comparison with SCANS using the TN-FSV geometry.**

Results from ADOC were also compared with results from the SCANS (Shipping Cask Analysis System) computer code for the TN-FSV<sup>(6)</sup> Transport Packaging. The following table, taken from the TN-FSV SAR, Rev. 1, demonstrates the agreement between ADOC and SCANS computer code.

Impact Angle	G load calculated by ADOC	G load calculated by SCANS
0°	71	69.7
15° First Impact	27.09	22.7
15° Second Impact	36.58	35
30°	19.56	17
45°	30.48	26.9
60°	38.91	35.9
75°	45.75	44.5
80°	47.85	46.6
90°	54.4	54.4

**2. b) Comparison with TN-FSV Scale Model Impact Limiter Static Crush Testing.**

In order to validate the ADOC computer code and verify the accuracy of the mechanical properties used for the impact limiter wood, the results from the ADOC computer code have been compared to the results from static crush tests. In particular, the maximum forces and displacements measured during the static crush tests for the TN-FSV transport cask impact limiters have been compared with results computed by ADOC. The following table shows force and displacement information measured during the TN-FSV static crush test and computed by ADOC, using both maximum and minimum wood crush strength.

Test Angle		Computed by ADOC		TN-FSV Static Crush Test
		Minimum Wood Properties	Maximum Wood Properties	
0° Side Crush	Maximum Force (kips)	330	423	435
	Maximum Displacement (in.)	4.8	4.0	3.6
80° Corner Crush	Maximum Force (kips)	575	643	590
	Maximum Displacement (in.)	8.9	7.0	6.5

The TN-FSV and TN-68 impact limiters are very similar in the follow respects.

- The specifications for the balsa wood and redwood used to construct the scale model TN-FSV impact limiters are the same as the specifications for the wood used in the TN-68 impact limiters.
- The shells and radial gussets for both the TN-FSV and TN-68 impact limiters are constructed from 304 stainless steel and have very similar geometry.
- Also, the arrangement of the wood blocks inside both the TN-FSV and TN-68 are similar.

Since the TN-FSV and TN-68 impact limiters are very similar, and the wood properties used as input to the ADOC program for the TN-FSV and TN-68 are identical, the ADOC code and wood properties used are deemed valid for the TN-68 impact limiter analysis.

**Conclusion:**

Based on the above, it is concluded that that the maximum and minimum force-deflection relationships for the impact limiters used in various drop orientations are valid.

2-9 With respect to the ADOC structural computer code:

2-9-1 Provide information regarding the validation of the ADOC code.

In addition to comparing with static crush test results, Section 2.10.8.4.1 also indicates that the ADOC code was benchmarked against other methods. However, no benchmarking data was provided. It is not clear as to how or what methods were used for the validation of the ADOC code.

**Response:** See response to question 2-8.

2-9-2 Describe how the stiffening effects of wood confinement were treated in the ADOC code.

It appears that the crush stress input for the ADOC code was taken from uniaxial, test results. The confining action of the steel jackets of the impact limiter will tend to cause actual axial crushing to occur at a higher stress level. Describe how this was addressed in the ADOC code analysis?

**Response:** The thickness of the steel shell and gussets (0.25 inches and 0.1875 inches respectively) are extremely thin relative to the size of the wood blocks, and therefore does not entirely preclude slight movement of the wood inside the impact limiters. Impact limiter testing (TN-FSV, TN-68) have shown that the confining action of the

**steel shell of the impact limiter has little affect on the crushing properties of the impact limiter wood (see response to question 2-8 and Appendix 2.10.9 rev. 1 attached to this response).**

2-9-3 Justify the values of “Locking Modulus” and “Unloading Modulus” shown in Table 2.10.8-2.

These Moduli values could potentially be strongly dependent on the type of confinement during crush. The locking modulus was set at 10 times the maximum crush stress. Provide the basis for these values.

**Response:** The TN-68 impact limiters have been designed using the ADOC program so that the strain in the impact limiters during all drop orientations is always less than the Locking Strain. Since the locking strain is never reached, the Locking Modulus and Unloading Modulus have no influence in the results of the ADOC analysis. The Locking Modulus was set at a conservatively high value of 10 times the maximum crush stress, so that the results of the ADOC analysis would clearly indicate if a “lock up” condition had been achieved.

The results of the TN-68 impact limiter testing program confirms that the impact limiter wood does not reach “lock up”, since the deformations measured in all drop orientations is either within, or slightly below, the bounds of the deformations computed by ADOC. The high level of agreement between the accelerations and deformations from the impact limiter testing results and the ADOC analysis also show that, in general, the wood properties and assumptions used in the ADOC analysis are reasonable (see attached Appendix 2.10.9, Rev. 1).

2-10 With respect to impact limiter testing:

2-10-1 Revise the application to include the results of the impact limiter testing stated in Appendix 2.10.9 of the SAR.

**Response:** Appendix 2.10.9 has been revised to include the impact limiter testing and is attached to this response.

2-10-2 Correlate the results of the impact limiter testing to the structural calculations that were performed using the ADOC computer code.

**Response:** Table 2.10.9-1 of Appendix 2.10.9 summarizes the maximum inertial loads measured during the TN-68 dynamic testing program, as well as the maximum inertial loads computed by ADOC and used in the TN-68

cask and basket analyses. Table 2.10.9-1 demonstrates that the inertial loads calculated in Appendix 2.10.8 are reasonable and that the inertial loads used in the analyses in Appendices 2.10.1 and 2.10.2 are conservative.

**G Loads Used for Structural Analyses  
Vs.  
G Loads Measured by Drop Test and Computed by ADOC Program  
(Reproduced From Table 2.10.9-1 of Appendix 2.10.9)**

30 foot Drop Orientation	Maximum G Load, Measured by Drop Test	Maximum G Load, Computed by ADOC	Input Loading Used in FEA (Appendix 2.10.1)
90° End Drop	75 G Axial	66 G Axial	80 G Axial
0° Side Drop	35 G Transverse	53 G Transverse	80 G Transverse

\* Conservatively Using Higher G loads

A detailed description of the TN-68 dynamic testing program and results is provided in the attached Appendix 2.10.9, Rev. 1.

- 2-11 Revise the analysis to show that the impact limiters remain attached to the cask body after 30-foot drops in various orientations.

The impact limiter attachment analysis of Section 2.10.8.6 does not include a structural analysis dealing with the adequacy of brackets which are welded to the outer shell of the cask and are threaded into each impact limiter. Failure of these brackets during 30-foot drops (including corner, oblique, end, and side drop orientations) may cause separation of the impact limiter from the cask.

**Response:** The thirteen tie rods attached to both impact limiters are designed to hold the impact limiter on the cask during all drop scenarios without the aid of the attachment bolts. The structural analyses of the tie rods are described in Section 2.10.8.6 of TN-68 SAR. The purpose of the eight attachment bolts and brackets is to hold the top impact limiter on the cask body during a tip over event immediately following a near 90° corner drop. After a high angle corner drop (45° to 90°) the crushing of the impact limiter (from inside where the cask contacts the impact limiter) on the bottom (impact side) could cause the tie rods to become loose. In the event that the tie rods become loose, and the package tips over (second impact) the attachment bolts will hold the top impact limiter in place. The following calculation shows that the attachment bolts and brackets are structurally adequate to withstand

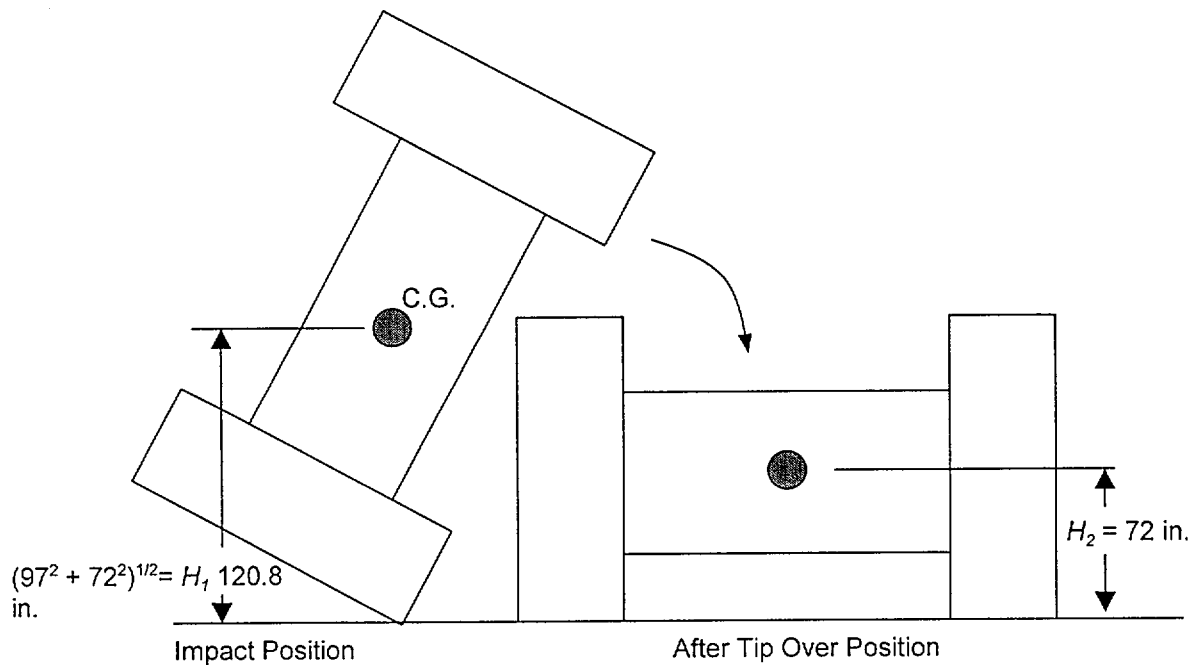
the load corresponding to a tip over (second impact) event.

#### Attachment Bolt / Bracket Analysis:

Four 1½ – 8UN bolts are used to prevent the top impact limiter from falling off the cask in the event of a 30 foot corner drop where the impact limiter crushing exceeds 12.75 inches from the inside. These bolts and brackets are designed to hold the top impact limiter on the cask during tip over (immediately after a corner drop) when the top impact limiter's inertia would tend to pull it off the cask.

During the tip over, after a corner drop, simple energy conservation laws are used to determine the maximum axial acceleration that the top impact limiter could experience.

All of the potential energy of the package in the C.G. over corner drop impact position is assumed to be converted into rotational energy (the C.G. over corner drop impact position yields the highest potential energy). This is conservative since some of the potential energy in the package is converted to vertical translational energy. The following figure shows the height of the center of gravity of the package in the impact position,  $H_1$ , and after the tip over,  $H_2$ .



The potential energy change of the package during tip over,  $\Delta PE$ , is therefore:

$$\Delta PE = W \Delta H = 271,950 \text{ lb.} \times (120.8 - 72) = 1.327 \times 10^7 \text{ in. lb.}$$

Where  $W$  is the weight of the TN-68 Package, and  $\Delta H$  is the change in height of the package during tip over. This energy is assumed to be converted entirely into rotational energy of the package,  $\Delta KE$ , which is equal to the following:

$$\Delta KE = \frac{1}{2} I \omega^2$$

Where  $I$  is the moment of inertia of the package about the pivot point, and  $\omega$  is the rate of rotation of the cask after tip over. The moment of inertia of the TN-68 transport package about its center of gravity,  $I_{CG}$ , is  $3.76 \times 10^6$  lbf.in.sec<sup>2</sup>. Therefore the moment of inertia of the package about the pivot point is:

$$I = I_{CG} + m r^2 = 3.76 \times 10^6 + (271,950/386.4) \times 120.8^2 = 14.03 \times 10^6 \text{ lbf.in.sec}^2.$$

Then,

$$\Delta PE = \Delta KE = \frac{1}{2} I \omega^2$$

$$\Rightarrow \omega^2 = 2 \Delta KE / I = 2 \times 1.327 \times 10^7 / 14.03 \times 10^6 = 1.89 \text{ (rad./sec.)}^2$$

The axial centripetal acceleration,  $a$ , associated with this angular velocity is:

$$a = r \omega^2 = 278.8 \times 1.89 = 526.93 \text{ in.sec.}^{-2}$$

Here,  $r$ , is the distance from the pivot point to the end of the top impact limiter ( $r = [269.33^2 + 72^2]^{1/2} = 278.8$  in.). The corresponding  $G$  load is  $a / g = 526.93/386.4 = 1.36$  Gs.

Therefore, for analysis purpose, assume that the top impact limiter undergoes 5 Gs during tip over, which is very conservative. The tensile force applied to the four bolts is then,

$$15,450 \times 5 = 77,250 \text{ lbs.}$$

The tensile force per bolt is

$$77,250 / 4 = 19,313 \text{ lb/bolt.}$$

The tensile stress area for a 1½ – 8UN bolt is 1.4899 in<sup>2</sup>. Therefore the tensile stress is

$$19,313 / 1.4899 = 12,962 \text{ psi} \approx 13.0 \text{ ksi}$$

The impact limiter bolt material is A540 Class1 with allowable stress =  $S_u = 165$  ksi, which is well above the calculated bolt stress.

The load applied to the bracket by the bolt is counteracted by shear force in the fillet weld between the bracket and the outer shell. The resulting shear stress in the weld is calculated below.

The throat area of the weld is  $.75 \times \cos 45^\circ = 0.530$  in.

The weld shear area is  $7 \times .530 = 3.71$  in<sup>2</sup>. (weld length is 7 inches, so that the bolt holes are not welded over.)

Shear stress per bracket is  $19,313 / 3.71 = 5,206$  psi  $\approx 5.2$  ksi

The bracket material is A516 Grade 70. Therefore the allowable shear stress is  $.42S_u$  or 29.4 ksi., which is well above the calculated shear stress.

Bending stress in bracket:

Conservatively assume that only the 5 inch tall plate carries the bending load.

$$I = \frac{10 \times 0.75^3}{12} = 0.3516 \text{ in}^4.$$

$$M = 19,313 \times 2.52 = 48,669 \text{ in. lb.}$$

$$\sigma_b = \frac{Mc}{I} = \frac{48,669 \times (0.75/2)}{0.3516} = 51,908 \text{ psi} \approx 52.0 \text{ ksi} < 70.0 \text{ ksi}$$

The attachment bolt and bracket are therefore structurally adequate, since all calculated stresses are less than their corresponding allowable stresses.

- 2-12 Show that the cask closure seals will exclude water under the deep immersion test specified in 10 CFR 71.61.

The requirements of 10 CFR 71.61 state that packages with irradiated spent fuel must be designed to withstand an external water pressure of 290 psi for a period of not less than one hour without collapse, buckling, or inleakage of water. There is no analysis demonstrating the seals prevent inleakage of water under these conditions.

**Response:** The containment lid is 5 in. thick and is fastened to the body by 48 bolts. Double metallic O-ring seals are provided for the lid closure. There are two penetrations through the containment vessel which are in the lid. These penetrations are for draining and venting. Double metallic seals are also utilized on these two lid penetrations.

Appendix 2.10.2 of TN-68 SAR evaluates the ability of the cask closure to maintain a leak tight seal under normal and accident conditions. Lid bolt analyses described

in that appendix are in accordance with NUREG/CR-6007<sup>(7)</sup>. The forces acting on the lid bolt due to normal and accident loads are summarized in the Appendix 2.10.2 table (page 2.10.2-7 of TN-68 SAR) and are repeated here as follows:

Lid Bolt Individual Load Summary

Load Case	Applied Load	Tensile Force, F <sub>a</sub> (lbs)
Preload	Maximum Torque (2,100 ft-lbs)	135,200
	Minimum Torque (2,050 ft-lbs)	131,200
Gasket	Seating Load	13,200
Pressure	100 psig Internal Pressure	8,696
Thermal	300°F	0
Impact	1 Foot Normal Condition Drop	14,280
	30 foot Accident Condition Drop	119,000
Puncture	Drop on Six Inch Dia. Rod	0
Immersion	290 psig External pressure	See Calculation Below

The axial force per bolt due to 290 psig external pressure is calculated per NUREG/CR-6007, Table 4.3,

$$F_a = \frac{\pi D_{lg}^2 (P_{li} - P_{lo})}{4N_b}$$

Where,       $D_{lg}$  = Closure lid diameter at the seal (outer) = 72.9 in.  
                   $P_{li}$  = Inside pressure of the cask  
                   $P_{lo}$  = External pressure of the cask  
                   $N_b$  = Total number of the closure bolt, 48

Therefore, for 290 psig external pressure, F<sub>a</sub> is:

$$F_a = \frac{\pi(72.9^2)(0 - 290)}{4(48)} = -25,218 \text{ lb./bolt.}$$

This force is negative (inward acting), and will not reduce the positive (compressive) load produced by the bolt preload. Therefore, the lid closure will maintain a leak tight seal under the 290 psig external pressure. The stresses in the lid, inner shell (both cylinder and bottom) and closure flange due to 290 psig external pressure are evaluated using the finite element model. Table 2-102 of TN-68 SAR shows the maximum combined stress of lid bolt preload, fabrication stress and 290 psi external pressure. The maximum stress intensity for this combined loads at the lid (location 22, at center of the lid, Figure 2-4 of SAR) is 6.45 ksi, which is well below the allowable stress intensity of 49.0 ksi.

Each of the vent and drain cover is bolted to the lid using eight (8) ¾-10 UNC bolts. The forces acting on the lid bolt due to normal and accident loads are summarized in the following table.

Vent and Drain Bolt Individual Load Summary

Load Case	Applied Load	Tensile Force, F <sub>a</sub> (lbs)
Preload	Maximum Torque (65 ft-lbs)	83,200
	Minimum Torque (60 ft-lbs)	76,800
Gasket	Seating Load	37,922
Pressure	100 psig Internal Pressure	1,871
Thermal	300°F	0
Immersion	290 psig External pressure	See Discussion Below

The force acting on the vent and drain cover plate due to the 290 psig external pressure will result in a negative (inward acting) force, and will not reduce the positive (compressive) load produced by the bolt preload. Therefore, the vent and drain closure will maintain a leak tight seal under the 290 psig external pressure.

For the 1.0 in. thick vent and drain cover plates with a mean radius of 4.5 in., an external pressure of 290 psi will produce a compressive hoop stress of: (reference to formulas for Stress and Strain by Raymond Roark<sup>(8)</sup>, fourth edition, Table X, Case 1, edges supported, uniform load over entire surface)

$$\begin{aligned} \sigma &= (3W/8\pi m t^2)(3m + 1) \\ &= [3 (290 \times \pi \times 4.5^2) / 8\pi \times 3.33 \times 1] [(3 \times 3.33 + 1) ] \\ &= 7.3 \text{ ksi} \end{aligned}$$

This maximum stress is less than the allowable stress intensity of 46.2 ksi ( 0.7 × S<sub>u</sub> of cover plate material SA-240 type 304, at 300°F).

Conclusion:

Based on the above calculations, it is concluded that the stresses in the lid, vent and drain cover plates are less than the allowable stresses and a positive (compressive load due to bolt preload) load is maintained during the immersion accident condition. Therefore, the lid, vent and drain closures will maintain a leak tight seal under the 290 psig external pressure.

- 2-13 Revise the application to include a calculation of the hoop stress in the inner containment vessel due to the interference fit with the gamma shield, considering the tolerances of

those shells (see related RAI 1-1-4.)

10 CFR 71.33 requires that the packaging and contents be described in sufficient detail to provide an adequate basis for its evaluation.

**Response:** The cask body shells are assembled to provide the best possible contact at the interface of the inner containment shell and gamma shield shell. The thickness of the inner containment shell is 1.5 in. minimum and the combined thickness of the inner containment shell and gamma shield shell is 7.5 in. (+0.13”/-0.00”). The gamma shield shell is shrunk fit onto the inner containment shell. The outside diameter of the inner shell and the inside diameter of the gamma shield shell are machined and measured prior to the shrink fit. The nominal radial interference between the inner and outer shell is 0.015 inches. TN drawing 972-71-2 is revised to include this requirement. The thicknesses of the inner containment shell and gamma shield shell may vary due to fabrication tolerances. However, the nominal radial interference between the inner and outer shell will be controlled by machining the outside diameter of the inner shell and the inside diameter of the gamma shield shell. This interference results in an interface pressure of 403.4 psi between the outer surface of the inner shell and inner surface of the gamma shell. For cylinders of same modulus of elasticity and radial interference,  $\delta$ , the interference pressure, P, is given by reference 9, page 59:

$$P = [E \times \delta/b] [(b^2 - a^2)(c^2 - b^2)/(2 \times b^2) (c^2 - a^2) ]$$

Where

E = modulus of elasticity,  $29.5 \times 10^6$  psi

$\delta$  = radial interference, 0.015 in.

a = inner radius of inner shell, 34.75 in.

b = outer radius of inner shell, 36.25 in.

c = outer radius of gamma shield shell, 42.25 in.

Substituting the values given above,

$$P = [29.5 \times 10^6 \times 0.015/36.25] [(36.25^2 - 34.75^2)(42.25^2 - 36.25^2)/(2 \times 36.25^2)(42.25^2 - 34.75^2) ] = 403.4 \text{ psi}$$

As described in SAR Section 2.10.1.3, page 2.10.1-7, the two-dimensional axisymmetric finite-element model was modified by removing all the couplings between the inner and outer cylinders. A run was made by applying a pressure of 403.4 psi to the outer surface of inner containment vessel and the inner surface of outer gamma shield cylinder.

The stress intensities from the ANSYS run at the selected locations of the containment vessel and gamma shield are presented in Tables 2.10.1-3 and 4 of the SAR. As indicated in Tables 2-18 and 2-58 of TN-68 SAR, these stress intensities (specified as fabrication stresses) are included in all Normal and Accident load

combinations.

Further analysis was performed to show that the inner containment shell would not buckle when subjected to the 403.4 psi. fabrication pressure. A 403.4 psi external pressure generates the following hoop stress,  $\sigma_h$ , in the containment shell.

$$\sigma_h = \frac{PR}{t} = \frac{(403.4)(35.50)}{1.50} = 9,547 \text{ psi.}$$

Where  $P$  is the pressure due to shrink fit,  $R$  is the nominal radius of the inner containment shell, and  $t$  is the thickness the containment shell.

The analytical method provided in ASME Code Case N-284-1<sup>(3)</sup> is used to determine the adequacy of the inner shell with respect to buckling due to the fabrication stress. The same procedure used to compute the allowable buckling stress due to axial compression (see response to RAI 2-5) was used to compute the allowable buckling stress due to fabrication stress.

The following table summarizes the Code Case N-284 buckling stress calculations.

Summary of Code Case N-284 Buckling Stress Calculations

Code Case N-284 Reference Paragraphs	Stress Calculations
Fabrication Stress Based on 403.4 psi. Radial External Pressure.	9.55 ksi
Factor of Safety Normal Conditions (Para. 1400)	2.00
	19.1 ksi
Capacity Reduction Factor (Para. 1500)	0.8
Elastic Amplified Stress	23.88 ksi
Plastic Reduction Factor (Para. 1600)	1
Plastic Amplified Stress	23.88 ksi
Theoretical Buckling Stress (Para. 1712)	44.9 ksi
Analysis Result	23.88 ksi < 44.9 ksi

**It is concluded that the allowable buckling load of the inner shell is much higher than load caused by fabrication pressure. Therefore, the inner containment shell will not buckle due to fabrication stress.**

**It may be pointed out that the buckling stress calculations are very conservative. Actually, the buckling capacity of preshrunk inner cylinder is much higher than a simple cylinder subjected to external pressure. It is a rather defined pattern, depending on its relative dimensions and conditions of restraint at its ends or periphery. The most common form assumed is the two lobe buckling which gives the lowest buckling pressure. In this mode, the ideal circular section is deflected into an oval or elliptical section. However, in a preshrunk internal cylinder, the outer cylinder resists the formation of the lobes, i.e., the change of the circular section to an oval section. This restraint prevents the buckling of the inner shell like an ordinary unstiffened cylinder.**

## Chapter 2 references

1. American National Standards Institute, ANSI N14.6, American National Standard for Special Lifting Devices for Shipping Containers Weighing 10,000 Pounds or More for Nuclear Materials, 1993.
2. Machine Design, August 17, 1967, "Eccentrically Loaded Joints", Richard T. Berger.
3. ASME Section III, Code Case No. N-284, "Metal Containment Shell Buckling Design Methods", August, 1980.
4. ANSYS Engineering Analysis System, Users Manual for ANSYS Rev. 5.6, Swanson Analysis Systems, Inc., Houston, PA, 1998.
5. NUREG/CR-4554, "SCANS A Microcomputer Based Analysis System for shipping Cask Design review", April, 1989.
6. Safety Analysis Report for the TN-FSV Packaging, Rev. 1, 1994.
7. NUREG/CR-6007 "Stress Analysis of Closure Bolts for Shipping Casks", By Mok, Fischer, and Hsu, Lawrence Livermore National Laboratory, 1992.
8. Formulas For Stress and Strain, By R. Roark, Fourth Edition.
9. Theory and Design of Modern Pressure Vessel, By J. Harvey, Second Edition, 1974.

**Figure 2-1**  
**Finite Element Model**

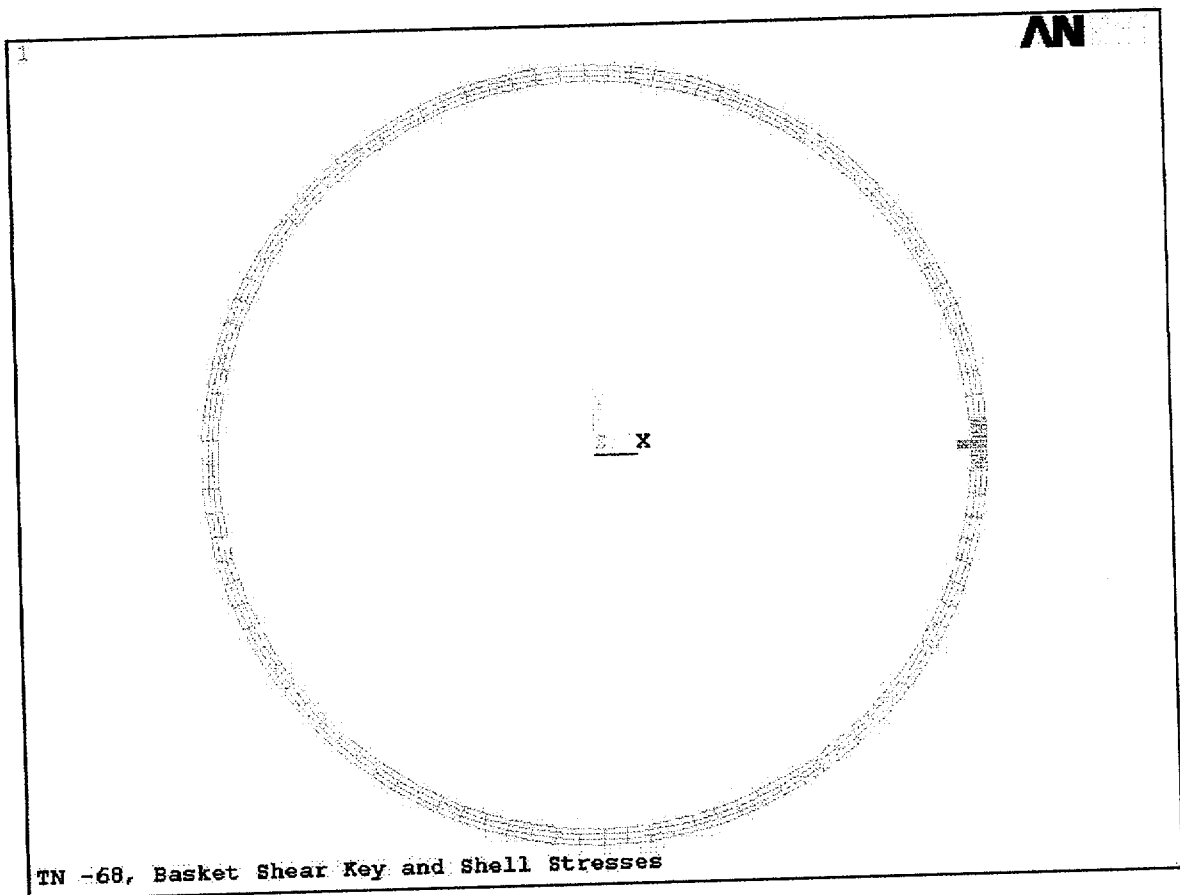


**Figure 2-2**  
**Constraint of Finite element Model**

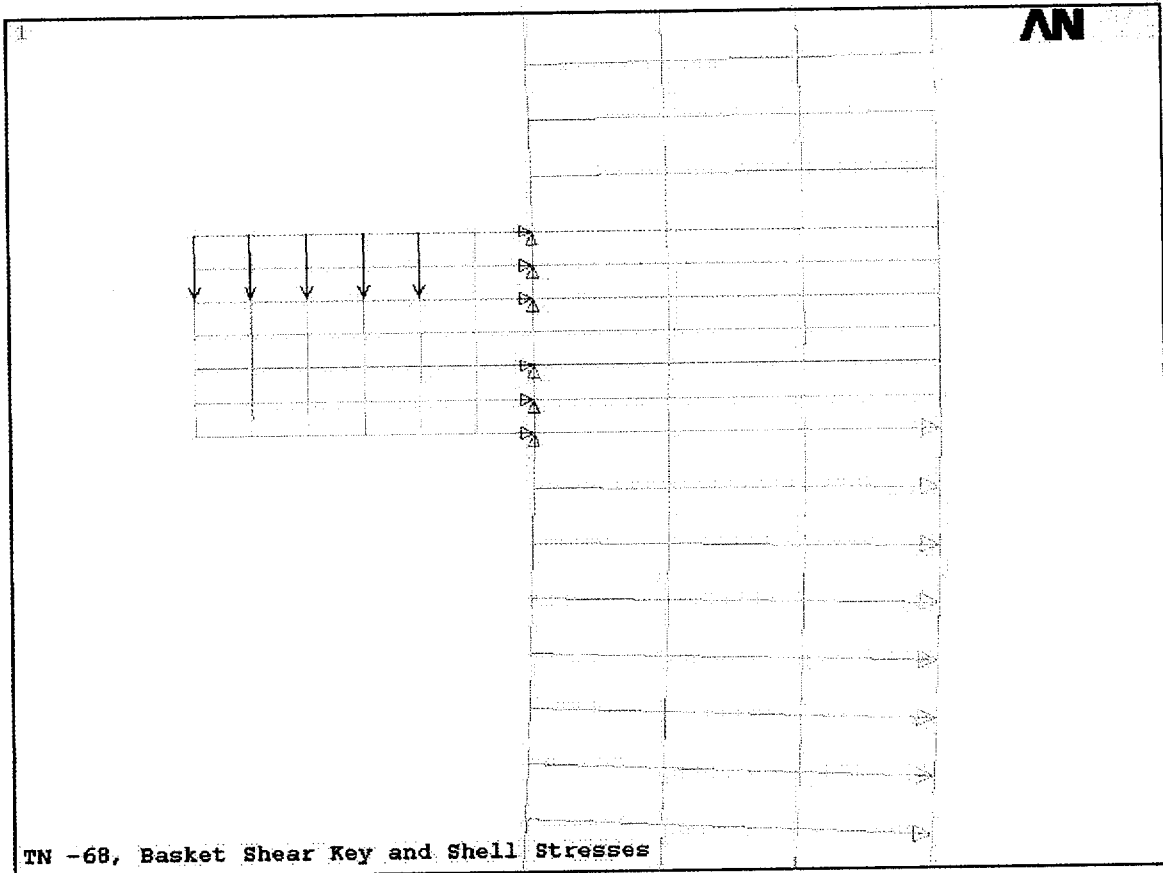


**Figure 2-3**  
**Loading and Boundary Conditions**

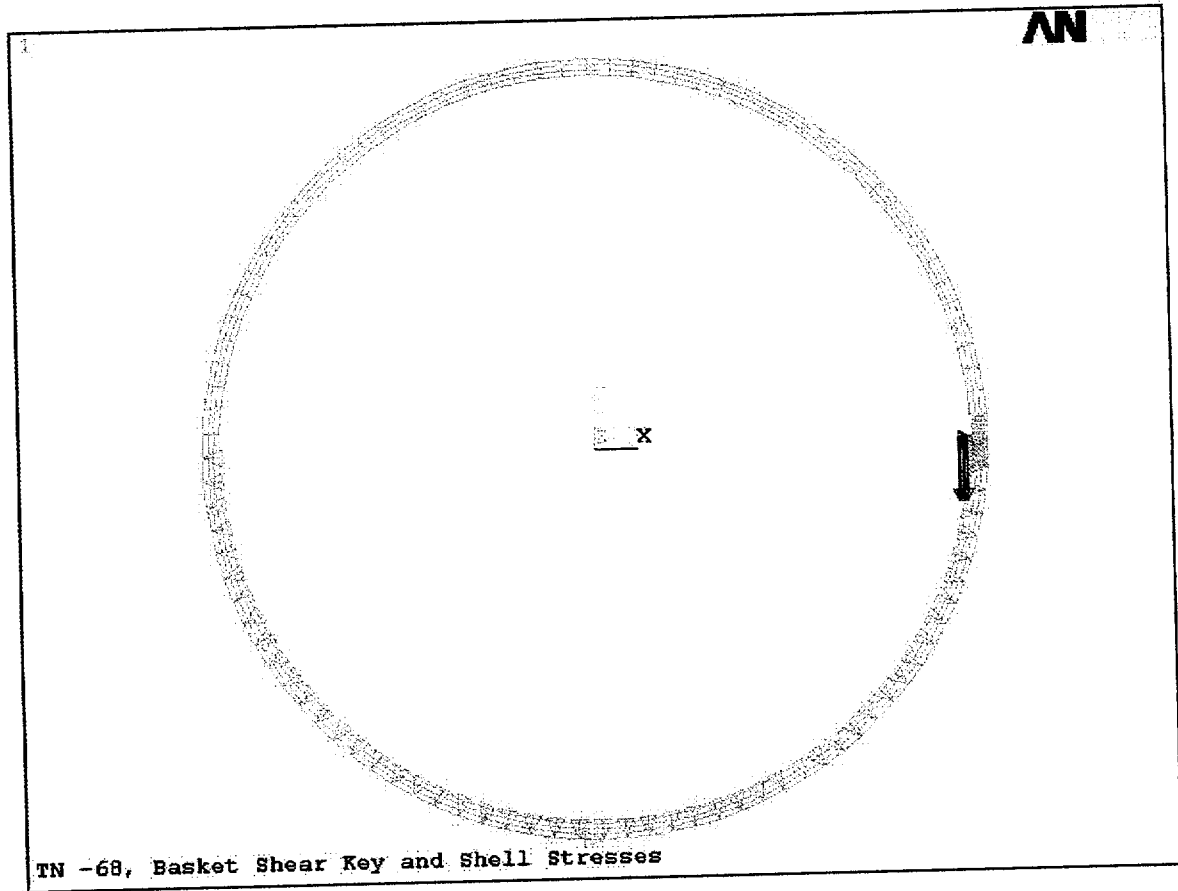
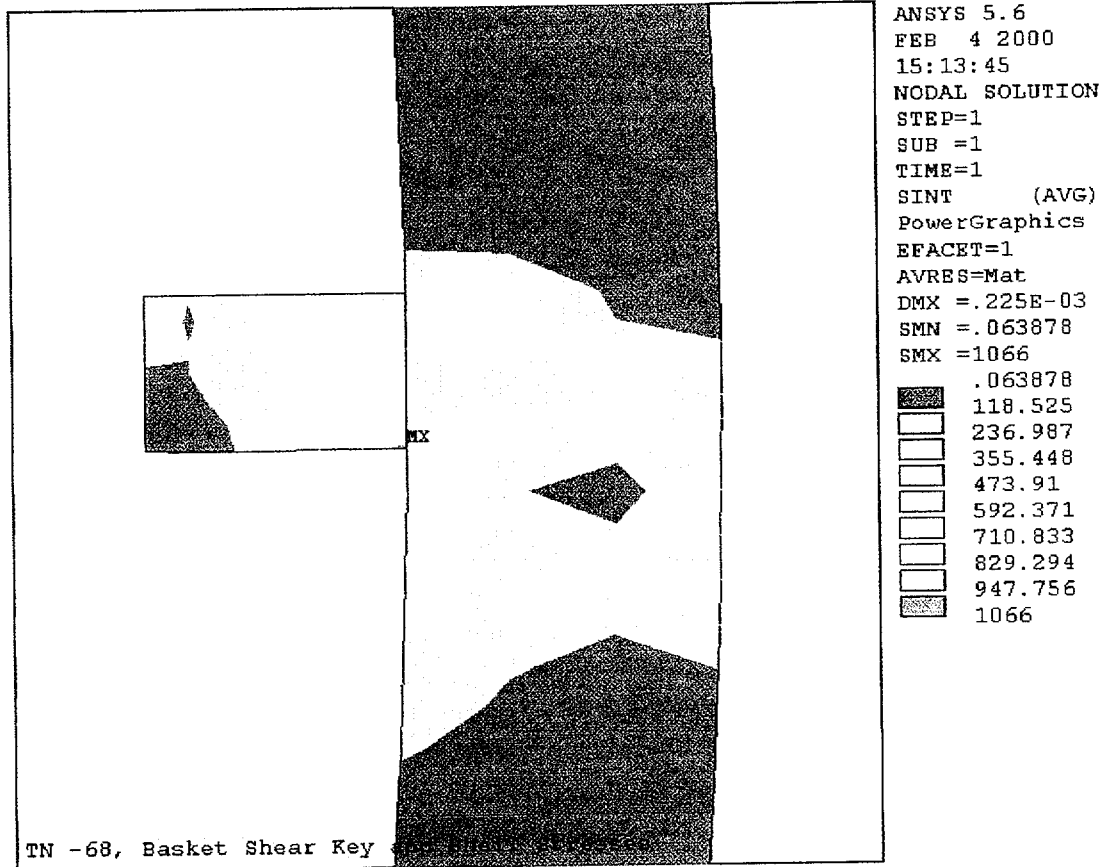


**Figure 2-4**  
**Maximum Stress Intensity Plot**



Chapter 3 Thermal

3-1 Provide an analysis of the effects of the structures and/or components that will be placed around the exterior of the TN-68 transport cask and include design details on the package certification drawings, as appropriate. Specifically:

3-1-1 SAR page 1-2, indicates that a tarp is placed over the cask during transport (see related RAI 1-5.)

**Response:** The application will be revised to delete the statement that a tarp is placed over the cask during transport.

3-1-2 SAR pages 3-2 and 3-12, indicate that a “crib frame” or equivalent barrier surrounds the packaging.

**Response:** The application will be revised to delete the statement that a “crib frame” or equivalent barrier surrounds the packaging during transport.

3-1-3 Quantify the effect of the transport cover on package temperatures during normal conditions of transport.

**Response:** No transport cover will be used to cover the packaging during transport conditions.

3-1-4 Quantify the maximum accessible surface temperature of the enclosure under the conditions of 10 CFR 71.43 (g).

**Response:** The application is revised to include a 3-D, 1/12 symmetry finite element model of the cask body, lid, impact limiter spacer, and front and rear impact limiters in order to determine the accessible impact limiter surface temperature in the shade.

**The front and rear impact limiters and tie rods prevent access to the cask body during transport conditions. Additionally, railing(s) may be attached to the transport frame or rail car to further prevent access. The readily accessible surfaces of the packaging are limited to the impact limiters which extend radially past the rail car.**

**The maximum accessible surface temperature is 110 °F.**

The SAR, page 3-2 paragraph 1, 2nd sentence states “The crib frame is sufficiently far away from the packaging such that it has a negligible effect on the heat dissipated from the package.” A similar statement is made on page 3-12. However, neither the tarp nor the “crib frame” appear to be included in the drawings nor in the thermal analysis for the normal conditions of transport. The correlation for heat transfer from the cask surface

assumes an open environment at a constant temperature of 100 °F which will not to be the case if a cover (i.e. the tarp and crib frame) is in place. In addition, the effects of the transport cover need to be described. 10 CFR 71.33(a)(5)(iii) requires a description of external structures to provide a sufficient basis for evaluation of the package. Also, SRP chapter 3.5.4 states that the thermal impedance of personnel barriers placed around the cask be considered when determining temperatures for normal conditions of transport.

The applicant reports that the “maximum accessible surface temperature of the enclosure in the shade will be 100°F.” However, it is unclear how this surface temperature was determined considering that 10 CFR 71.43 (g) requires an ambient temperature of 100°F in addition to heat generated by the package contents.

- 3-2 Recalculate the Maximum Normal Operating Pressure (MNOP) based on the input assumptions in the Draft Standard Review Plan, NUREG-1617(SRP.)

The calculation of MNOP in SAR section 4.2.2, assumes a 3% rod failure. However, the SRP, Section 3.5.3.4, recommends that the calculation should assume 100% rod failure.

The Regulatory requirements of 10 CFR § 71.33 that the packaging and contents must be described in sufficient detail to provide an adequate basis for its evaluation are applicable to questions 3-3 through 3-5.

**Response: The MNOP has been calculated assuming 100% rod failure as recommended in NUREG-1617. Section 4.2.2 of the TN-68 Transport SAR has been revised accordingly and is attached to this submittal.**

- 3-3 Provide the basis for the 0.312 kW per assembly reported on SAR p. 3-11.

**Response: The basis for the 0.312 kW is an SAS2H analysis performed for a 7x7 fuel assembly, with 3.3 %wt average enrichment, an assembly average burnup of 40,000 MWD/MTU, and a cooling time of 10 years. The fuel assembly parameters and the SAS2H input file are given in Sections 5.2 and 5.6.1 respectively of the TN-68 SAR.**

- 3-4 Confirm that the design basis fuel of 40000 MWD/MTU and 10 years cooling meets the per assembly heat generation criterion.

**Response: See response to RAI 3-3 above.**

- 3-5 Provide the calculation or reference the calculation (if previously submitted to NRC) for normal fuel cladding temperature limits.

**Response: The calculation for normal fuel cladding temperature limits was provided in Section 3.5.1 of the TN-68 storage application.**

- 3-6 For normal conditions of transport, confirm that the thermal environment does not degrade the materials (wood, adhesives, etc.), cause changes in material properties, or adversely affect the ability of the impact limiters to perform intended safety functions.

The package must be designed, constructed, and prepared for transport so that there will be no significant decrease in packaging effectiveness under the tests specified in 10 CFR 71.71 (normal conditions of transport.)

**Response:** The structural properties for wood given in NUREG/CR-0322, for temperatures up to 230 °F, bound those used in the structural analysis. The application is revised to include a 3-D, 1/12 symmetry finite element model of the cask body, lid, impact limiter spacer, and front and rear impact limiters in order to determine maximum wood temperatures. Wood temperatures are below the 230 °F temperature limit.

The adhesive used in the impact limiters can withstand temperatures in excess of the wood temperature limit of 230 °F.

The structural performance of the impact limiters under minimum ambient normal conditions is verified via testing. Cold temperatures result in increasing the stiffness of the impact limiter, and hence increasing the g loads. Therefore the end drop test was performed using an impact limiter which had been cooled to -20°F. The results of this test are presented in Appendix 2.10.9.

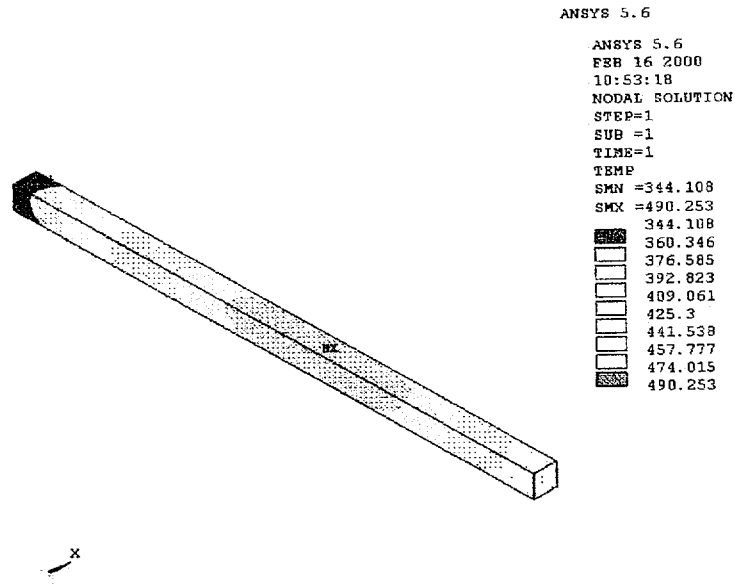
- 3-7 Provide the axial temperature profile of: (1) the hot assembly and (2) the cask inside wall for normal conditions of transport.

The packaging and contents must be described in sufficient detail to provide an adequate basis for its evaluation (10 CFR 71.33.)

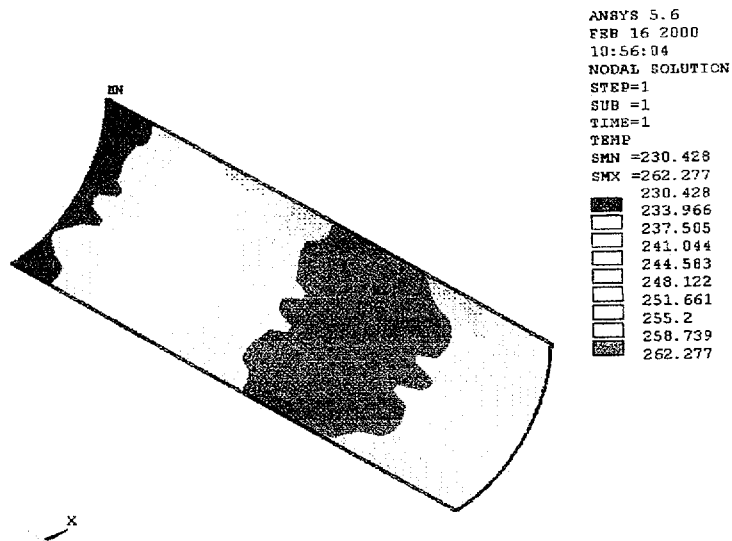
The package must be evaluated to demonstrate that it satisfies the thermal requirements specified in 10 CFR Part 71.71, normal conditions of transport.

Response: The requested figures are found below.

**“Hot” Fuel Assembly, Normal Conditions of Transport**



**Cask Inner Wall, Normal Conditions of Transport**



- 3-8 Revise the application to show that the maximum seal temperatures are within allowable limits under fire test conditions, considering impact limiter damage from the sequential 30-foot and 40-inch puncture tests.

The SAR evaluation calculates seal temperatures without considering the extent to which the impact limiter wood may be charred or no longer present in the crushed areas and where the puncture pin may penetrate the impact limiter. See related RAI 2-7.

The package design must be evaluated for the hypothetical accident conditions in 10 CFR 73 sequentially to determine the effects of the conditions and tests under a hypothetical accident. The 30-minute, 800°C (1475°F) thermal test of 10 CFR 71.73(c)(4) must be evaluated on a damaged package.

**Response:** The application is revised to show the effects of impact limiter damage. Two 3-D, 1/12 symmetry finite element models are created to represent:

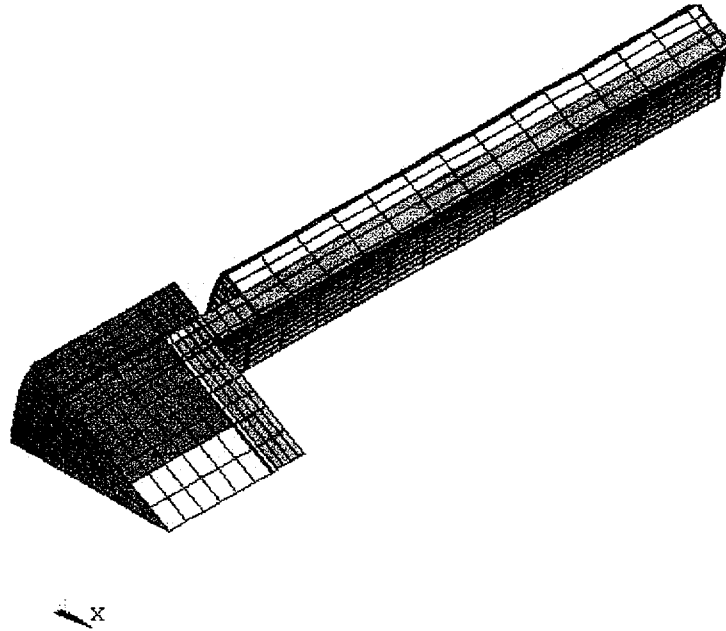
- 1) A crushed impact limiter corresponding to a 15° drop resulting in the shortest distance between the fire ambient and the Helicoflex o-ring between the lid and cask body.
- 2) A crushed impact limiter corresponding to a 70° drop resulting in the shortest distance between the fire ambient and the Helicoflex o-rings within the port covers.

The balsa and redwood within the impact limiters are treated as a homogenized mass given bounding material properties. During the fire accident condition the wood is given a bounding maximum thermal conductivity and no thermal mass in order to maximize heat flow into the seals. During the pre-fire and post-fire conditions the wood is given a bounding minimum conductivity (0.0019 Btu/hr-in<sup>2</sup>-°F) and no thermal mass in order to minimize heat flow out of the seals.

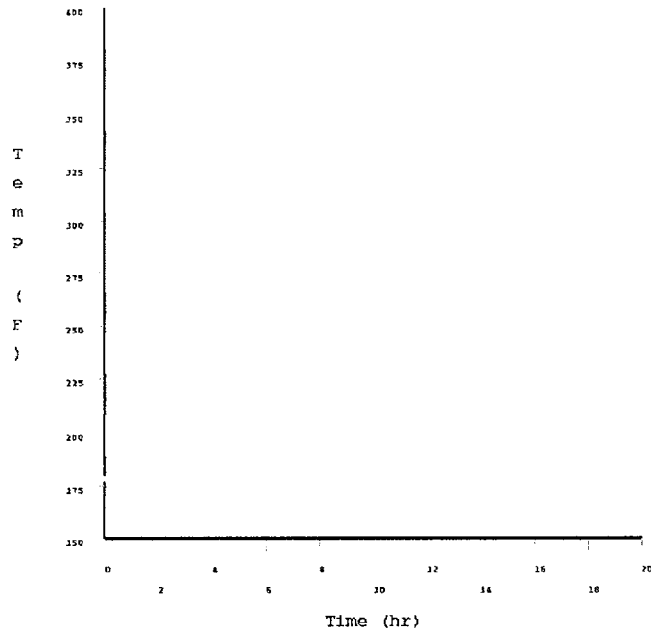
The bounding minimum conductivity is equivalent to that of air. This bounds the effects of the altered conduction path through the wood due to the 40-inch puncture test and wood that has charred.

Plots of the finite element models and the transient seal temperatures for each of the crush configurations are shown below. The analysis demonstrates that the peak transient seal temperatures remain below 375 °F.

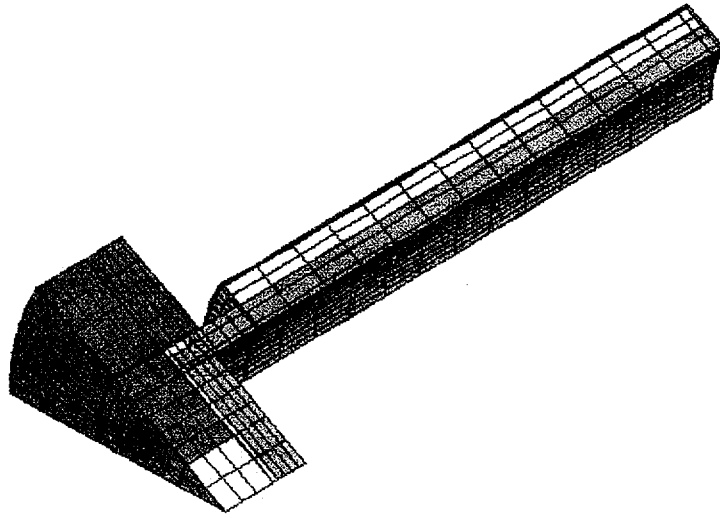
**15° Drop Configuration, Finite Element Model**



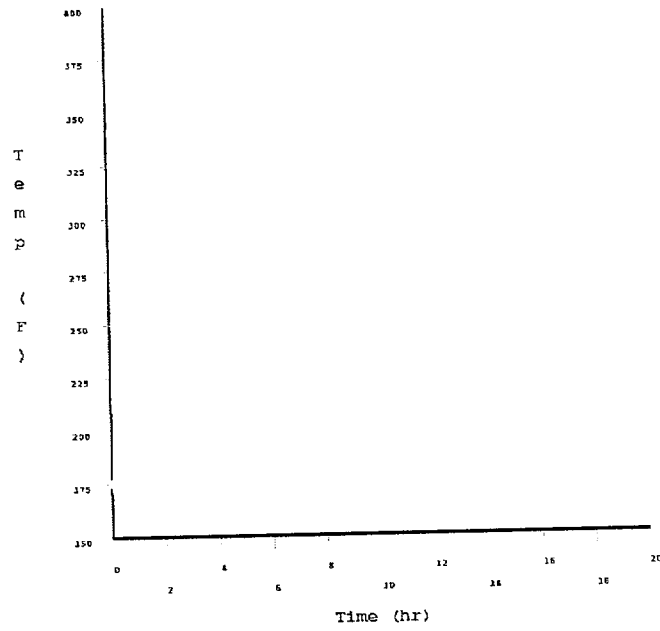
**15° Drop Configuration, Transient Seal Temperature**



## 70° Drop Configuration, Finite Element Model



## 70° Drop Configuration, Transient Seal Temperature

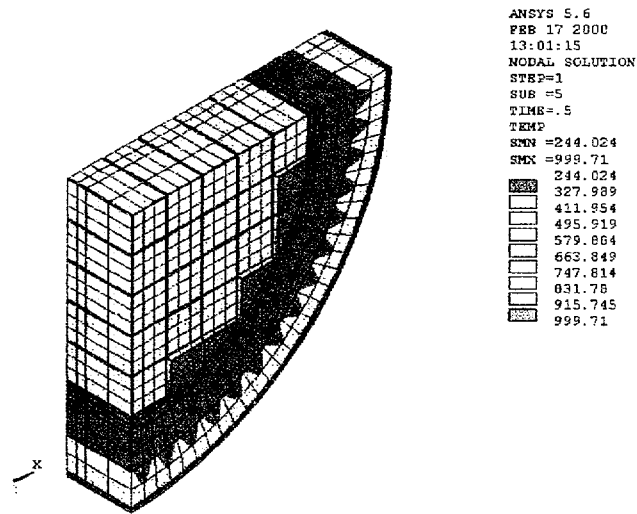


3-9 With respect to the hypothetical accident conditions thermal analysis:

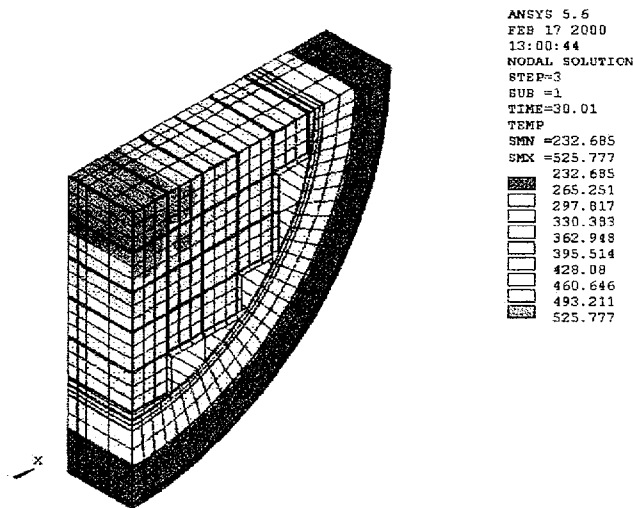
3-9-1 Provide figures representing the cross section model and calculated temperature distributions for the fire transient at the end of the fire and after equilibrium is established in the post fire phase.

**Response:** The application will be revised using a post fire absorptivity of unity. (see response to RAI 3-9-3) The requested figures, using the revised absorptivity, are shown below:

**Temperature Distribution, End of Fire Condition**



**Temperature Distribution, Post Fire Steady State**



3-9-2 Provide the axial temperature profile of:

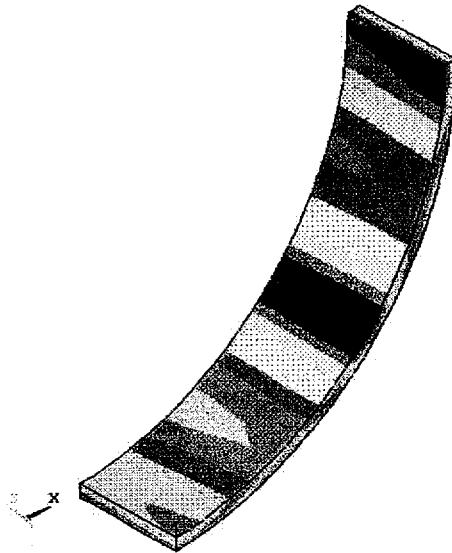
(A) the cask inside wall at time = 2.3 hours and

(B) the hot assembly at time = 21.3 hours.

**Response:** The analysis of the fire accident condition consists of finite element models of the seal region, and of the hottest cross section of the packaging. Neither provide axial temperature profiles of the fuel assemblies and the cask inner wall during accident conditions.

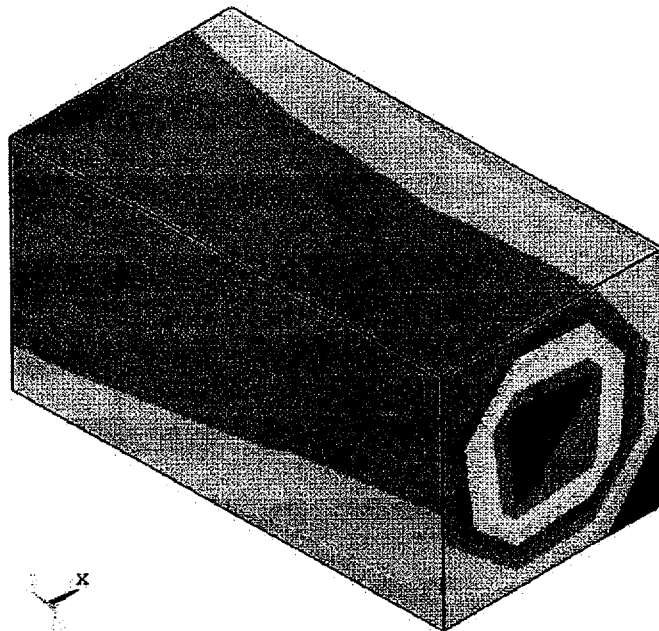
The application will be revised using a post fire absorptivity of unity. (See response to RAI 3-9-3) Provided below are temperature distributions of the cask inner shell and the hot assembly, taken from the cross-section model, when they reach their peak transient temperatures.

**Cask Inner Shell @ time = 2.3 hours**



ANSYS 5.6  
FEB 17 2000  
12:58:49  
NODAL SOLUTION  
STEP=2  
SUB =12  
TIME=2.327  
TEMP  
SMN =370.689  
SMX =371.122  
370.689  
370.737  
370.786  
370.834  
370.882  
370.93  
370.978  
371.026  
371.074  
371.122

**Hot Fuel Assembly @ time = 22.6 hours**



ANSYS 5.6  
FEB 17 2000  
12:59:54  
NODAL SOLUTION  
STEP=2  
SUB =70  
TIME=22.571  
TEMP  
SMN =521.684  
SMX =554.519  
521.684  
525.333  
528.981  
532.629  
536.278  
539.926  
543.574  
547.223  
550.871  
554.519

3-9-3 Provide the post fire, solar absorptivity and confirm that the correct value was used in the analysis.

No figures for temperature in the fuel regions and cask body were provided. In the post fire cooldown discussion on p. 3-16 of the TN-68 SAR, the absorptivity of white paint was given vs. soot.

The packaging and contents must be described in sufficient detail to provide an adequate basis for its evaluation (10 CFR 71.33.)

The package must be evaluated to demonstrate that it satisfies the thermal requirements specified in 10 CFR 71.73, hypothetical accident conditions.

**Response:** An absorptivity of 0.30 had been used for the post fire condition. The application will be revised using a post fire absorptivity of unity to account for the effect of soot on cask surfaces following the fire accident condition. The effect of this on the peak transient temperatures is less than 3 °F. The updated peak transient temperatures for the accident conditions are shown below:

<u>Component</u>	<u>Maximum Transient</u>
Outer Surface	1000°F (End of Fire)
Seal	375°F (2.0 hours)
Radial Neutron Shield	82°F (End of Fire)
Gamma Shell	379°F (1.3 hours)
Basket Rail	390°F (5.0 hours)
Inner Shell	371°F (2.3 hours)
Basket	537°F (22.1 hours)
Fuel Cladding	555°F (22.6 hours)
Average Cavity Gas	423°F (14.6 hours)

## Chapter 4     Containment

4-1     Provide data and supporting calculations for the following:

4-1-1     Surface area of the fuel rods used in crud calculation.

4-1-2     Free volume in the cask.

In chapter 4.2.1.1, page 4-7, the surface area of a fuel rod is used in the calculation of crud activity. The free volume inside the containment vessel is also given in this section. These parameters are key inputs to the source term calculations used in the containment analysis.

The packaging and contents must be described in sufficient detail to provide an adequate basis for its evaluation (10 CFR 71.33).

**Response:     The calculations of the fuel rod surface area and the cask free volume have been added to Section 4.2.1.1.**

4-2     Provide the basis or calculation for the values, 4.425 E-03 kg-moles and 2.2 atm-abs, used on page 4-10 to calculate P<sub>3%</sub> rod failure and p. 4-12 to calculate P<sub>100%</sub> rod failure.

These parameters are key inputs to cask internal pressure calculations used in the containment analysis. The packaging and contents must be described in sufficient detail to provide an adequate basis for its evaluation (10 CFR 71.33).

**Response:     The basis for the cavity pressures and gas mixtures has been added to Chapter 4. The calculations for MNOP have been updated to assume 100% rod failure.**

4-3     Provide a complete listing of the input parameters used to calculate permissible leakage rates under hypothetical accident conditions given in Table 4-5 of the TN-68 SAR. The information requested is similar to the information presented on pages 4-8 and 4-9 of the SAR for normal conditions of transport.

These parameters are key inputs to cask accident leak rate calculations used in the containment analysis. The packaging and contents must be described in sufficient detail to provide an adequate basis for its evaluation (10 CFR 71.33). The package must be evaluated to demonstrate that it satisfies the containment requirements of 10 CFR Part 71, Subpart E, under the conditions and tests of Subpart F.

The package must meet the containment requirements of 10 CFR 71.51(a)(2) for hypothetical accident conditions, with no dependence on filters or a mechanical cooling system. [10 CFR 71.51(c)]

**Response:     Additional detail has been added to Section 4.3.3. The conversion of**

**the permissible leakage rate to standard units of ref cm<sup>3</sup> / sec has also been added to this section.**

4-5 With respect to the calculation of effective A<sub>2</sub> values:

4-5-1 Justify the use of a limited number of radioactive isotopes as shown in SAR tables 4-1 and 4-3 for the calculation of effective A<sub>2</sub> values for spent fuel.

4-5-2 Justify the A<sub>2</sub> value of 13.5 Ci for Ba-137 given in SAR table 4-3.

Appendix A to 10 CFR 71 provides the methodology for determining A<sub>2</sub> values for various isotopes. This discussion provides a methodology for determining A<sub>2</sub> values for isotopes not listed in Table A-1, A<sub>2</sub> values for daughter products of radioactive isotopes, and effective A<sub>2</sub> values for mixtures of radioisotopes. A large number of isotopes are present in spent fuel and no basis was provided for considering only selected isotopes.

**Response: The source term for the containment analysis uses the methodology described in ISG-5 rev. 1. Slight modifications have been incorporated to this section. Ru-106 and Sb 125 have been added to the list of isotopes. Ba 137m has been removed since it is not required in accordance with 10 CFR 71 Appendix A.**

4-6 Provide additional details of the calculation of cask cavity gas mixtures under normal conditions of transport (page 4-9) and hypothetical accident conditions (p. 4-12).

This information given on pages 4-9 and 4-12 appear to support the assessment that there are no explosive mixtures present in the cask. However, sufficient detail has not been provided to verify the gas fractions given. SRP chapter 4.4.3 states that combustible gases should not exceed 5% of the cask free volume of any confined region.

The package must be made of materials and construction which assure that there will be no significant chemical, galvanic, or other reactions among the packaging components, among package contents, or between the packaging components and the package contents, including possible reaction resulting from in-leakage of water, to the maximum credible extent. The effects of radiation on the materials of construction must also be considered (10 CFR 71.43(d)).

**Response: Additional detail, including Tables 4-6 and 4-7, has been provided in Chapter 4 to support the calculation of the cask cavity gas mixture under normal transport and hypothetical accident conditions.**

## Chapter 5     Shielding

- 5-1     Revise Chapter 5 of the SAR to include bounding design-basis fuel specifications (i.e., initial enrichment and burnup) and minimum cooling times which are consistent with the contents that are proposed to be transported.

The applicant performed the shielding analysis assuming that the fuel has been cooled for a period of 20 years. The SAR states on page 5-1 that design basis fuel less than 20 years will be acceptable for transport as long as the measured dose rates meet 10 CFR 71.47. However, in order to demonstrate compliance with the regulatory external radiation standards for packages stated in 10 CFR 71.47, the analysis must be consistent with the proposed contents of the package. Chapter 1.2.3 of the SAR states that fuel that has been cooled for 10 years is proposed to be transported in the package and therefore the shielding analysis should assume the same cooling time. See related RAI 1-6-1.

**A discussion of the allowable contents for transport in the TN-68 cask was presented previously in response to question 1-6. In support of that response, MCNP dose rate calculations have been performed for the TN-68 transport packaging. An analysis was performed for the TN-68 cask containing 68 design basis (7x7) fuel assemblies with 40,000 MWD/MTU burnup, 3.3%wt enrichment, and cooled for 16 years. The results of this analysis are presented in the Table 5-1 below and they show that the dose rate criteria of 10CFR71 are met.**

**Additionally, an analysis was performed for the TN-68 cask containing 44 design basis fuel assemblies (40 GWD/MTU, 3.3% enriched, and 10 year cooled) and 24 medium burnup assemblies (21.5 GWD/MTU, 2.5% enriched, and 26 year cooled) on the periphery of the basket, surrounding the design basis fuel. This is a typical planned loading configuration for storage in the TN-68. The results of this analysis are presented in Table 5-2 below and they also show that the 10CFR71 limits are met. (Note: the ancillary shield ring has been increased from 1/2" thick to 1" thick.) As discussed in response 1-6, the design basis fuel, 40,000 MWD/MTU with 10 year cooling can be shipped in the TN-68 cask, depending on the number of assemblies, the location in which they are loaded, and the parameters of the other fuel loaded in the cask. Thermal, structural, and containment analyses are bounded by the design basis fuel (10 year cooling) and the number of design basis fuel assemblies that can be loaded is controlled by the dose rate that is required to be measured for the cask.**

**Source terms for 10 and 16 year cooled design basis fuel are shown in Tables 5-2 and 5-3 and will be included in the SAR.**

**Table 5-1 Dose Rates for 16 Year Cooled Fuel**

Axial Interval	MCNP Dose Rates (Mrem/hr)			16 year
	Radial			
	Total Dose Rates			
	<u>Cask Surface</u>	<u>Transport Vehicle Edge</u>	<u>2 M from Transport Vehicle</u>	
-314.68				
-275.94				1.9
-227.06				2.9
-190	0	0		4.6
-164.59	22	18		6.3
-146.3	27	22		6.9
-109.73	39	27		7.6
-73.15	39	29		9.2
-36.53	43	32		9.8
0	43	32		10
36.53	42	31		9.9
73.15	37	28		10
109.73	36	26		9.7
146.3	29	21		9.6
164.59	21	18		9.8
200	13	17		10
224.72	50	44		9.2
245.9	122	63		8.5
279.05				6.4
327.93				3.1
366.67				

<u>radius (cm)</u>	<u>top limiter*</u> <u>total (mrem/hr)</u>	<u>bottom limiter*</u> <u>total (mrem/hr)</u>
25	10.	8.5
50	9.7	7.8
75	7.3	6.2
101.4	4.3	3.4
124.5	1.7	1.3
152	0.72	0.48
182.9	0.34	0.19
352	0.92	0.75

\* - at surface of limiter

**Table 5-2 Dose Rates for Typical Storage Loading**

Axial Interval (cm)	Total Cask Dose Rate (mrem/hr) (44 dbf+24 mbf)		
	<u>Cask Surface</u>	<u>Transport Vehicle Edge</u>	<u>2 M from Transport Vehicle</u>
-314.68			
-275.94			0.95
-227.06			1.5
-190			2.3
-164.59	14.	10.	3.1
-146.3	14.	11.	3.3
-109.73	19.	13.	3.5
-73.15	16.	13.	4.3
-36.53	18.	13.	4.6
0	18.	13.	5.0
36.53	18.	14.	5.1
73.15	17.	13.	5.6
109.73	14.	11.	5.8
146.3	12.	9.6	6.7
164.59	8.9	9.7	7.7
200	11.	15.	8.7
224.72	60.	53.	8.9
245.9	151.	79.	8.9
279.05			6.4
327.93			2.9
366.67			

<u>radius (cm)</u>	<u>top limiter*</u> total (mrem/hr)	<u>bottom limiter*</u> total (mrem/hr)
25	21.	17.
50	18.	15.
75	13.	10.
101.4	7.1	5.6
124.5	2.6	1.9
152	1.1	0.65
182.9	0.51	0.23
352	0.93	0.49

\* - at surface of limiter

**These results will be added to Chapter 5 of the SAR.**

TABLE 5-3  
 GENERAL ELECTRIC 7x7, BUNDLE AVERAGE ENRICHMENT 3.3wt% U235,  
 40,000 MWD/MTU, AND 10 YEAR COOLING TIME WITH CHANNELS

PRIMARY GAMMA SOURCE SPECTRUM

<u>Scale Group</u>	<u>Energy Interval, MeV</u>	<u>Active Fuel Zone</u>	<u>γ/sec/assembly</u>		
			<u>Plenum Zone<sup>a</sup></u>	<u>Top Fitting Zone<sup>a</sup></u>	<u>Bottom Fitting Zone<sup>a</sup></u>
28	8.00E+00 to 1.00E+01	5.043E+04			
29	6.50E+00 to 8.00E+00	2.375E+05			
30	5.00E+00 to 6.50E+00	1.211E+06			
31	4.00E+00 to 5.00E+00	3.018E+06			
32	3.00E+00 to 4.00E+00	1.268E+08			
33	2.50E+00 to 3.00E+00	1.136E+09			
34	2.00E+00 to 2.50E+00	1.589E+10			
35	1.66E+00 to 2.00E+00	4.586E+10			
36	1.33E+00 to 1.66E+00	4.982E+12	1.254E+11	3.981E+11	4.231E+11
37	1.00E+00 to 1.33E+00	3.563E+13	4.440E+11	1.410E+12	1.498E+12
38	8.00E-01 to 1.00E+00	3.593E+13			
39	6.00E-01 to 8.00E-01	6.627E+14			
40	4.00E-01 to 6.00E-01	5.862E+13			
41	3.00E-01 to 4.00E-01	1.378E+13			
42	2.00E-01 to 3.00E-01	2.240E+13			
43	1.00E-01 to 2.00E-01	8.007E+13			
44	5.00E-02 to 1.00E-01	1.023E+14			
45	1.00E-02 to 5.00E-02	2.678E+14			

Total (α,n plus spontaneous fission) Neutron Source

<u>Scale Group</u>	<u>Energy Interval (MeV)</u>	<u>Source Term (n/sec/assembly)</u>
1	6.430E+00 - 2.000E+01	1.65E+06
2	3.000E+00 - 6.430E+00	1.88E+07
3	1.850E+00 - 3.000E+00	2.09E+07
4	1.400E+00 - 1.850E+00	1.18E+07
5	9.000E-01 - 1.400E+00	1.59E+07
6	4.000E-01 - 9.000E-01	1.73E+07
7	1.000E-01 - 4.000E-01	3.39E+06
	Total	8.98E+07

**TABLE 5-4**  
**GENERAL ELECTRIC 7x7, BUNDLE AVERAGE ENRICHMENT 3.3wt% U235,**  
**40,000 MWD/MTU, AND 16 YEAR COOLING TIME WITH CHANNELS**

PRIMARY GAMMA SOURCE SPECTRUM

<u>Scale Group</u>	<u>Energy Interval, MeV</u>	<u>Active Fuel Zone</u>	<u>γ/sec/assembly</u>		
			<u>Plenum Zone<sup>a</sup></u>	<u>Top Fitting Zone<sup>a</sup></u>	<u>Bottom Fitting Zone<sup>a</sup></u>
28	8.00E+00 to 1.00E+01	4.03E+04			
29	6.50E+00 to 8.00E+00	1.90E+05			
30	5.00E+00 to 6.50E+00	9.67E+05			
31	4.00E+00 to 5.00E+00	2.41E+06			
32	3.00E+00 to 4.00E+00	9.12E+06			
33	2.50E+00 to 3.00E+00	2.33E+08			
34	2.00E+00 to 2.50E+00	1.67E+09			
35	1.66E+00 to 2.00E+00	3.02E+10			
36	1.33E+00 to 1.66E+00	2.10E+12	5.694E+10	1.808E+11	1.922E+11
37	1.00E+00 to 1.33E+00	2.03E+13	2.016E+11	6.402E+11	6.805E+11
38	8.00E-01 to 1.00E+00	1.28E+13			
39	6.00E-01 to 8.00E-01	5.38E+14			
40	4.00E-01 to 6.00E-01	1.62E+13			
41	3.00E-01 to 4.00E-01	1.15E+13			
42	2.00E-01 to 3.00E-01	1.82E+13			
43	1.00E-01 to 2.00E-01	6.24E+13			
44	5.00E-02 to 1.00E-01	8.57E+13			
45	1.00E-02 to 5.00E-02	2.99E+14			

Total (α,n plus spontaneous fission) Neutron Source

<u>Scale Group</u>	<u>Energy Interval (MeV)</u>		<u>Source Term (n/sec/assembly)</u>
1	6.43E+00	- 2.00E+01	1.31E+06
2	3.00E+00	- 6.43E+00	1.50E+07
3	1.85E+00	- 3.00E+00	1.68E+07
4	1.40E+00	- 1.85E+00	9.38E+06
5	9.00E-01	- 1.40E+00	1.26E+07
6	4.00E-01	- 9.00E-01	1.38E+07
7	1.00E-01	- 4.00E-01	2.69E+06
		Total	7.16E+07

- 5-2 Justify the use of ICRP-51 for flux to dose rate conversion factors for the shielding calculations of the TN-68 package or revise the calculation using dose conversion factors from ANSI/ANSI 6.1.1-1977.

Table 5.4-1 of the SAR provides dose conversion factors which were derived from Table 6 of ICRP 51. The draft SRP states in chapter 5.5.4.3 that ANSI/ANS 6.1.1-1977 should be used for dose conversion factors in the shielding analysis. External dose rate calculations using dose conversion factors from ANSI/ANS 6.1.1-1977 are more conservative than those that would be calculated with ICRP 51.

**The response functions from ANSI/ANSI 6.1.1-1977 and ICRP 51 are shown in Figure 5-1 below. As shown in the Figure, the response functions for both gamma and neutron are virtually identical in the energy range of interest, i.e., around 1 MeV for gamma and above 0.1 MeV for neutron.**

- 5-3 Revise the application to provide the basis for determining the bounding fuel assembly type for shielding, considering neutron dose end effects for fuel assembly types that contain natural uranium blankets and a cooling time of 10 years.

The SAR did not provide information related to the neutron dose rates for fuel assembly types that have natural uranium blankets. The applicant should revise the SAR to summarize the dose rate results at the cask end locations and the external cask side locations that are not covered by the neutron shielding for assemblies with natural uranium blankets. In addition, a discussion of the treatment of end effects of applicable assemblies in the development of source terms and neutron/photon peaking distributions should be provided. The SAR should also use source term inputs from 10 year cooled fuel as stated in RAI 5-1 above.

An evaluation of this issue is required to determine compliance with the external radiation limits specified in 10 CFR Parts 71.47.

**New source terms (SAS2H runs) were created for zones 1 and 12 shown in Table 5.2-7 of the SAR assuming the uranium was natural. The calculated neutron source for the natural uranium zones was 1.094E5 and 1.652E5 for zones 1 and 12 respectively. (Note: The gamma sources decreased slightly and were not further evaluated.) A modified Table 5.2-7 is shown below.**

**The revised axial profile was input into the MCNP model and the neutron dose rates recalculated with the new axial profile due to natural uranium ends in the fuel assemblies.**

**A comparison of the neutron dose rate results from this calculation with those from the previous calculation show a slight increase in the dose rate at the top and bottom of the cask.**

At the cask surface just above the bottom impact limiter, the neutron dose rate increases from 4.23 mrem/hr to 4.40 mrem/hr and on the cask surface, just below the top impact limiter, the neutron dose increases from 15.7 mrem/hr to 16.7 mrem/hr. The neutron dose at locations in between are essentially the same. At the edge of the rail car, the neutron dose at the top impact limiter area increases from 7.20 mrem/hr to 7.51 mrem/hr while at the bottom, no significant change is apparent. At 2 meters, the neutron dose rates from the two cases are essentially identical.

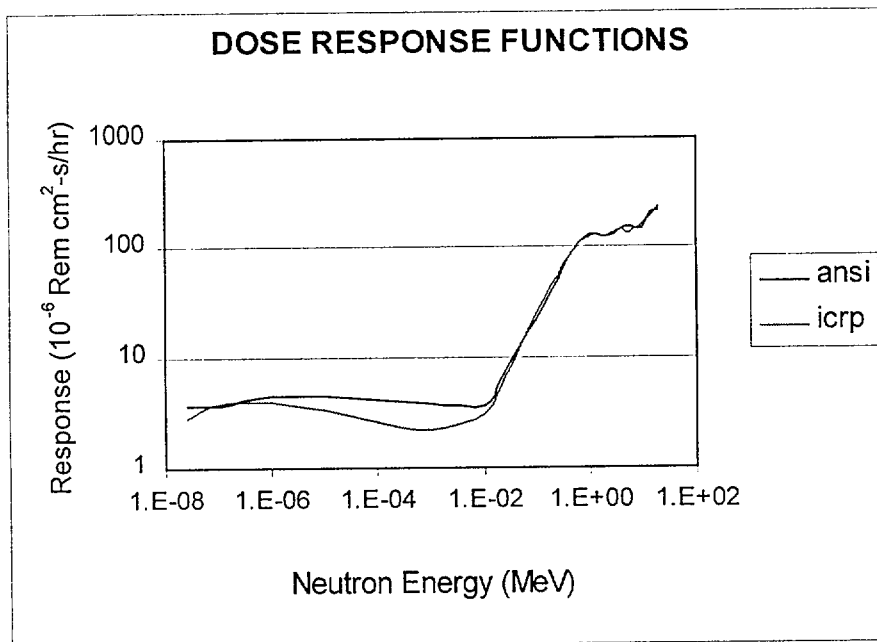
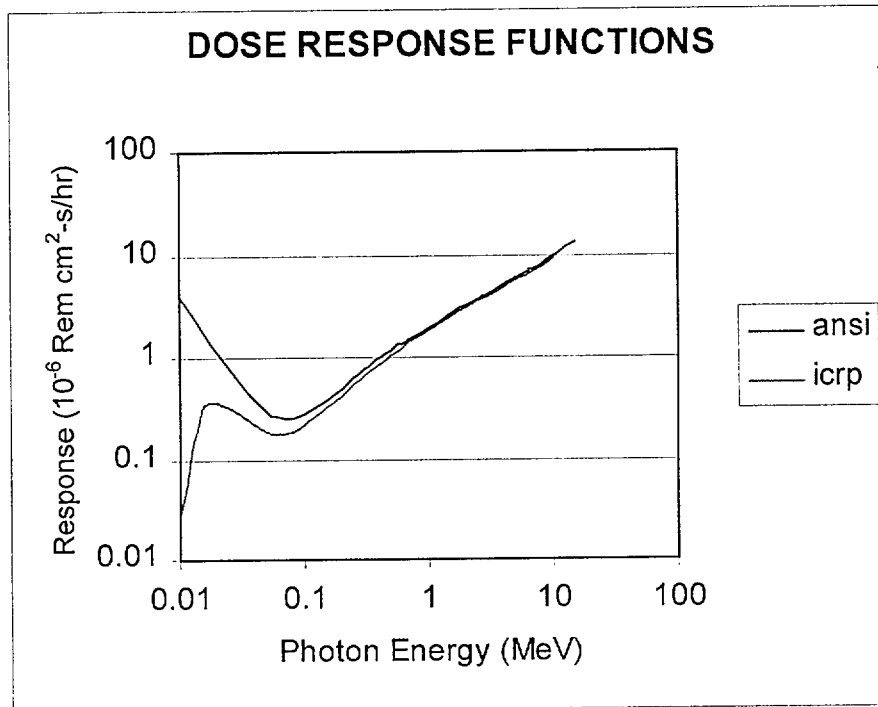
If one compares the total dose rates for the two cases, one again sees that at the surface, the dose rate increases by 1 mrem/hr around the impact limiters and at the rail car edge, the dose rate around the top limiter increases by 0.2 to 0.3 mrem/hr. Again no significant difference occurs at 2 meters.

Thus, it is shown that a change in the neutron dose rate due to the natural uranium ends occurs, as expected, toward the top and bottom end of the cask. The maximum increase in the neutron dose rate occurs just below the top limiter at the cask surface and is approximately 6.5%. The maximum increase in the total dose rate is approximately 1% and occurs just below the top impact limiter. The natural uranium ends has no significant effect on the dose rates calculated at 2 meters.

Modified SAR Table 5.2-7

Output File Name	Zone	Frac Core Height	Peaking Factor	Burnup (MWd/MtU)	SAS2H Power (MW)	Water Density (g/cc)	Neutron Source (n/s)	Neutron Peaking Factor	Gamma Source (g/s)	Gamma Peaking Factor
7x7-9-36nu.output	12	0.95-1.0	0.2410	9640	1.205	0.3609	1.652E+05	0.0277	1.476E+13	0.2162
7x7-25-36.output	11	0.90-0.95	0.6330	25320	3.165	0.3631	6.500E+05	0.1090	4.275E+13	0.6264
7x7-36-37.output	10	0.8-0.9	0.8973	35891	4.486	0.3701	6.005E+06	0.5036	1.238E+14	0.9066
7x7-43-39.output	9	0.7-0.8	1.0766	43065	5.383	0.3861	1.274E+07	1.0685	1.499E+14	1.0980
7x7-46-41.output	8	0.6-0.7	1.1515	46061	5.758	0.4118	1.647E+07	1.3814	1.535E+14	1.1243
7x7-47-43.output	7	0.5-0.6	1.1912	47649	5.956	0.4375	1.859E+07	1.5592	1.663E+14	1.2182
7x7-48-47.output	6	0.4-0.5	1.2000	48000	6.000	0.4708	1.877E+07	1.5743	1.674E+14	1.2262
7x7-48-53.output	5	0.3-0.4	1.2000	48000	6.000	0.5251	1.819E+07	1.5256	1.671E+14	1.2241
7x7-47-59.output	4	0.2-0.3	1.1836	47345	5.918	0.5945	1.649E+07	1.3830	1.644E+14	1.2044
7x7-43-70.output	3	0.1-0.2	1.0750	43001	5.375	0.7008	1.005E+07	0.8429	1.484E+14	1.0869
7x7-31-75.output	2	0.05-0.1	0.7746	30985	3.873	0.7541	1.002E+06	0.1680	5.245E+13	0.7685
7x7-9-76nu.output	1	0.0-0.05	0.2357	9426	1.178	0.7603	1.094E+05	0.0184	1.443E+13	0.2114
<b>Average/Total</b>			0.9917	39670	4.959	0.5016	1.192E+08	1.0000	1.365E+15	1.0000
<b>Uniform Case</b>		0.0-1.0	1	40000	5	0.432	8.976E+07		1.379E+15	
<b>Ratio to Non-Uniform Case</b>							1.328		0.990	

Figure 5-1 ANSI vs ICRP Response Function



Chapter 6      Criticality

- 6-1      Revise the criticality safety analysis to either include preferential flooding or justify why preferential flooding is not credible.

The above scenario needs to be considered to demonstrate that the requirements of 10 CFR 71.55(b) are met.

**The following will be added as the last paragraph in Section 6.1:**

**“Non-uniform flooding of the basket is not evaluated because all the spaces in the basket are interconnected, and therefore this is not a credible condition.”**

## Chapter 7 Operating Procedures

The regulatory requirements of 10 CFR 71.87 regarding routine determinations apply to RAI 7-1 through 7-4.

- 7-1 Revise chapter 7.1.2.3 of the loading procedures to ensure that fuel loaded into the package meets the fuel specifications in chapter 1.2.3 of the SAR.

The SAR states that procedures will be developed to ensure that fuel loaded into the cask meets fuel specifications.

**Section 7.1.2.3 will be revised as follows:**

**7.1.2.3 Load the pre-selected spent fuel assemblies into the basket compartments. Procedures shall be developed to ensure that the fuel loaded into the cask meets the fuel specifications in chapter 1.2.3 of the SAR.**

- 7-2 Revise chapter 7.1.2.8 of the loading procedures to discuss acceptable methods for draining the water in the cask.

The SAR states that water will be drained according to the procedures but does not specify what procedures are being referred to.

**Response: Para. 7.1.2.8 of the SAR will be revised as follows. Reference to procedures has been deleted:**

**7.1.2.8 Using the drain port in the lid, drain the water from the cask. The cask is drained by connecting one end of a drain hose to the Hansen coupling in the drain port and routing the other to a pump. This may be done either before or after lifting the cask out of the pool. While lifting the cask out of the pool, the exterior of the cask may be rinsed with clean deionized water to facilitate decontamination.**

- 7-3 Revise the torque values for the impact limiter attachment bolts specified in chapter 7.1.3.17 to match the package drawings.

The torque value stated in the operating procedures for the impact limiter attachment bolts (400 ft-lbs) is not consistent with the value on drawing 972-71-2 (250 to 300 ft-lbs).

**Response: The torque value specified in the operating procedures for the impact limiter attachment bolts will be revised to make them consistent with the value on TN drawing 972-71-2. The torque value (250 to 300 ft-lbs) specified in the drawing is correct.**

- 7-4 Revise the operating procedures to include a step in which the vent and drain cover bolts are properly installed and torqued to the levels specified on the package drawings.

**Response:** The last statement in paragraph 7.1.3.6 will be revised as follows:

**Install the vent and drain cover bolts and torque to 35 ft-lbs in the first pass and to 60 - 65 ft-lbs in the final pass following the torquing sequence shown in Figure 7-1 prior to leak testing.**

## 9. General

### 9-1 With respect to cask fabrication and oversight:

- 9-1-1 Clarify the statements made in the SAR on pages 2-51 and 4-2:  
“Surveillances are performed by TN and utility personnel rather than by an Authorized Nuclear Inspector (ANI).” For these personnel, describe (1) the scope of the surveillances, (2) the organization(s), (3) the qualifications, and (4) the duties and authorities.

**Response: Surveillances are performed by TN personnel to ensure that the requirements imposed on our fabrication subcontractors through procurement documents are met. These surveillances are performed under the guidance of TN’s Quality Assurance Manager through documentation review and witnessing of fabrication and testing. Witnessing of fabrication for the TN-68 cask include (a) witnessing of leak testing, hydrotesting, functional and load tests. It also includes other inspections and witness or verifying any other examinations and additional investigations, which, in the judgment of the person performing the surveillance or the QA manager, are necessary to ascertain whether the item being inspected is being constructed in accordance with the procurement documents. These other examinations may include review of NDE reports, witnessing of NDE inspections, taking measurements to ensure that dimensional requirements or witnessing of fabrication processes to ensure that code requirements are met. TN either performs these surveillances through the use of TN personnel or outside contractors under the direction of the TN Quality Assurance Manager and in accordance with the TN nuclear QA program. The qualifications of these personnel are dependent on the type of surveillance required. In all cases, the surveillance personnel are trained in the TN QA program and surveillances are performed in accordance with written checklists. Surveillance personnel have experience in fabrication and NDE processes, calibration requirements and nuclear QA requirements. Surveillance personnel have the responsibility to accurately report any activity at the fabrication facility which he/she deems is adverse to the quality of the product, assure that further processing, delivery, installation or use of non-conforming items is controlled until proper disposition has occurred, and to perform day to day surveillance to verify that QA requirements are met.**

- 9-1-2 Clarify what is meant by “utility personnel” in the statements made in the SAR on pages 2-51 and 4-2.

The draft SRP states on page 2-6, that NRC will accept deviations from the ASME Boiler and Pressure Vessel Code (B&PV Division 3) provided the applicant’s justification is stated in the SAR and is acceptable to the NRC. The overall requirements, scope of activities, duties, and responsibilities for the ANIs are in Article NCA-5000 of the ASME Code. The scope, of surveillances, organization, personnel qualifications, and duties and authorities of personnel proposed by TN are not provided in the SAR. Also there have

been quality problems with vendor oversight programs as described in NRC Information Notice 95-29, "Oversight of Design and Fabrication Activities for Metal Components used in Spent Fuel Dry Storage Systems," and NRC Inspection Report Nos. 72-1007/97-212 and 72-1004/95-202. The applicant needs to provide additional information to demonstrate the adequacy of the alternative measures proposed in the SAR.

**Response: Reference to utility personnel will be deleted. Utility personnel, as the ultimate users of the casks, generally provide oversight of fabrication activities. However, TN has no authority to state the qualifications, duties or authorities of the utility personnel.**

10. Editorial changes / Typographical errors

- 10-1 Correct or clarify the apparent error on SAR p. 4-9 which states  $L_{std} = 1.70E-05$  ref  $cm^3/sec$  and on p. 4-10 which states  $L_{std} = 1.78E-05$  ref  $cm^3/sec$ .

**Response: The correct value is  $1.70E-05$  ref  $cm^3/sec$ . Section 4.2.3 of the SAR has been corrected.**

- 10-2 Revise chapter 6.1 and 6.2 to reference chapter 1 instead of chapter 2 for the cask contents.

**Response: References have been corrected.**

- 10-3 On page 8-1, last paragraph, ASME code exceptions regarding the containment vessel are stated to be described in "Chapter 7". This information is not provided in Chapter 7. Provide the correct cross-reference to this information.

**Response: Reference has been corrected to refer to ASME Code Exceptions listed in Section 2.11 of Chapter 2.**

- 10-4 The SAR references Appendix 6A in chapter 6.4.2.C, but no such appendix exists. It appears that the proper reference is Appendix 2.10.7.

**Response: The reference has been corrected.**

**FIGURE WITHHELD AS SENSITIVE UNCLASSIFIED  
INFORMATION**

1	2/22/02	SEE DCN 972-108	972	PS	PS		WRS	1/1/02	
NO.	DATE	REVISIONS	DWN.	CHK'D.	M.D.	O/A	PROJ.		
APPROVALS	DATE	 <b>TRANSNUCLEAR, INC.</b> <small>HAWTHORNE, N.Y.</small> <b>TN-68 PACKAGING GENERAL ARRANGEMENT</b> <span style="float: right;">SAR</span>							
PROJ.	T.J.N.								19 MAY 98
O/A	W.R.S.								19 MAY 98
MECH. DES.	P.S.								19 MAY 98
CHK'D. BY	P.S.								19 MAY 98
DWN. BY.	J.T.G.	18 MAY 98	NONE	B	972-71-2	1			
		SCALE	SIZE	DWG. NO.	REV.				

**FIGURE WITHHELD AS SENSITIVE UNCLASSIFIED  
INFORMATION**

~~SECRET~~

2	1/2/99	SEE DCN 972-125	JTG	JMC	PS					
1	2/28/00	SEE DCN 972-109	JTG	PS	PS			WRS	T.JN	
NO.	DATE	REVISIONS	DWN.	CHKD.	M.D.	N/T	O/A	PROJ.		
APPROVALS	DATE	<p align="center">   <b>TRANSNUCLEAR, INC.</b>  <small>HAMPSHIRE, NY</small>  <b>TN-68 PACKAGING</b>  <b>GENERAL ARRANGEMENT</b>  <b>PARTS LIST &amp; DETAILS</b> </p>								
PROJ.	T.JN									19 MAY 99
O/A	WRS									19 MAY 99
MECH. DES.	PS									19 MAY 99
CHKD. BY	PS									19 MAY 99
DWN. BY	JTG	18 MAY 99	NONE SCALE	B SIZE	972-71-3 DWG. NO.				SAR 2 REV.	

**FIGURE WITHHELD AS SENSITIVE UNCLASSIFIED  
INFORMATION**

2	5/2/68	SEE DCN 972-126	972	LMC	PS			
1	5/2/68	SEE DCN 972-10	JTG	PS	PS		WRS	T.JM
NO.	DATE	REVISIONS	DWN	DRD	HD.		O/A	PROJ
APPROVAL	DATE	 <b>TRANSNUCLEAR INC.</b> HAWTHORNE, N.Y.						
PROJ.	T.JM	MAY 68	<b>TN-68 PACKAGING</b> <b>LID ASSEMBLY &amp; DETAILS</b>					
O/A	WRS	MAY 68						
MECH. DES.	PS	MAY 68						
CHKD. BY	PS	MAY 68	NONE SCALE   B SIZE   972-71-4 DWG. NO.   2 REV.					
DWN. BY	JTG	MAY 68						



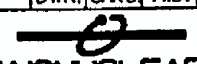
**FIGURE WITHHELD AS SENSITIVE UNCLASSIFIED  
INFORMATION**

I	2/2/99	SEE DCN 972-III	Q/A	PS	PS	WRS	2/2/99	
NO.	DATE	REVISIONS	DWN.	CHK'D	M.D.	N/T	O/A	PROJ.
APPROVALS	DATE	 <b>TRANSNUCLEAR, INC.</b> <small>HAWTHORNE, N.Y.</small> <b>TN-68 PACKAGING BASKET</b> <b>TYPICAL CROSS SECTION</b>						
T.J.N.	19 MAY 99							
PROJ.								
W.R.S.	19 MAY 99							
O/A								
P.S.	19 MAY 99							
MECH. DES.								
P.S.	19 MAY 99							
CHK'D. BY								SAR
J.T.G.	18 MAY 99	NONE	B	972-71-6	I			
DWN. BY		SCALE	SIZE	DWG. NO.	REV.			

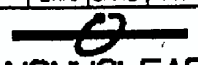
**FIGURE WITHHELD AS SENSITIVE UNCLASSIFIED  
INFORMATION**

2	4/1/99	SEE DCN 972-127	JTG	MC	PS		SDZ	JIN
1	2/28/00	SEE DCN 972-12	JTG	PS	PS		WRS	T.JN
NO.	DATE	REVISIONS	DWN.	CHKD.	FLD.		O/A	PROJ.
APPROVALS	DATE	 <b>TRANSNUCLEAR, INC.</b> <small>SAFETY-CORE, INC.</small> <b>TN-68 PACKAGING DETAILS</b> <div style="float: right; border: 1px solid black; padding: 2px;">SAR</div>						
PROJ.	T.JN							
O/A	WRS							
MECH. DES.	PS							
CHK'D. BY	PS							
DWN. BY.	JTG	NONE	B	972-71-7	2			
		SCALE	SIZE	DWG. NO.	REV.			

**FIGURE WITHHELD AS SENSITIVE UNCLASSIFIED  
INFORMATION**

1	PS	SEE DCN 972-113	PS	PS	WRS		
NO.	DATE	REVISIONS	DWN.	CHKD.	M.D.	O/A	PRJ.
APPROVALS	DATE	<p align="center">   <b>TRANSNUCLEAR, INC.</b>  <small>HARTSDALE, N.Y.</small>  <b>TN-68 PACKAGING</b>  <b>CASK ON TRANSPORT FRAME</b>  <span style="float: right;">SAR</span> </p>					
PROJ.	T.J.N.						19 MAY 98
O/A	W.R.S.						19 MAY 98
MECH. DES.	P.S.						19 MAY 98
CHK'D. BY.	P.S.	19 MAY 98	NONE	B	972-71-8	1	
DWN. BY.	J.T.G.	18 MAY 99	SCALE	SIZE	DWG. NO.	REV.	

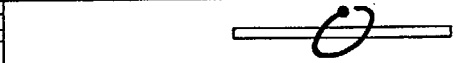
**FIGURE WITHHELD AS SENSITIVE UNCLASSIFIED  
INFORMATION**

1		4/20/99	SEE DCN 972-14	972	PS	PS	WRS/TJN			
NO.	DATE	REVISIONS		DWN	D-KD	M.D.	Q/A	PROJ.		
APPROVALS	DATE	 <b>TRANSNUCLEAR, INC.</b> <small>HAWTHORNE, N.Y.</small>  <b>TN-68 PACKAGING</b> <b>TRANSPORT IMPACT LIMITER</b> <b>ASSEMBLY</b>								
PROJ.	T.J.N.							19	MAY	99
Q/A	W.R.S.							19	MAY	99
MECH. DES.	P.S.							19	MAY	99
D-KD. BY	P.S.							19	MAY	99
DWN. BY	J.T.G.	18	MAY	99	NONE	B	972-71-9	I		
		SCALE	SIZE	ENG. NO.	REV.					

ASME Code Exceptions

The cask containment boundary is designed, fabricated and inspected in accordance with the ASME Code Subsections NB/WB to the maximum practical extent. The basket is designed, fabricated and inspected in accordance with ASME Code Subsection NG to the maximum practical extent. The gamma shielding, which is primarily for shielding, but also provides structural support to the containment boundary during accident events, was designed in accordance with Subsection NF of the code. Inspections of the gamma shielding are performed in accordance with ASME code Subsection NF. Other cask components, such as outer shell and neutron shielding are not governed by the ASME Code.

Component	Reference ASME Code/Section	Code Requirement	Exception, Justification & Compensatory Measures
TN-68 Cask	NB-1100/ Subsection NCA NB-2000 or WB-1100/ WB-2000	Stamping and preparation of reports by the Certificate Holder, Surveillances, Use of ASME Certificate Holders	The TN-68 cask is not N/TP stamped, nor is there a code design specification or stress report generated. A design criteria document is generated in accordance with TN's QA Program and the design and analysis is performed under TN's QA Program and presented in the SAR. The cask may also be fabricated by other than N-stamp holders and materials may be supplied by other than ASME Certificate holders. Surveillances are performed by TN and utility personnel rather than by an Authorized Nuclear Inspector (ANI)
TN-68 Cask	NCA-3800	QA Requirements	The quality assurance requirements of 10 CFR 71 are imposed in lieu of NCA-3800 requirements.
Containment Vessel	NB-6200/WB-6200	Hydrostatic Testing	The containment vessel is hydrostatically tested in accordance with the requirements of the ASME B&PV Code, Section III, Articles NB-6200/WB-6200 with the exception that the containment vessel is installed in the gamma shield shell during testing. The containment vessel is supported by the gamma shield during all design and accident events.
Weld of bottom inner plate to the containment shell	NB-5231/WB-5231	Full penetration corner welded joints require the fusion zone and the parent metal beneath the attachment surface to be UT after welding.	The required UT inspection will be performed on a best efforts basis. The joint will be examined by RT and either PT or MT methods in accordance with ASME Subsection NB/WB requirements. The joint may be welded after the containment shell is shrink fitted into the gamma shield shell. The geometry of the joint does not allow for UT inspection.
Containment Shell Rolling Qualification	NB-4213/WB-4213	The rolling process used to form the inner vessel should be qualified to determine that the required impact properties of NB-2300/WB-4213 are met after straining by taking test specimens from three different heats.	If the plates are made from less than three heats, each heat will be tested to verify the impact properties.
Containment Vessel	NB-7000	Vessels are required to have overpressure protection	No overpressure protection is provided. Function of containment vessel is to contain radioactive contents under normal and accident conditions of transport. Confinement vessel is designed to withstand maximum internal pressure considering 100% fuel rod failure and maximum accident temperatures.
Containment Vessel	NB-8000/WA-8000	Requirements for nameplates, stamping and reports per NCA-8000	TN-68 cask is to be marked and identified in accordance with 10 CFR71 requirements. Code stamping is not required. QA data package to be in accordance with Transnuclear approved QA program.
Containment Vessel	NB-1131/WB-1132	The design specification shall define the boundary of a component to which other component is attached.	A code design specification was not prepared for the TN-68 cask. A TN design criteria was prepared in accordance with TN's QA program.
Basket poison and aluminum plates	NG-2000	Use of ASME Materials	The poison material and the aluminum plates are not used for structural analysis, but to provide criticality control and heat transfer. They are not code materials.
Basket Rails	NG-2000	Use of ASME Materials	The basket rail material is not a Class I material. It was selected for its properties. Aluminum has excellent thermal conductivity and a high strength to weight ratio. NUREG-3854 and 1617 allow materials other than ASME Code materials to be used in the cask and basket fabrication. ASME Code does provide the material properties for the aluminum alloy up to 400°F and also allows the material to be used for Section III applications (Class 2 and 3). The construction of the aluminum rails will meet the requirements of Section III, Subsection NG.

NO.	DATE	REVISIONS	DWN.	CHK'D.	M.E.	Q/A	PROJ.
APPROVALS DATE		 <b>TRANSNUCLEAR, INC.</b> HAWTHORNE, N.Y.					
PROJ.	JIM	2/1/00					
Q/A	WRS	2/24/00					
MECH. ENG.	PS	2/24/00					
CHK'D. BY	PS	2/24/00					
DWN. BY	JTB	17 FEB. 00	NONE	B	972-71-14	0	
			SCALE	SIZE	DWG. NO.	REV.	

# TN 68 TRANSPORT PACKAGING

## APPENDIX 2.10.9

### TABLE OF CONTENTS

	<u>Page</u>
2.10.9	IMPACT LIMITER TESTING
2.10.9.1	Introduction..... 2.10.9-1
2.10.9.2	Scaling Relationships..... 2.10.9-3
2.10.9.3	Test Model Description..... 2.10.9-4
2.10.9.4	Test Description..... 2.10.9-6
2.10.9.5	Test Data and Results..... 2.10.9-8
2.10.9.6	Conclusions..... 2.10.9-17
2.10.9.7	References..... 2.10.9-18

### LIST OF TABLES

2.10.9-1.	Comparison of Calculated vs. Measured <i>G</i> Loadings
-----------	---

## LIST OF FIGURES

- 2.10.9-1 One-Third Scale Test Model
- 2.10.9-2 Accelerometer Locations
- 2.10.9-3 TN-68 Scale Model 15° Slap Down Drop Test Setup
- 2.10.9-4 TN-68 Scale Model 90° End Drop Test Setup
- 2.10.9-5 TN-68 Scale Model 0° Side Drop Test Setup
- 2.10.9-6 TN-68 Scale Model 90° Puncture Drop Test Setup
- 2.10.9-7 Impact Limiter Number 4 (Second Impact), Damaged During 15° Slap Down Drop
- 2.10.9-8 Impact Limiter Number 1 (1<sup>st</sup> Impact), Damaged During 15° Slap Down Drop
- 2.10.9-9 Test Model After 90° End Drop
- 2.10.9-10 Impact Limiter Number 2 After 90° End Drop
- 2.10.9-11 Test Model After 0° Side Drop
- 2.10.9-12 Impact Limiter Number 3 After 0° Side Drop
- 2.10.9-13 Test Model After 40 Inch Puncture Drop
- 2.10.9-14 Impact Limiter Number 2 After 40 Inch Puncture Drop
- 2.10.9-15 Unfiltered Acceleration Time History, 90° End Drop, Accelerometer 2
- 2.10.9-16 Acceleration Time History, with 600 Hz. Low-Pass Filter, 90° End Drop, Accelerometer 2
- 2.10.9-17 Unfiltered Acceleration Time History, 0° Side Drop, Accelerometer 1
- 2.10.9-18 Unfiltered Acceleration Time History, 0° Side Drop, Accelerometer 2

## APPENDIX 2.10.9

### IMPACT LIMITER TESTING

#### 2.10.9.1 Introduction

A series of dynamic tests have been performed on one-third scale models of the TN-68 impact limiters. The tests were performed to evaluate the effect of the 30 foot free drop hypothetical accident defined in 10 CFR 71.73(c)(1)<sup>(1)</sup>. The test results will be used to verify the analyses performed for the TN-68 cask and basket. The objectives of the TN-68 impact limiter test program are to:

- Demonstrate that the inertia  $g$  values and forces calculated in Appendix 2.10.8 and used in the analyses presented in Appendices 2.10.1 and 2.10.2 are conservative.
- Demonstrate that the extent of crush depths are acceptable, i.e., limiters do not bottom out and trunnions would not impact target.
- Demonstrate the adequacy of the impact limiter enclosure.
- Demonstrate adequacy of attachment design.
- Evaluate the effects of low temperature (-20° F) on the crush strength and dynamic performance of the impact limiters.
- Evaluate the effects (puncture depth and shell damage) of a 40 inch drop onto a six inch diameter puncture bar on a previously crushed impact limiter, as per 10 CFR 71.73(3).

The four 1/3 scale impact limiters that were constructed are identified as 1, 2, 3, and 4. The various drop test orientations were performed in the following sequence.

Test Number	Drop Orientation	Drop Height	Impact Limiter Number	Location of Impact Limiter	Comments
1	15° Slap Down	30 feet	1	Top (1 <sup>st</sup> Impact)	
			4	Bottom (2 <sup>nd</sup> Impact)	
2	90° End Drop	30 feet	1	Top	Bottom impact limiter (2) chilled to -20° F
			2	Bottom (Impact End)	
3	0° Side Drop	30 feet	1	Top	
			3	Bottom	
4	90° End Drop	40 inches	2	Top (Puncture End)	Drop onto 6 inch diameter puncture bar.
			3	Bottom	

The 15° slap down drop was chosen to be performed because the 15° orientation puts the highest load on the tie rods and attachment bolts. Also, second impact will absorb approximately 60% to 65% of the entire energy, it will provide a reasonable estimate of the likelihood of the trunnions impacting the target.

The 90° end drop orientation was chosen to be performed because the 90° orientation was expected to cause the highest axial deceleration. For the 90° end drop, the bottom impact limiter was chilled to -20° F in order to acquire the most conservative estimate of the highest axial g load.

The 0° side drop was performed because this orientation generates the highest transverse acceleration as well as significant deformation. The 0° side drop will also provide a reasonable estimate of the likelihood of the trunnions impacting the target.

A 40 inch drop onto a 6 inch diameter puncture bar was performed in accordance with 10 CFR 71.73(3) in order to evaluate the effects of this drop on the TN-68 transport package. The test model was dropped in the 90° end drop orientation and the puncture bar was centered over test model's center of gravity. This orientation was chosen because it assures that the puncture impact absorbs 100% of the drop energy. Also the center of the impact limiter outer plate, where the puncture impact occurred, is the weakest portion of the impact limiter since there are no gussets in this location.

### 2.10.9.2 Scaling Relationships

The TN-68 and impact limiter models are constructed with a geometric scale factor of  $1/\lambda = 1/3$ . Consequently, the following scale factors apply.

Length:

$$L_p = \lambda L_m$$

Surface area:

$$A_p = \lambda^2 A_m$$

Moment of inertia:

$$I_p = \lambda^4 I_m$$

Section modulus:

$$S_p = \lambda^3 S_m$$

Weight:

$$W_p = \lambda^3 W_m$$

Energy absorbed during drop (from same height  $h$ ):

$$E_p = W_p h = \lambda^3 W_m h = \lambda^3 E_m$$

Velocity at beginning of impact:

$$V_p = \sqrt{2gh} = V_m$$

where  $\lambda$  is the scale factor, the subscript  $p$  refers to the full size, and the subscript  $m$  refers to the model.

During impact, the impact limiter materials will deform or crush. Since the model and full size impact limiters are made of the same materials, they deform under the same stress,

$$S_p = S_m.$$

Therefore we have the following relationships.

Force during impact:

$$F_p = S_p A_p = S_m \lambda^2 A_m = \lambda^2 F_m$$

Deformation:

$$D_p = E_p / F_p = \lambda^3 E_m / \lambda^2 F_m = \lambda D_m$$

Impact duration:

$$T_p = D_p / V_p = \lambda D_m / V_m = \lambda T_m$$

Impact deceleration:

$$a_p = V_p / T_p = V_m / \lambda T_m = 1/\lambda a_m$$

### 2.10.9.3 Test Model Description

The test model for the dynamic tests consists of a solid carbon steel test body with an impact limiter on each end. The test model, shown in Figure 2.10.9-1, is constructed to be as close as possible to one-third of the full size packaging.

#### 2.10.9.3.1 Model Test Body

The model test body provides the proper one-third scale weight, CG location, and dimensions. The test body is 66.25 inches long with a gamma shield outside diameter of 28.17 inches, and an outer shell outside diameter of 32.67 inches. The reduced diameter portion, located in the axial center of the dummy is not important dimensionally, but is required to provide the proper overall weight and CG location. Important test model and full size packaging dimensions are provided below.

Test Model vs. Full Size Packaging

Component	Test Model (in)	Full Size Packaging (in)
Body Length (with spacer)	66.25	198.75
Length Including Impact Limiters	89.08	267.25
Gamma Shield Diameter	32.67	98.00
Outer Shell Diameter	28.17	84.50

The outer shell of the TN-68 package is simulated by welding a hollow ¼ inch carbon steel shell to the dummy body. The geometry of the outer shell model is shown in Figure 2.10.9-1. The outer shell model is broken up into two separate pieces because of the central reduced diameter section of the dummy body. Modeling the outer shell is important because it will reveal any influence the outer shell has on the performance of the bottom impact limiter, as well as

providing an accurate simulation of the structure that the impact limiter bolt brackets are attached to.

The attachment bolts, bolt brackets, tie rods, and tie rod brackets are made of the same material specified for the full size limiters, but their dimensions are scaled down by a factor of one-third.

### 2.10.9.3.2 Impact Limiters

The one-third scale model impact limiters are scale models of the full size limiters with some minor exceptions which are described below. The steel impact limiter structure is the same as that described in Appendix 2.10.8, steel shells closed off by flat plates and reinforced by sixteen (16) radial gussets. The model and full scale configurations are almost identical, except that all linear dimensions in the model are one-third of those in the full scale impact limiter.

The spaces within the steel shells and gussets are filled with wood blocks, which are formed by gluing together a number of smaller pieces of wood. The balsa and redwood used in the model are consistent with that specified for fabrication of the full scale impact limiters. The model contains the same number of wood blocks as the full size impact limiters. The wood blocks are made up of a number of smaller pieces of wood glued together with phenol resorcinol adhesive, using the same procedure to be used on the full size impact limiters.

The differences between the model and full size limiters are as follows:

- a) The nearest standard plate thicknesses corresponding to one-third scale were used. The following dimensions for the scale model impact limiter components do not exactly conform to one-third scaling:

Component	Full-size Thickness	One-third Scale	Model Thickness
Stainless Steel Shell	0.25 in.	0.083 in.	0.0897 (13 Gauge)
12 Radial Gussets	0.19 in.	0.063 in.	0.0598 (16 Gauge)

- b) The support angles used as legs to allow the limiters to stand upright for storage are not included on the models.
- c) The weld between the 12 radial gussets and the 12 outer flat plate segments were a 0.09 inch plug weld instead of a 0.09 inch fillet weld.
- d) The fusible plugs that provide pressure relief during a fire are excluded. Only two openings diametrically opposite from each other are included in the model. Steel plugs are used instead of fusible plugs for sealing these openings and for leak testing.
- e) The lifting lugs are made larger than one-third scale to facilitate lifting.

#### 2.10.9.4 Test Description

These tests were performed at National Technical Systems (NTS) drop pad facility, in Acton Massachusetts. The drop test was performed in accordance with approved written procedures. Much of the information presented here is taken from NTS documentation. Test data plots, e.g., acceleration versus time, are reproductions from NTS data sheets and were obtained from Reference 2.

The quick release mechanism used to drop the cask consisted of a hydraulic piston that applies a tensile force to a single bolt that supports the test model via a rigging system. The bolt has a reduced diameter section so that the hydraulic piston can fail the bolt in tension in a controlled manner, causing the test model to drop.

An inclinometer was placed on the test body to measure the initial angle ( $\pm 1^\circ$ ) of its longitudinal axis with respect to the drop pad (i.e., impact surface). A measured line, 30 feet long (+ 1.0, -0.0 inches), was attached to the lowest point on the test dummy in order to assure the proper drop height.

The impact surface was an essentially unyielding horizontal surface. The drop pad base consists of an unyielding concrete pad weighing more than 250,000 lb. and resting on bedrock. An A-36 hot rolled mild steel plate, two (2) inches thick, has been securely attached to the concrete pad.

Accelerometers were used to measure the inertial  $g$  load during impact for the three 30 foot drops performed. The accelerometers were mounted to aluminum brackets, which were bolted to the exterior of the test body at  $0^\circ$ ,  $90^\circ$ ,  $180^\circ$ , and  $270^\circ$  orientations at the approximate center of gravity location and adjacent to each impact limiter. The twelve (12) accelerometer locations are shown in Figure 2.10.9-2. Accelerometers were not mounted in locations that would result in certain destruction of the accelerometer or it's mounting block. However, at least eight (8) accelerometers were used during each 30 foot drop.

The test setup for the  $15^\circ$  slap down drop is shown in Figure 2.10.9-3. The accelerometers located at the center of gravity and near the top impact limiter (1<sup>st</sup> impact) were oriented to measure accelerations  $75^\circ$  from the axis of the test model (perpendicular to the drop pad surface when the test model is oriented at a  $15^\circ$  angle). The accelerometers near the bottom impact limiter (2<sup>nd</sup> impact) were oriented to measure accelerations perpendicular to the test model axis (perpendicular to the drop pad surface during slap down when the test modal axis is parallel to the drop pad surface).

The test setup for the end drop is shown in Figure 2.10.9-4. The package was oriented with the cask bottom facing down so that the impact occurred on the bottom end of the package. This was conservatively done because the increased surface area created by the outer shell may increase axial  $g$  loads. For the end drop test, the accelerometers were oriented to measure accelerations in the drop (axial) direction. The bottom impact limiter (impact limiter number 2) was kept in a conditioning chamber held at a temperature of  $-20^\circ$  F for six (6) days. The time between removal of the impact limiter from the conditioning chamber and the test article drop was roughly 3 hours.

The test setup for the 0° side drop is shown in Figure 2.10.9-5. For the side drop test, the accelerometers were oriented to measure accelerations in the drop direction (perpendicular to the drop pad surface).

The test setup for the 90° puncture drop is shown in Figure 2.10.9-6. During the puncture drop the package was oriented with the cask top facing down so that the puncture bar impacted on the top (lid) end of the package. A 6 inch diameter solid cylindrical puncture bar, 18 inches long was used. The puncture bar was constructed from mild steel and was welded to the drop pad with its long axis oriented in the vertical direction. The top of the bar was horizontal and its edge rounded to a radius of 0.25 inches. Accelerometer data was not taken during the puncture drop.

Data was collected by accelerometers capable of measuring data at a minimum frequency response of 6,000 Hz per channel. The lowest natural vibration frequencies of the test body, which are excited during the test, are much lower than this. These body vibrations involve small displacements (low stresses) at high frequencies, which excite the accelerometers and tend to mask the low frequency rigid body acceleration. This low frequency acceleration is masked, because both low frequency rigid body and high frequency natural vibration accelerations superimpose and the net acceleration is recorded. Filtering the data was used to remove these high frequency accelerations. A cutoff filter will be used to eliminate data above a specified cutoff frequency. The cutoff frequency used to filter the data was set at a value slightly below the significant natural frequency of the test body.

Acceleration data was recorded using a Data Physics data acquisition system. This unit is equipped with a PCB signal conditioner and data recording and reduction devices. A TEAC DAT recorder was used as a backup data storage device. The overall frequency response measured by the instrumentation system was 5,000 Hz. A computer was used to calibrate and control the data acquisition and recording equipment and to reduce the test data.

The following data was measured and recorded before, during, and after each drop test.

1. Prior to each drop test.
  - a. Torque of the impact limiter bolts.
  - b. Impact limiter dimensions.
  - c. Height from test article to drop pad.
  - d. Angular orientation of the test article to the impact surface.
  - e. Atmospheric condition data, *i.e.*, ambient temperature, wind speed, barometric pressure immediately and prior to the release of the test article.
  
2. During each drop test.
  - a. Test article behavior on videotape.
  - b. Date and time of test.
  - c. Observations of damage or unexpected behavior of the test article
  - d. Impact acceleration time histories and frequency responses (excluding the puncture drop test).

3. Following each drop test.
  - a. Observations of the damage to the test article on features other than the limiters, *i.e.*, tie rods, and attachment bolts.
  - b. Measurements of deformation to each impact limiter to fully describe the extent of the damage. These measurements include:
    - i. Depth of external crushing on the impact limiter.
    - ii. Overall thickness of each impact limiter after each test.
    - iii. Width of impact footprint.

#### 2.10.9.5 Test Data and Results

For purposes of reviewing test results, it should be noted that the energy to be absorbed by the scale model is approximately 1/27 of the full scale TN-68 value. The acceleration of the model is approximately three times that of the full size cask, and the crush deformation of the model limiter is approximately one-third that of the full size limiter. The impact force applied to the model is determined by multiplying the mass by the rigid body acceleration ( $F = ma$ ). The model force is 1/9 of the full scale force.

##### 2.10.9.5.1 15° Slap Down Test

The first drop test performed was the 15° slap down drop. Impact limiters 1 and 4 were placed on the top and bottom of the test model respectively. The cask was oriented such that the top (lid) end impacted the drop pad first. A four point chain rigging system was used to lift the test model by its four lifting lugs. The four legs of the rigging system join at a single point that was shackled to the quick release mechanism. Figure 2.10.9-3 depicts the test setup up for the 15° slap down test.

##### Accelerometer Data

Inspection of the accelerometer data revealed the accelerometers failed to record accurate data. The acceleration time history plots show a very short period (1 – 2 msec.) of what appears to be good data, after which an extreme instantaneous dc offset occurs in all accelerometer plots. In most channels the offset is several times the magnitude of the first bit of good data and in the opposite direction of the test model's acceleration.

Further analysis of the damaged test model and videotape showed that all accelerometer wires were either cut or severely crimped during the drop. The most probable cause of this damage was determined to be either the chain rigging system or a portion of the quick release mechanism impacting the accelerometer wires.

The two main purposes of the 15° slap down dynamic test are as follows:

- Demonstrate adequacy of the attachment design.
- Demonstrate that the limiters do not bottom out and the trunnions would not impact the target.

Despite the loss of the acceleration data, the 15° slap down test was successful in accomplishing the two main goals of the test program.

### Crush Depth Measurements

After the slap down test the impact limiters were removed from the test model body and their crush depths were measured. There was evidence of both inside and outside crushing. The following table summarizes the measured and predicted crush depths for the bottom impact limiter (slap down impact). A springback of 0.25 inches is assumed (based of previous crush tests).

	Second Impact (impact limiter number 4)
Maximum Inside Crush Depth (in.)	2.00
Maximum Outside Crush Depth (in.)	2.875
Spring Back	0.25
Total Maximum Crush Depth (in.)	5.125
Predicted Total Maximum Crush Depth $\times$ 1/3 (in.)	5.17 – 6.28

The highest accelerations generated during a slap down drop occur during the second impact. Even though the acceleration data was lost during the 15° drop, the predicted g loads are considered reasonable, since there is a direct relation between the impact limiter crush depth and package acceleration, and there is good agreement between the measured and predicted crush depths. Figures 2.10.9-7 and 2.10.9-8 are photographs of impact limiter numbers 4 and 1 respectively after the 15° slap down drop.

It should also be noted that the trunnions would not contact the target during the impact. The full scale distance between the end of the trunnion face and the outside diameter of the impact limiter is 21.3 inches. Therefore, a clearance of 5.925 in. (full scale,  $21.3 - 5.125 \times 3 = 5.925$ ) would remain between the crushed plane of the impact limiter (secondary impact) and the end of the trunnion face, based on the measured crush depth.

### Damage Assessment

Both impact limiters remained attached to the cask during and after the slap down impact. All tie rods and tie rod brackets also remained intact. The tie rod brackets in the region where crushing occurred were bent.

All attachment bolts and brackets remained intact. Two of the screws that hold one of the attachment bolts brackets on the lid (first impact) end failed in shear. The remaining two screws were slightly bent, but the attachment bolt and bracket remained intact and in the proper orientation. Please noted that these attachment bolts are designed for the end drop or closed to the end drop case where some of the impact limiter crushing occurs from the inside. This brings the impact limiters closer together, and can loosen some of the tierods. To prevent the top impact limiter from falling off the cask during secondary impact, eight 1½ – 8UN bolts (four per impact limiter) are employed. For all other drop orientations, the tie rods are designed to take all the drop loads.

Two welds in the stainless steel shell opened on Impact Limiter number 4 (second impact). The first weld was located between the outer cylindrical shell and the top flat plate of the impact limiter. The weld tear spanned a roughly 105° arc, and had a maximum opening between plates of roughly 2.5 inches. The second broken weld was located between the inside cylindrical shell and the circular flat plate that is flush with the bottom of the cask dummy. The second torn weld spanned a 105° arc, and had a maximum opening between plates of roughly 2.0 inches. All of the wood in the impact limiter remained confined inside the shell despite the welds.

One weld in the shell of Impact Limiter number 4 (first impact) opened. The torn weld was located between the inside cylindrical shell and the circular flat plate that is flush with the top of the cask dummy. The torn weld spanned a 60° arc, and had an opening too small for wood to be seen.

#### 2.10.9.5.2 90° End Drop Test

The second drop test performed was the 90° end drop. Impact limiters 1 and 2 were placed on the top and bottom of the test model respectively. The cask was oriented such that the bottom end impacted the drop pad. Since the chain rigging system was believed to be the cause of the damage to the accelerometer wires during the slap down drop, two straps were used instead of chains to suspend the test model. The straps were attached to the model body's top two lifting lugs and to the quick release mechanism with shackles. The shackles and the components of the quick release mechanism that fall with the test model were wrapped in foam to prevent them from impacting the model body, causing it to ring. Figure 2.10.9-4 depicts the test setup up for the 90° end drop test.

#### Accelerometer Data

The acceleration time history plots for the 90° end drop test appeared qualitatively reasonable. The plots generally show a single rounded peak 10 – 15 msec. long, with a high frequency low amplitude signal superimposed on top of it.

A Fast Fourier Transform (FFT) was performed in order to acquire a frequency response spectrum of the raw data. The frequency response plots show a large initial peak between 10 Hz. and 100 Hz., followed by a series of higher frequency harmonics. This initial peak, along with its higher frequency harmonics, represents the primary rigid body inertial acceleration of the test model.

Just below 1,000 Hz. and at roughly 2,000 Hz. there are other large peaks that do not coincide with the higher harmonics of the primary rigid body acceleration. These higher frequency peaks represent the natural frequency vibration (ringing) of the test model body. Each peak represents a different mode of vibration.

A 600 Hz. low-pass filter was used to filter the data above 600Hz. in order to eliminate the ringing effect of the test model body. The filtered time history plots show a smoother curve with a single peak. The height of this peak is taken to be the maximum inertial acceleration of the test model.

Both the filtered and unfiltered acceleration plots from accelerometers located on the outer shell near the bottom impact limiter displayed extreme ringing with a relatively low maximum amplitude. The ringing completely masked all rigid body acceleration, and was most likely caused by the hollow nature of the outer shell. The acceleration data from these accelerometers is excluded from the results that follow.

The following table shows the axial acceleration measured by five of the accelerometers, during the 90° end drop, as well as the range of axial acceleration predicted by ADOC.

Accelerometer Location (see figure 2.10.9-2)	Measure Axial Acceleration** (gs)	Predicted Axial Acceleration Range (gs)
1	79	50 – 66
2	82	
3	78	
4	70	
5	65	
Average	75	

\*\* Higher than predicted acceleration is attributed to the fact that the bottom impact limiter was chilled to -20° F prior to the drop test. The crush strength of balsa and redwood increases as temperature decreases.

The end drop acceleration data shows that chilling the impact limiter wood increases the wood crush strength by roughly 20%. An increase of 20% in the wood crush strength is acceptable for both axial and transverse accelerations, since the conservative *G* loads used to analyze the cask are more than 20% higher than the maximum crush strengths predicted by ADOC (see Table 2.10.9-1).

Figures 15 shows the acceleration time history measured by accelerometer 2, with a frequency response of 1,200 Hz. Figures 16 shows the same acceleration time history filtered at 600 Hz. These acceleration plots are characteristic of the end drop acceleration plots in general.

#### Crush Depth Measurements

Figure 2.10.9-9 is a photograph of the entire test model after the 90° end drop. After the end drop test the impact limiters were removed from the test model body and the crush depths of the bottom impact limiter were measured. There was evidence of both inside and outside crushing. The following table summarizes the measured and predicted crush depths for the bottom impact limiter (impact limiter 2). A springback of 0.25 inches is assumed.

	Bottom Impact Limiter (Impact Limiter Number 2)
Maximum Inside Crush Depth (in.)	1.24
Maximum Outside Crush Depth (in.)	0.75
Spring Back	0.25
Total Maximum Crush Depth (in.)	2.24
Predicted Total Maximum Crush Depth $\times$ 1/3 (in.)	2.32 – 2.95

The relatively low crush depth measured after the 90° end drop, compared with predicted values can be attributed to the fact that the bottom impact limiter was chilled to -20° F prior to the drop test.

#### Damage Assessment

Both impact limiters remained attached to the cask during the end drop impact. All tie rods and tie rod brackets also remained intact. Because of the crushing on the inside of the bottom impact limiter (on the body side of the impact limiter), the tie rods and attachment bolts were loosened by about 1.75 inches. However all tie rods and attachment bolts remained attached to the test model body.

All attachment bolts and brackets remained intact. All Four of the screws that hold one of the attachment bolt brackets on the bottom (impact) end failed in shear. Consequently, the bolt bracket became loose, even though the bolt remained threaded into the bottom impact limiter.

No welds in either impact limiter (1 or 2) were broken and no impact limiter wood was exposed during the end drop.

#### 2.10.9.5.2 0° Side Drop Test

The third drop test performed was the 0° side drop. Impact limiters 1 and 3 were placed on the top and bottom of the test model respectively. Four straps were used to support the test model. Again, the shackles and the components of the quick release mechanism that fall with the test model were wrapped in foam. Figure 2.10.9-5 depicts the test setup up for the 0° side drop test.

#### Accelerometer Data

The acceleration time history plots for the 0° side drop test qualitatively similar to those from the 90° end drop. The plots generally show a single rounded peak roughly 20 msec. long, with a high frequency low amplitude signal superimposed on top of it.

The following table shows the axial acceleration measured by six of the accelerometers during the 0° side drop, as well as the range of axial acceleration range predicted by ADOC.

Accelerometer Location (see figure 2.10.9-2)	Measured Transverse Acceleration (Gs)	Predicted Transverse Acceleration Range (Gs)
1	42	39 – 53
2	33	
3	30	
4	37	
7	30	
Average	35	

The accelerations measured during the side drop are at the low end of the range predicted by the ADOC computer program. The acceleration data presented in the above table is taken from unfiltered data having a frequency response of 1,200 Hz. Figures 17 and 18 show the unfiltered acceleration time histories from accelerometers 1 and 2 respectively, which are characteristic of the acceleration plots in general.

## Crush Depth Measurements

After the side drop test the impact limiters were removed from the test model body and the crush depths of both impact limiters were measured. Again, the impact limiters crushed from the inside and the outside. The following table summarizes the measured and predicted crush depths for both impact limiters.

	Impact Limiter Number 1 (Top)	Impact Limiter Number 3 (Bottom)
Maximum Inside Crush Depth (in.)	2.00	0.813
Maximum Outside Crush Depth (in.)	3.615	3.365
Spring Back	0.25	0.25
Total Maximum Crush Depth (in.)	5.865	4.428
Predicted Total Maximum Crush Depth $\times 1/3$ (in.)	4.51 – 5.27	

From the above table it can be seen that there is a relatively good correlation between the measured and predicted crush depths for the side drop event.

## Damage Assessment

Both impact limiters remained attached to the cask during the side drop impact. All tie rods and tie rod brackets also remained intact. Some of the tie rod brackets in the region where crushing occurred were bent.

All attachment bolts and brackets remained intact. Two of the screws that hold the one of the attachment bolt brackets on the bottom end failed in shear. The remaining two screws were slightly bent, but the attachment bolt and bracket remained intact and in the proper orientation.

Two welds in the stainless steel shell tore on Impact Limiter number 1 (top impact limiter). The first broken weld was located between the outer cylindrical shell and the top flat plate of the impact limiter. The weld tear spanned a roughly  $105^\circ$  arc, and had a maximum opening between plates of roughly 2.625 inches. The second torn weld was located between the inside cylindrical shell and the circular flat plate that is flush with the bottom of the cask dummy. The second torn weld spanned a  $120^\circ$  arc, and had a maximum opening between plates of roughly 2.0 inches. All of the wood in the impact limiter number 1 remained confined inside the shell despite the broken welds.

Two welds in the stainless steel shell tore on Impact Limiter number 3 (bottom impact limiter). The first torn weld was located between the outer cylindrical shell and the top flat plate of the impact limiter. The weld tear spanned a roughly 30° arc, and had a maximum opening between plates of roughly 1.563 inches. The second broken weld was located between the inside cylindrical shell and the circular flat plate that is flush with the bottom of the cask dummy. The second torn weld spanned a 90° arc, and had a maximum opening between plates of roughly 0.813 inches. All of the wood in the impact limiter number 3 remained confined inside the shell despite the broken welds.

#### 2.10.9.5.4 Puncture Drop Test

The final drop test performed was the puncture drop. Impact limiters 2 and 3 were placed on the top and bottom of the test model respectively. Two straps, attached to bottom two lifting lugs, were used to support the test model in the 90° vertical orientation with the test model's top end facing down. The puncture bar impacted impact limiter 2, which was previously crush during the 90° end drop. No accelerometer data was taken, since the purpose of the puncture drop is to obtain impact limiter deformation and damage only. Figure 2.10.9-6 depicts the test setup up for the 90° puncture drop test.

#### Crush Depth Measurements

The following table shows the measured crush depths for the 90° puncture drop. These deformations represent the crush depths beyond what was already crushed during the 90° end drop.

	Impact Limiter Number 2 (Top)
Maximum Inside Crush Depth (in.)	0.125
Depth of Puncture on Outside Surface (in.)	4.00

#### Damage Assessment

Both impact limiters remained attached to the cask during the puncture drop event. All tie rods and tie rod brackets also remained intact.

All attachment bolts and brackets remained intact. All Four of the screws that hold one of the attachment bolt brackets on the bottom (non puncture) end failed in shear. Consequently, the bolt bracket became loose, even though the bolt remained threaded into the bottom impact limiter.

The weld located between the 10 inch diameter circular flat plate and the central cylindrical gusset in impact limiter number 2 was torn all the way around (360°). This damage was caused by the inward punching force of the puncture bar during impact. All of the wood in the impact limiter remained confined inside the shell despite the broken weld.

#### 2.10.9.6 Conclusions

The predicted performance of the impact limiters in terms of accelerations and crush depths agrees very well with the measured data. Therefore, the g values and resulting forces used in the analyses in Appendices 2.10.1 and 2.10.2 are conservative.

The results of the dynamic tests demonstrate that:

- Table 2.10.9-1 summarizes the maximum inertial loads measured during the dynamic testing program, as well as the maximum inertial loads computed by ADOC and used in the TN-68 cask and basket analysis. Table 2.10.9-1 demonstrates that the inertial loads calculated in Appendix 2.10.8 are reasonable and that the inertial loads used in the analyses in Appendices 2.10.1 and 2.10.2 are conservative.
- The crush depths do not result in lockup of the wood in the limiters.
- The crush depths for the 0° side drop and 15° slap down cases would not result in the trunnions impacting the target.
- The predicted performance of the impact limiters in terms of decelerations and crush depths agrees well with the measured data.
- The impact limiter enclosure is structurally adequate in that it successfully confines the wood inside the steel shell.
- The impact limiter attachment design is structurally adequate in that the tie rods and attachment bolts hold the impact limiters on the ends of the cask during all drop orientations.
- The effects of low temperature (-20° F) on the crush strength of the impact limiters is minor, and is bounded by the conservative accelerations and forces used in the analysis in Appendices 2.10.1 and 2.10.2.
- A 40 inch drop onto a six inch diameter puncture bar, as per 10 CFR 71.73(3), does not significantly destroy the impact limiter. The impact limiter wood remains confined, and the maximum puncture depth represents only 1/3 the thickness of the impact limiter.

2.10.9.7 References

1. 10 CFR PART 71, Packaging and Transportation of Radioactive Material.
2. Dynamic Qualification Testing Report of the Transnuclear TN-68 1/3 Scale Model Impact Limiter.

TABLE 2.10.9-1

Comparison of Calculated vs. Measured *G* loadings

30 foot Drop Orientation	Maximum <i>G</i> Load, Measured by Drop Test (Appendix 2.10.9)	Maximum <i>G</i> Load, Computed by ADOC (Appendix 2.10.9)	Input Loading Used in FEA** (Appendix 2.10.1)
90° End Drop	75 G Axial	66 G Axial	80 G Axial
0° Side Drop	35 G Transverse	53 G Transverse	80 G Transverse

\*\* Conservatively Using Higher *G* loads

---

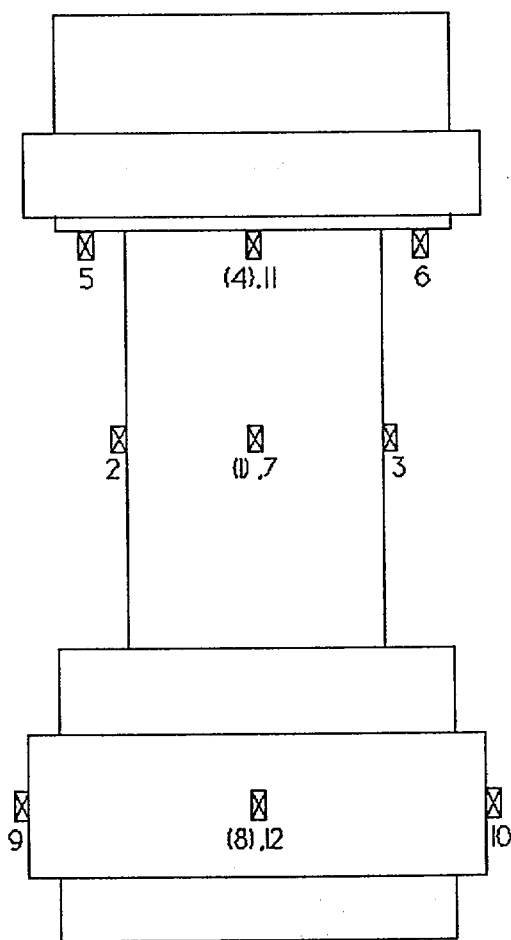
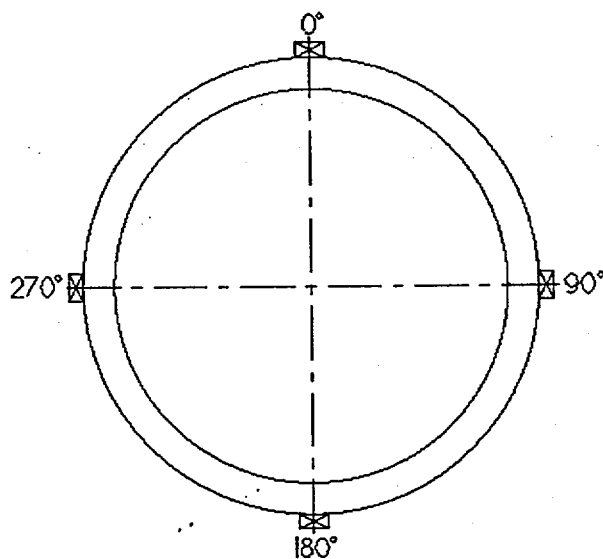
FIGURE 2.10.9-1  
One-Third Scale Test Model

---

**FIGURE WITHHELD UNDER 10 CFR 2.390**

FIGURE 2.10.9-2

Accelerometer Locations



☒ ACCELEROMETER

( ) DENOTES 0° SIDE

FIGURE 2.10.9-3

TN-68 Scale Model 15° Slap Down Drop Test Setup

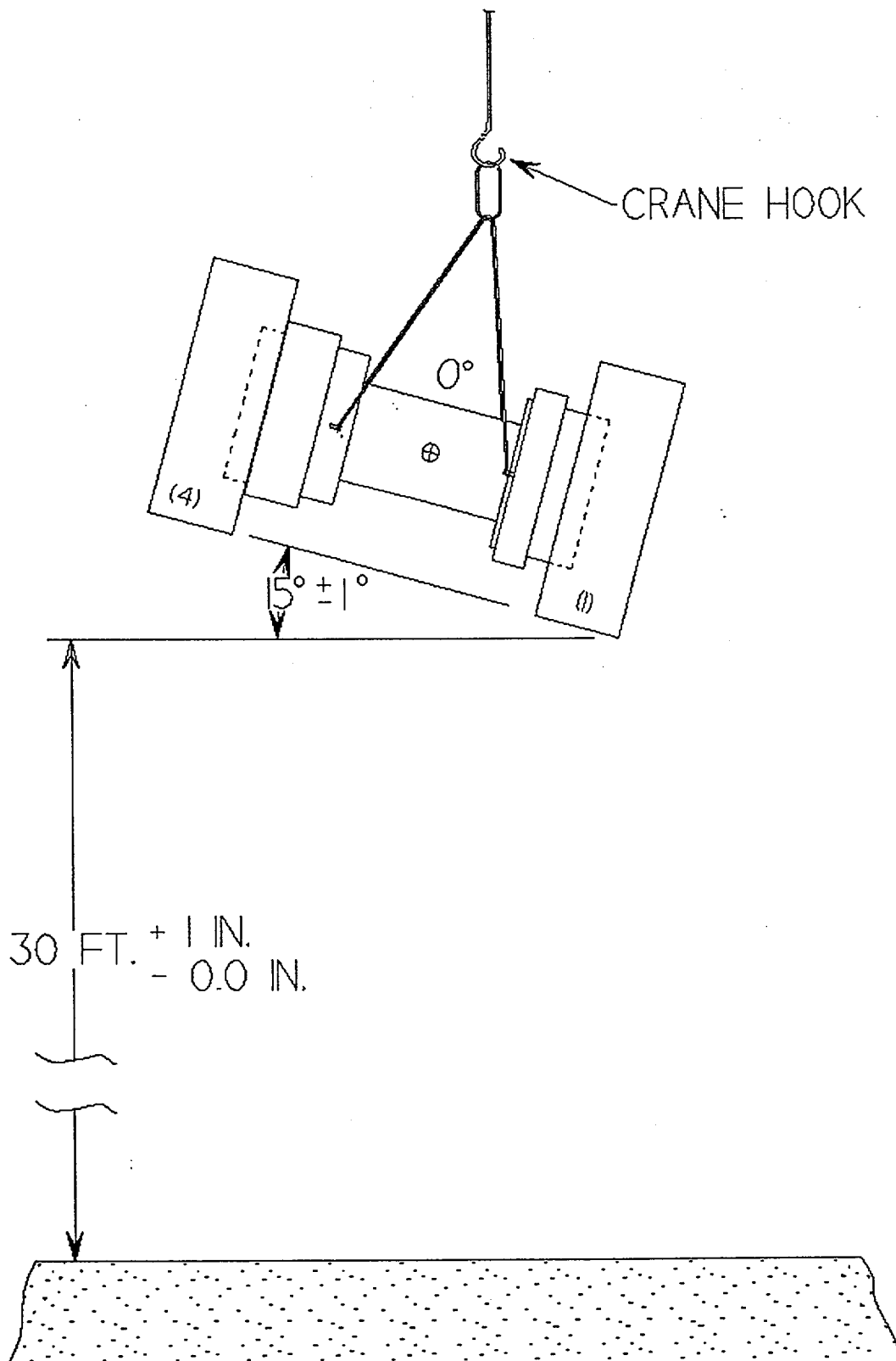


FIGURE 2.10.9-4

TN-68 Scale Model 90° End Drop Test Setup

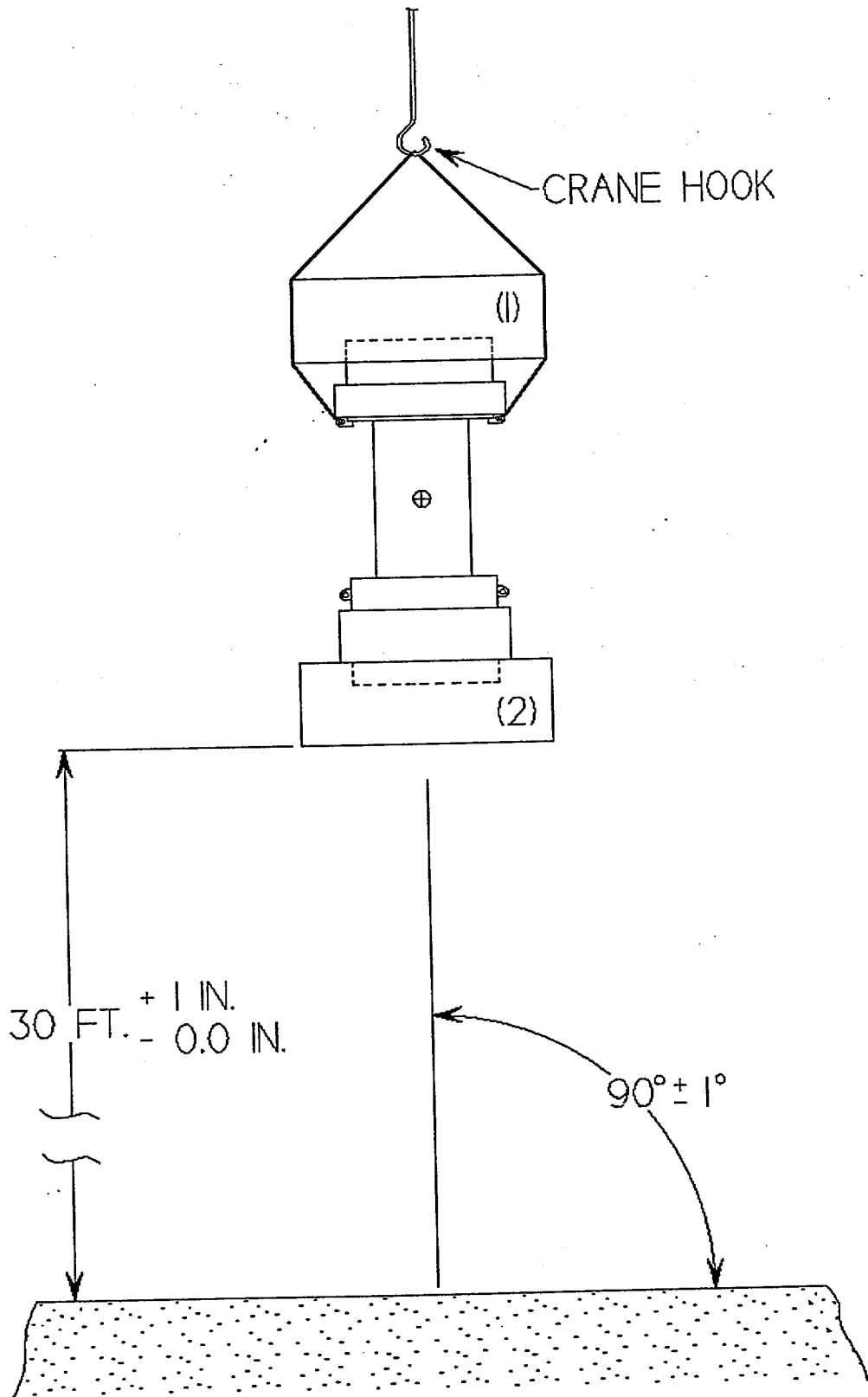


FIGURE 2.10.9-5

TN-68 Scale Model 0° Side Drop Test Setup

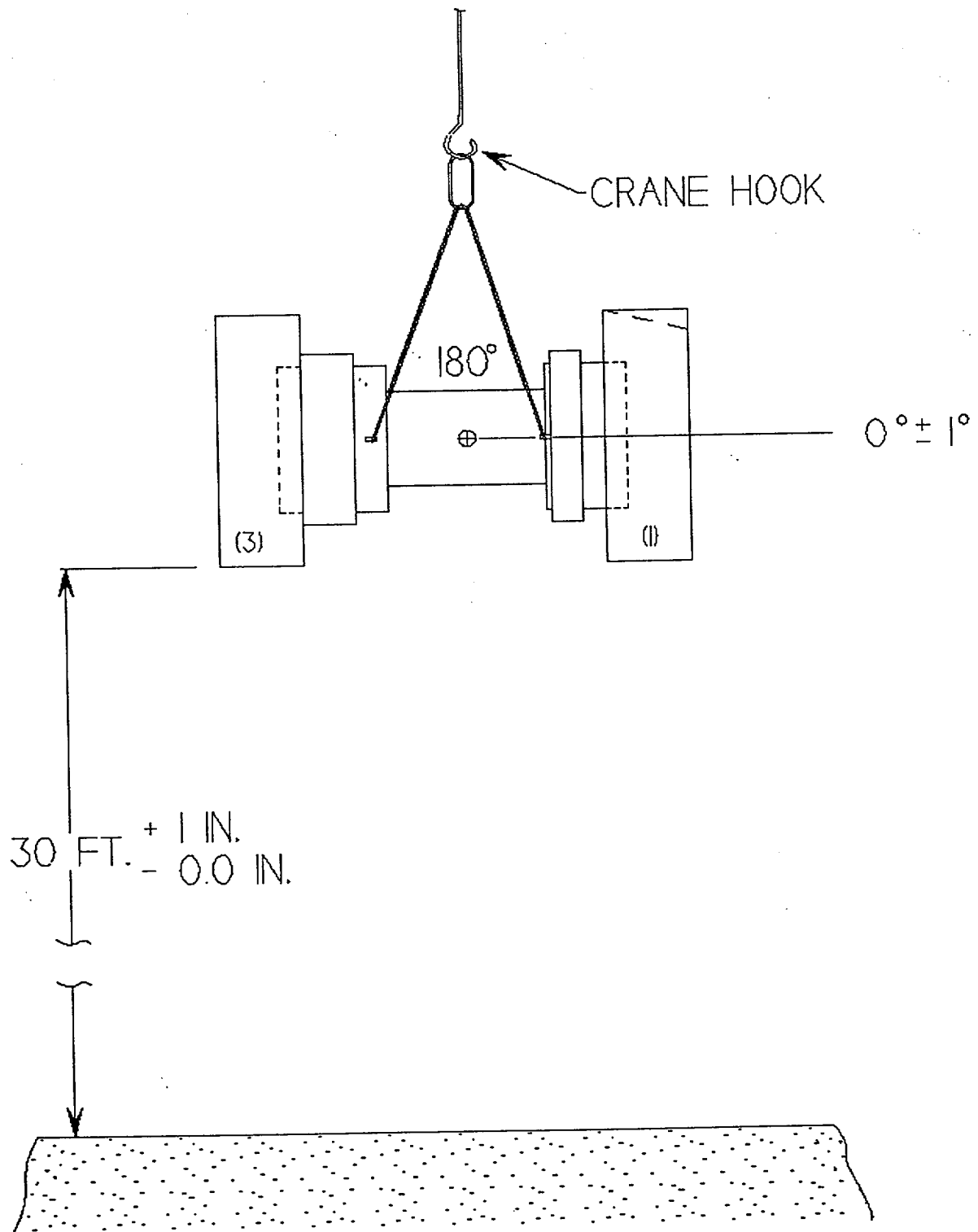


FIGURE 2.10.9-6

TN-68 Scale Model 90° Puncture Drop Test Setup

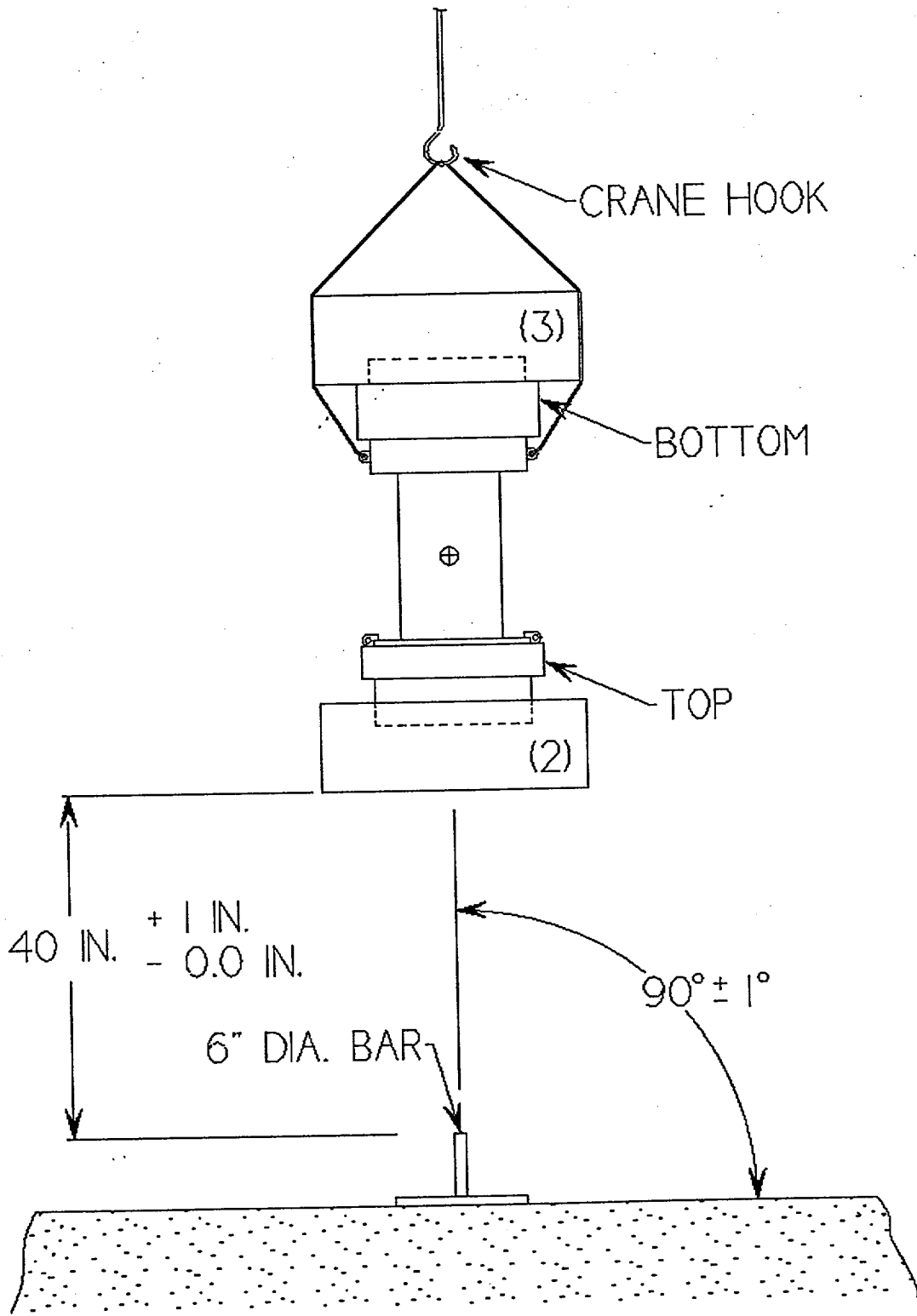


FIGURE 2.10.9-7

Impact Limiter Number 4 (Second Impact), Damaged During 15° Slap Down Drop

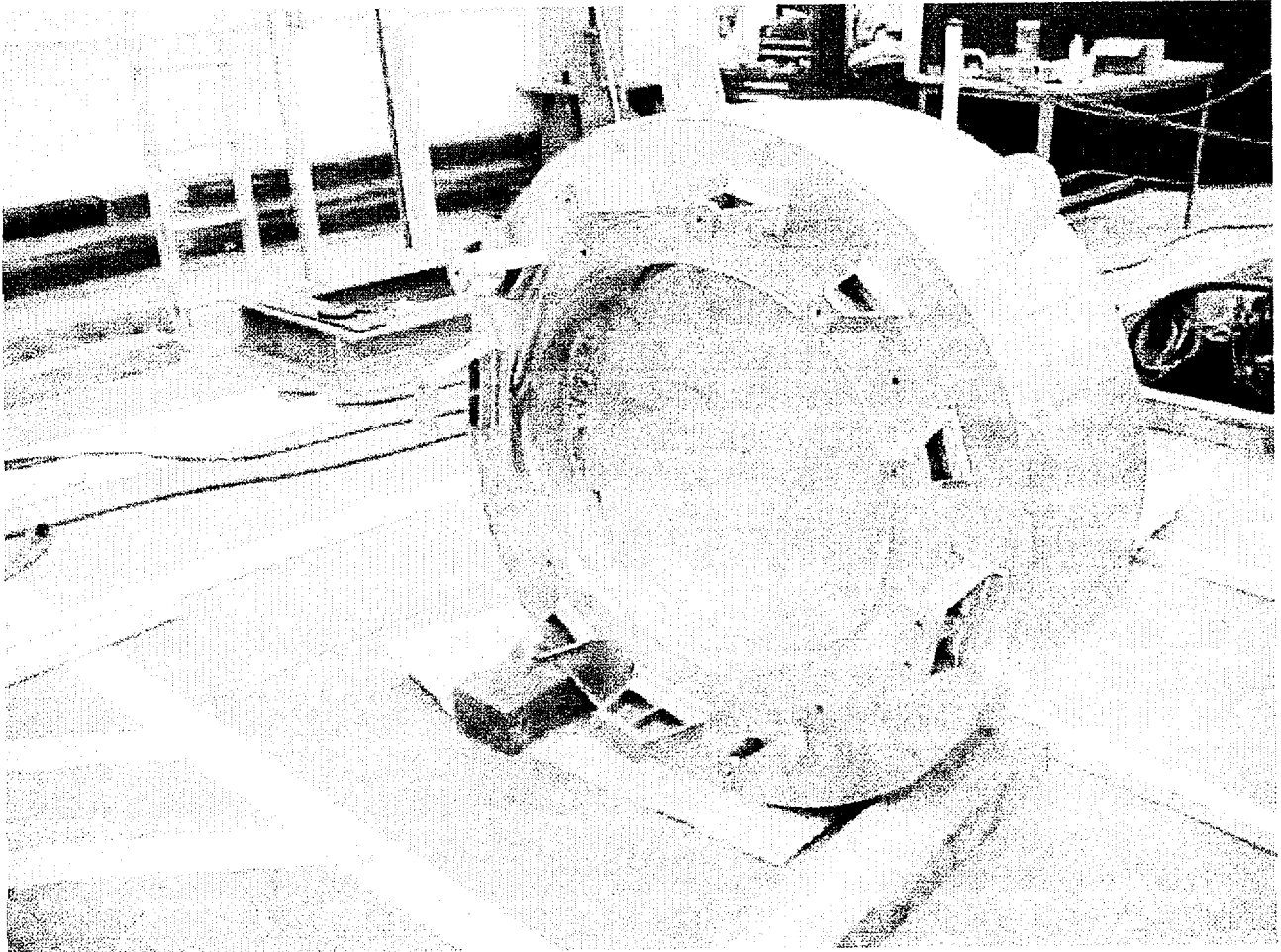


FIGURE 2.10.9-8

Impact Limiter Number 1 (1<sup>st</sup> Impact), Damaged During 15° Slap Down Drop

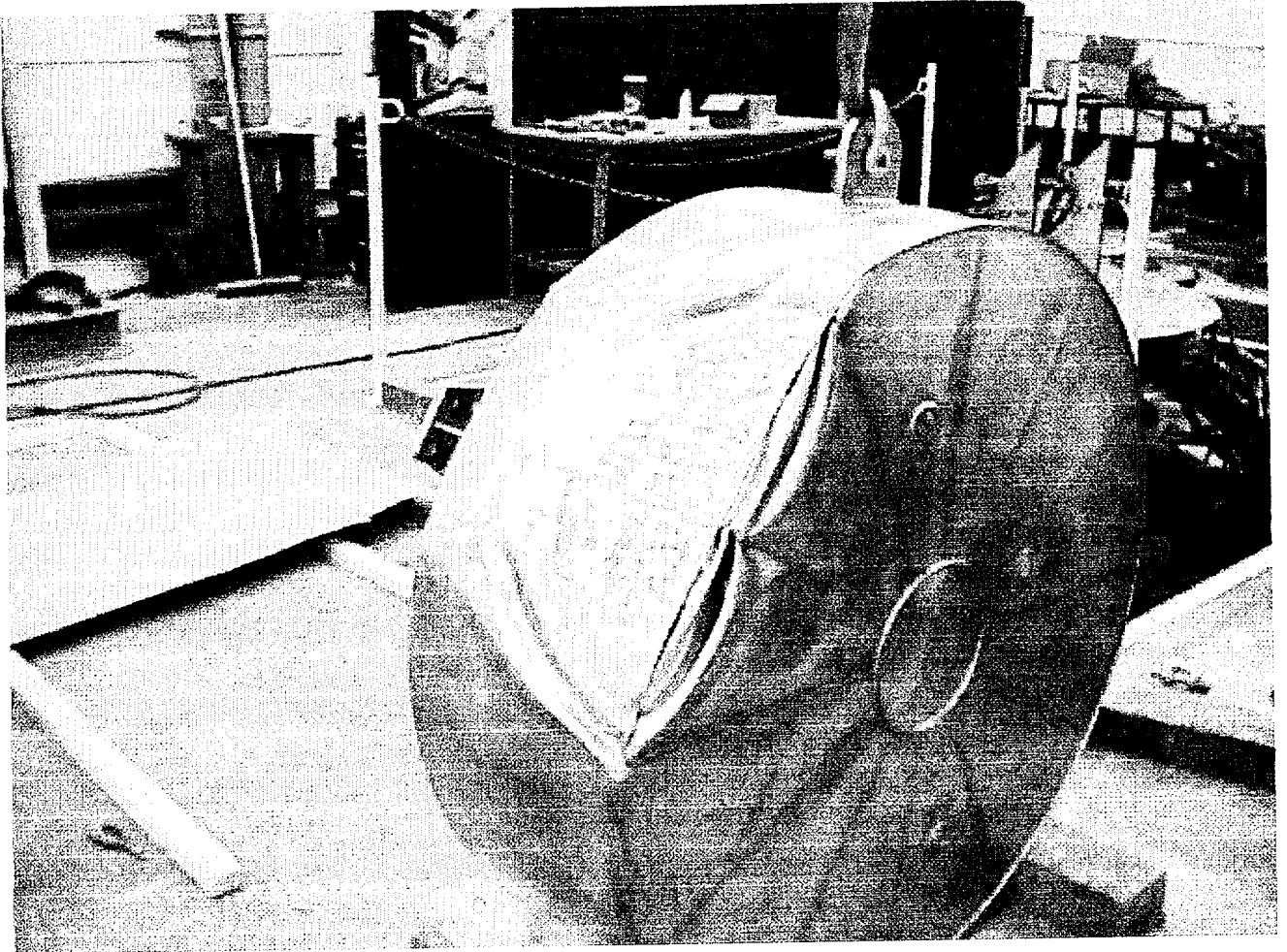


FIGURE 2.10.9-9

Test Model After 90° End Drop

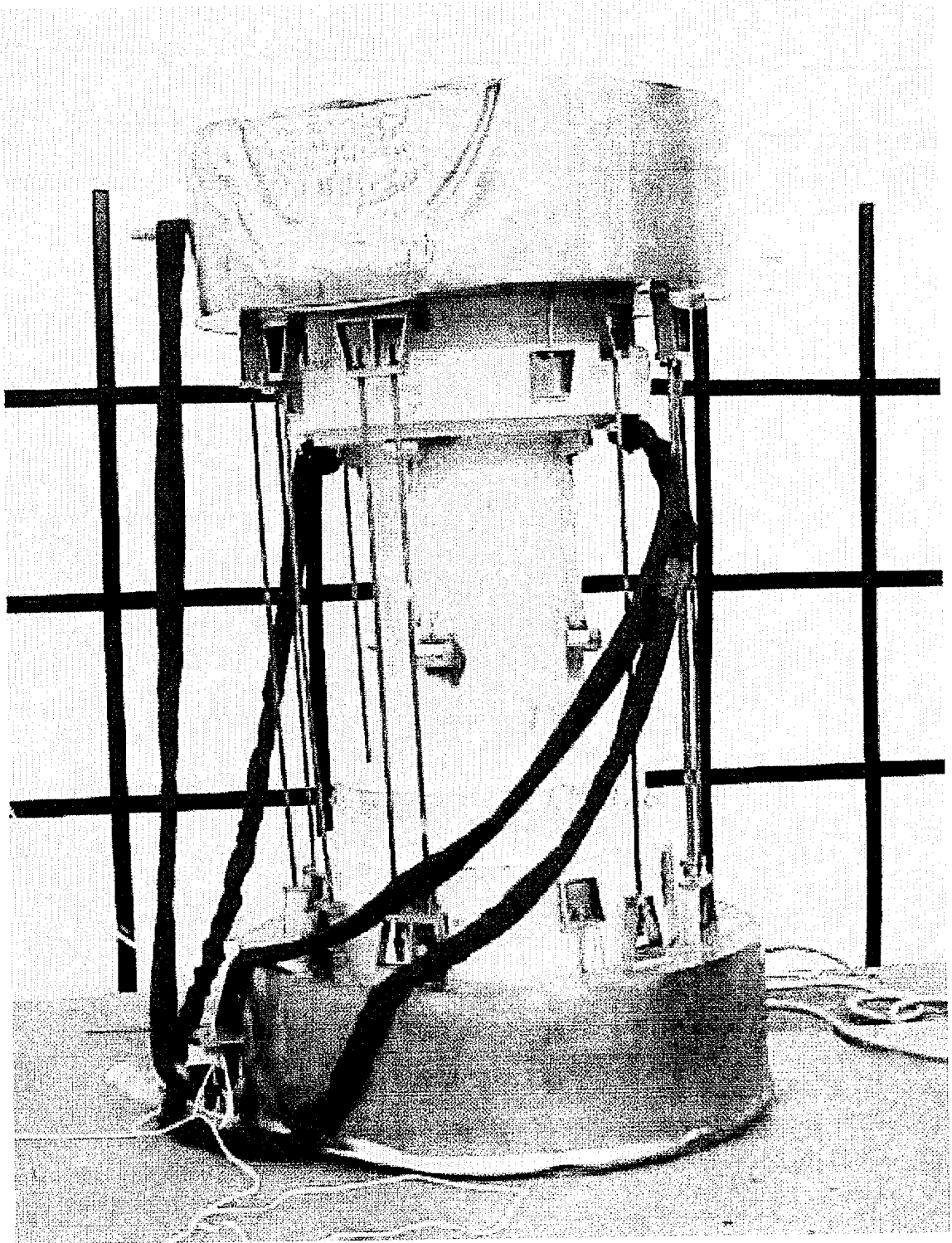


FIGURE 2.10.9-10

Impact Limiter Number 2 After 90° End Drop

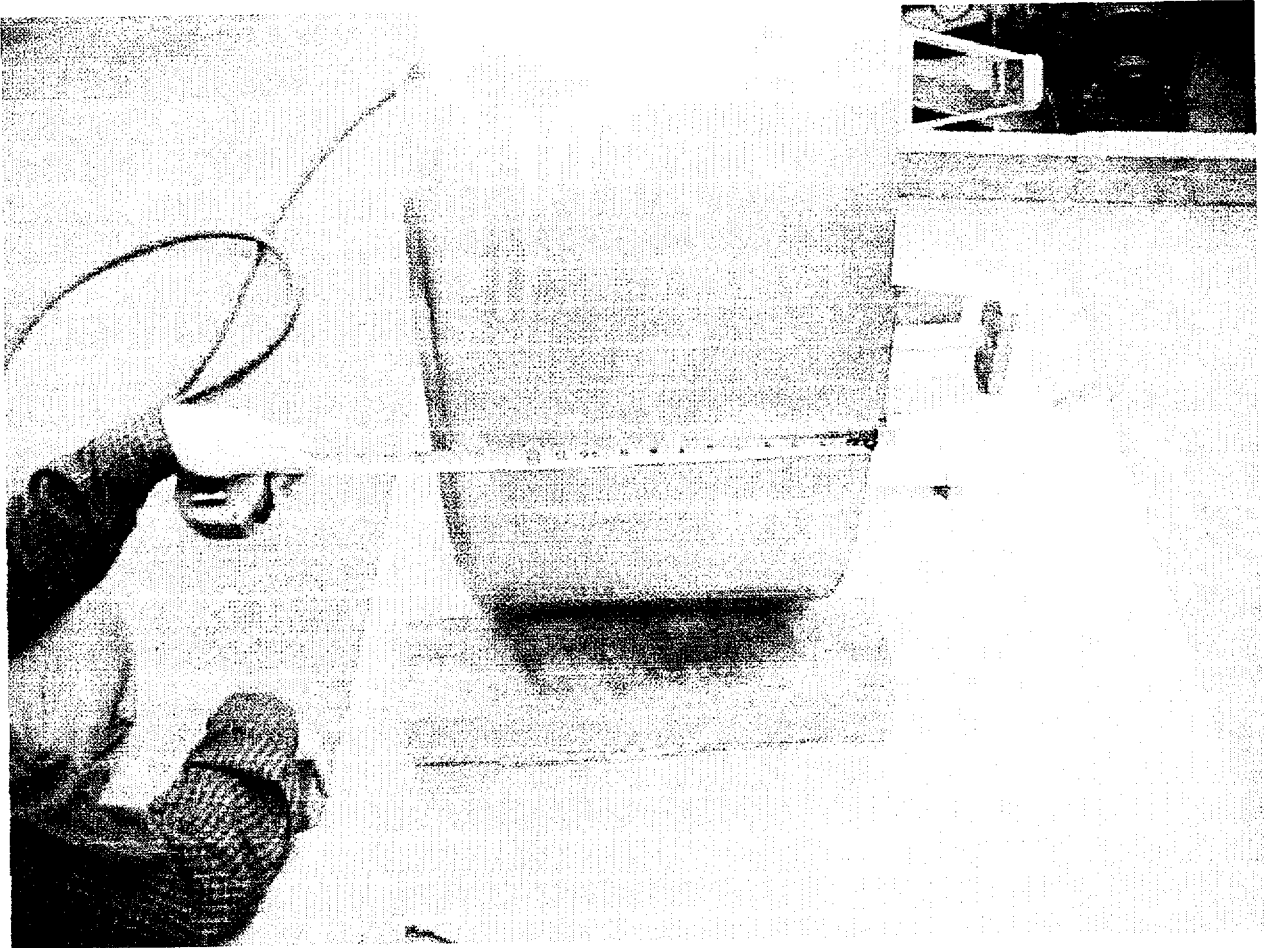


FIGURE 2.10.9-11

Test Model After 0° Side Drop

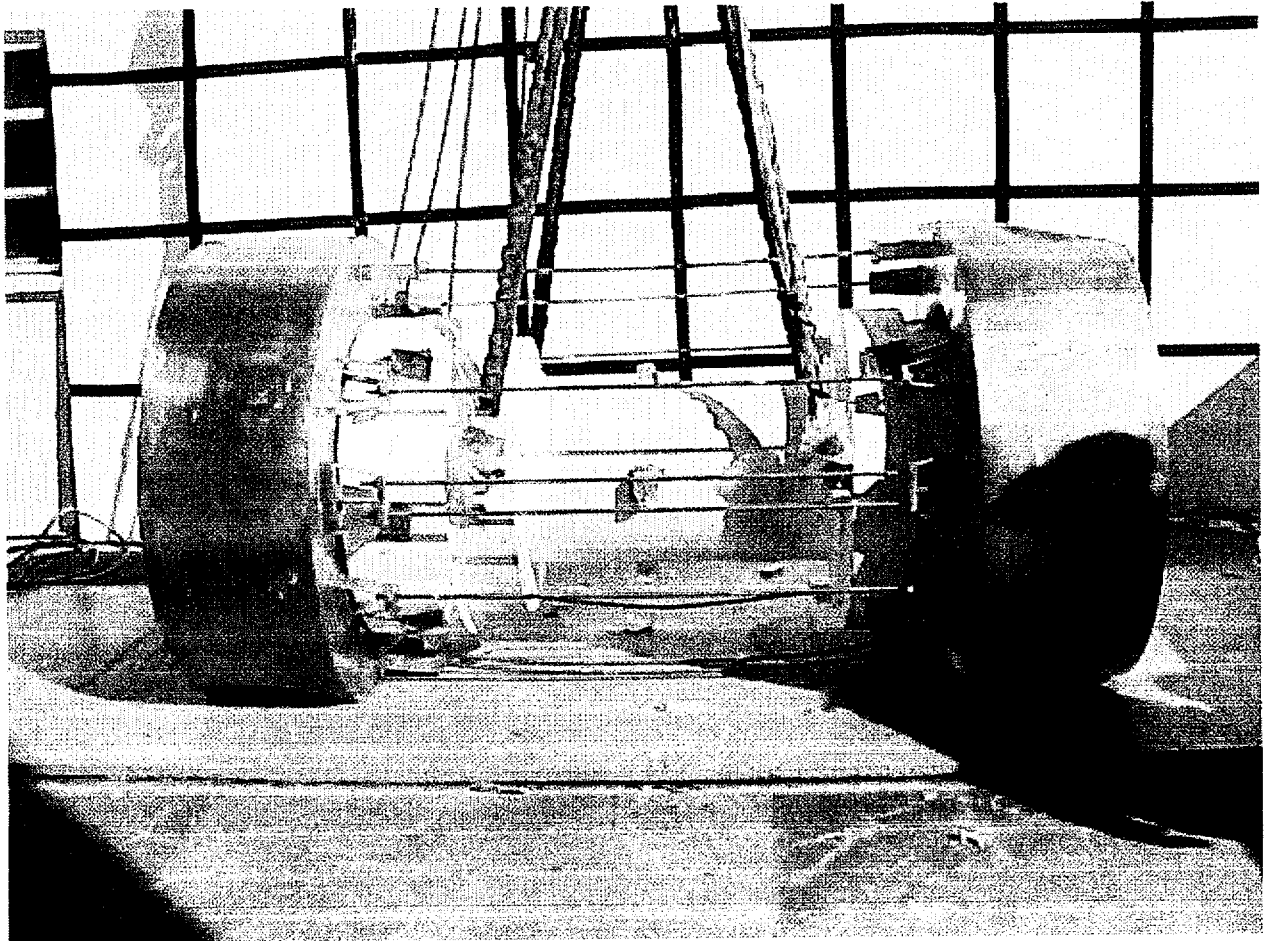


FIGURE 2.10.9-12

Impact Limiter Number 3 After 0° Side Drop

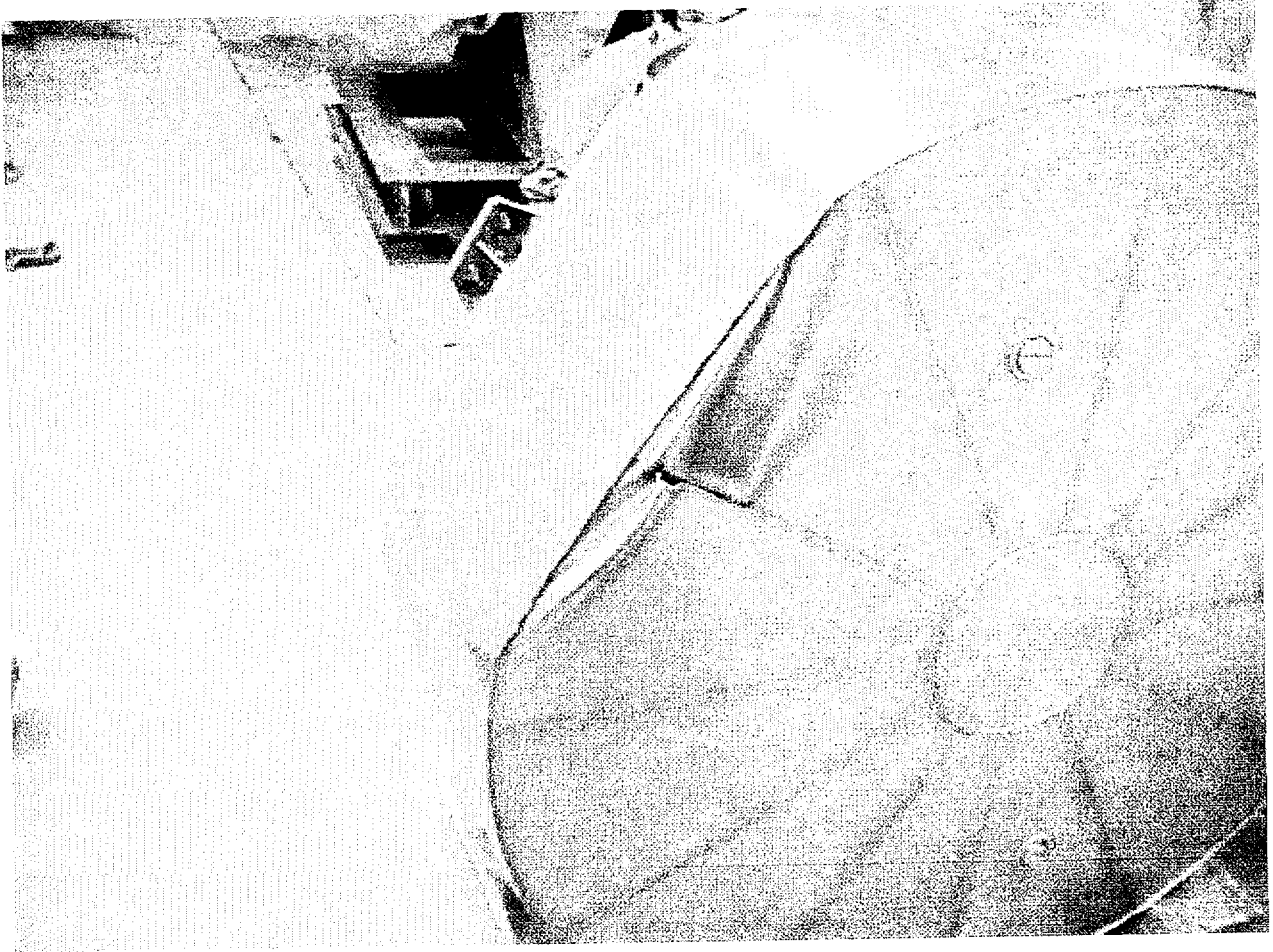


FIGURE 2.10.9-13

Test Model After 40 Inch Puncture Drop

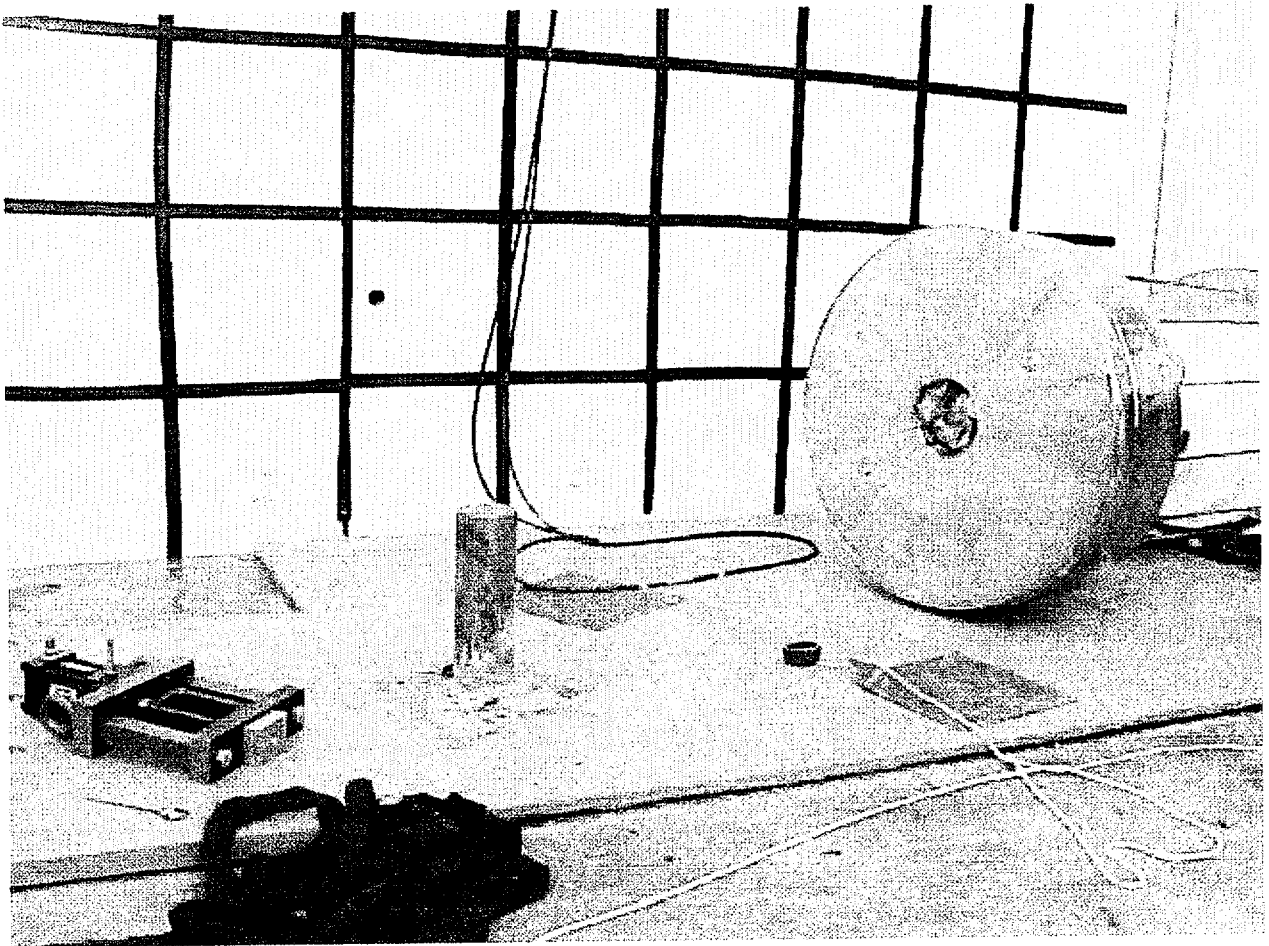


FIGURE 2.10.9-14

Impact Limiter Number 2 After 40 Inch Puncture Drop

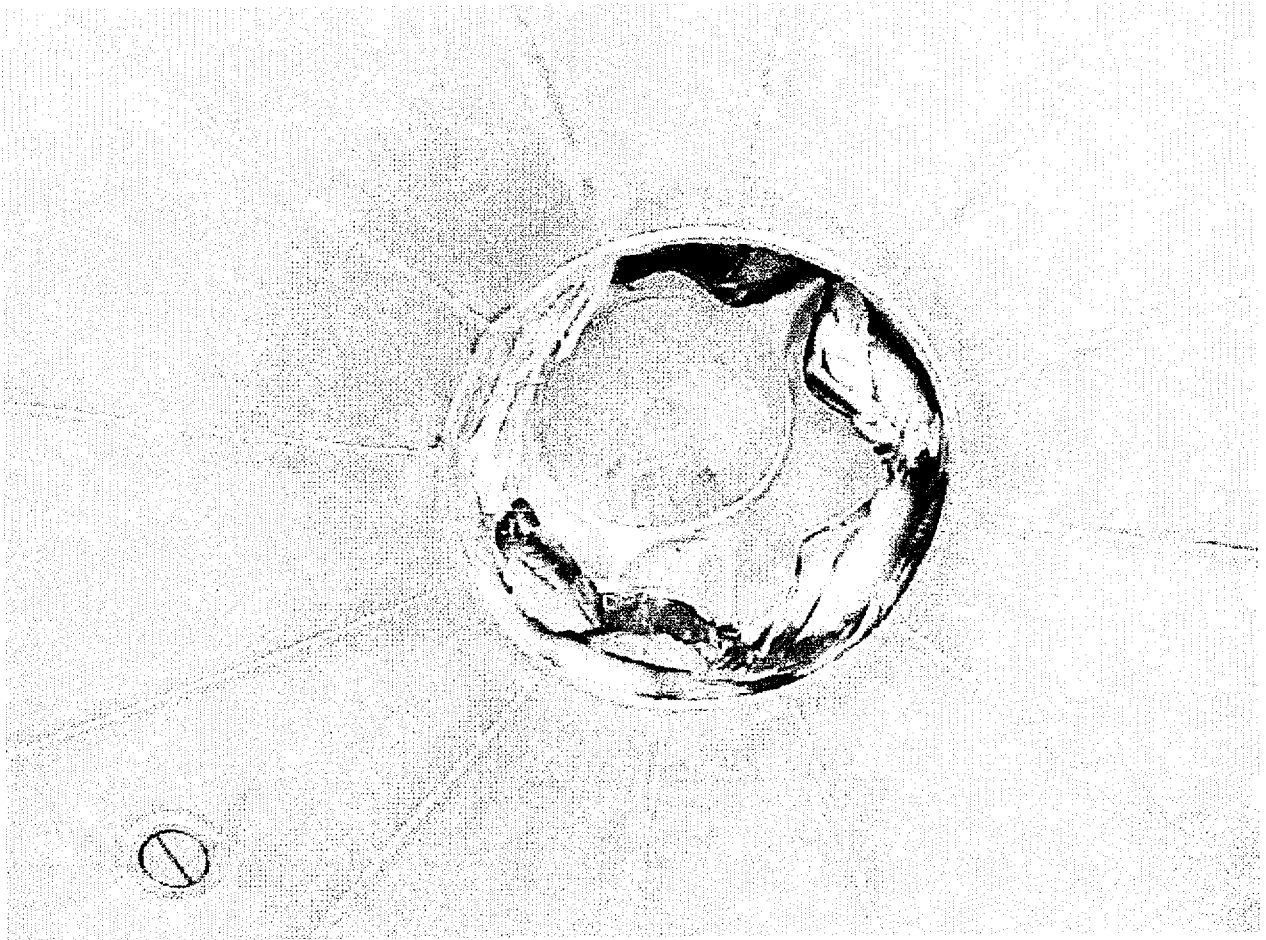


FIGURE 2.10.9-15

Unfiltered Acceleration Time History, 90° End Drop, Accelerometer 2

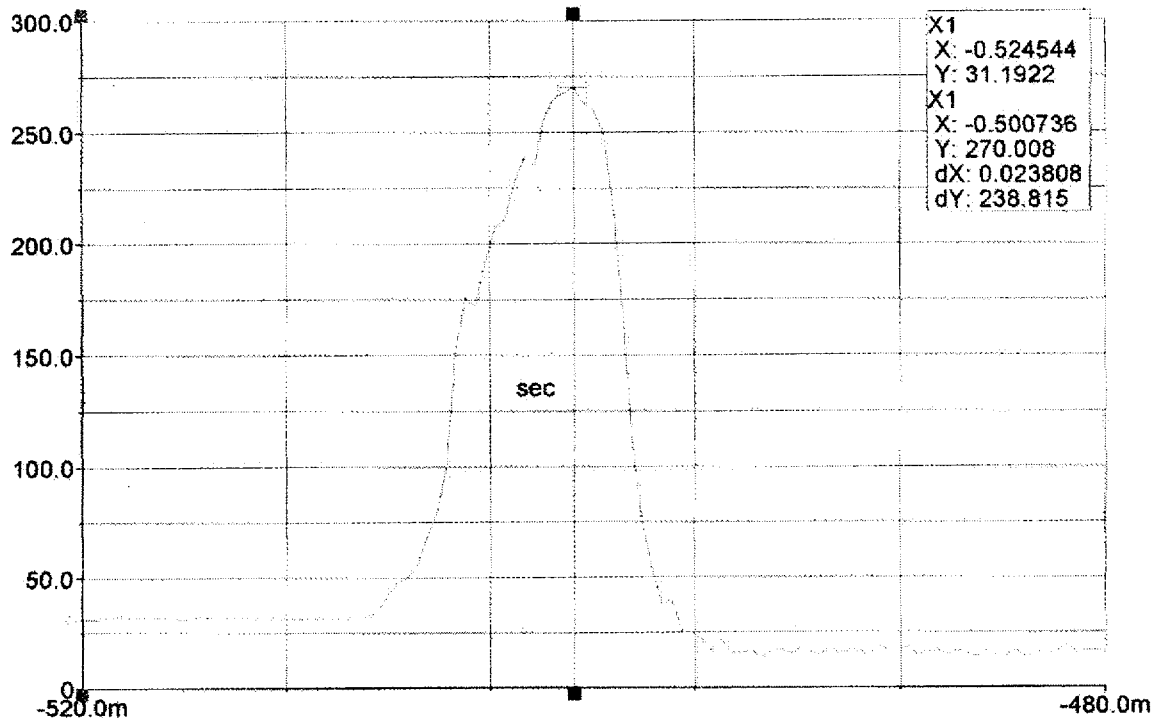


FIGURE 2.10.9-16

Acceleration Time History, with 600 Hz. Low-Pass Filter, 90° End Drop, Accelerometer 2

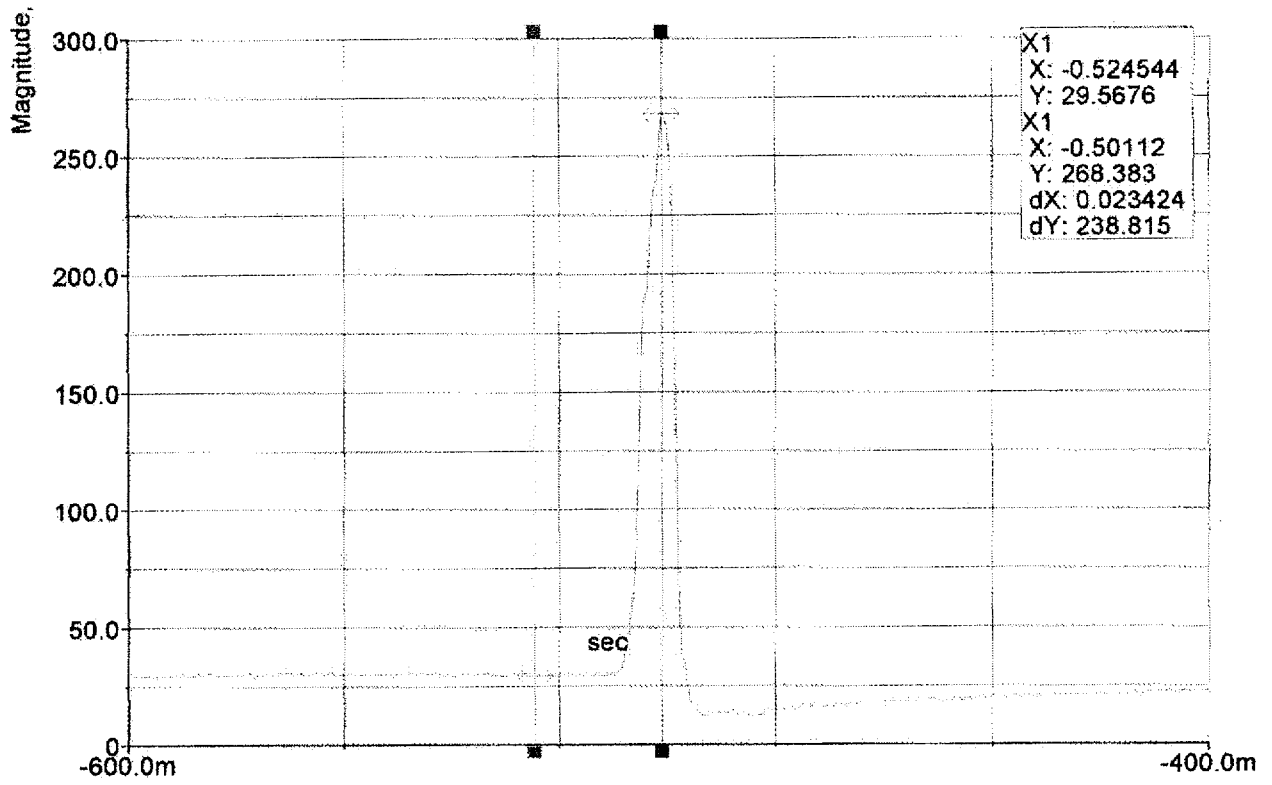


FIGURE 2.10.9-17

Unfiltered Acceleration Time History, 0° Side Drop, Accelerometer 1

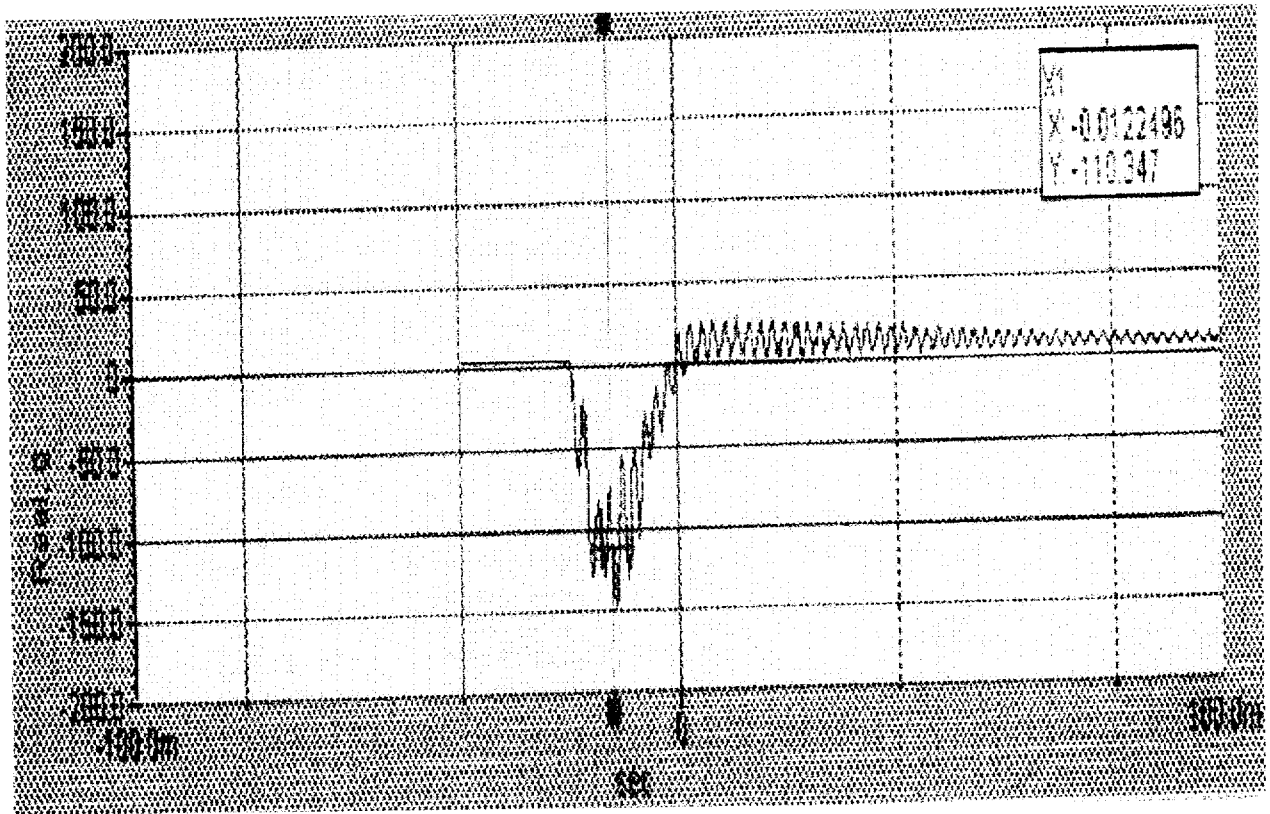
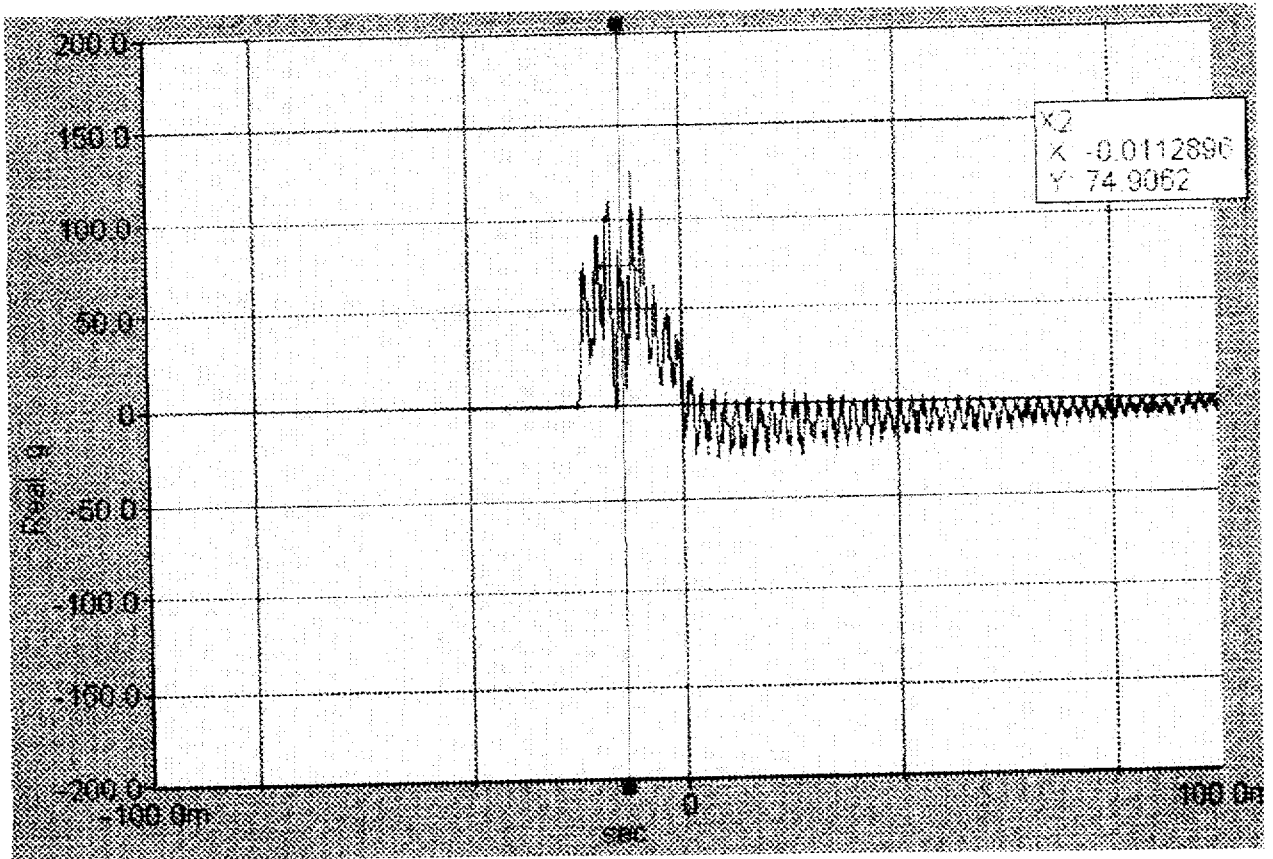


FIGURE 2.10.9-18

Unfiltered Acceleration Time History, 0° Side Drop, Accelerometer 2



# TN 68 TRANSPORT PACKAGING

## CHAPTER 4

### TABLE OF CONTENTS

	<u>Page</u>
4. CONTAINMENT	
4.1 Containment Boundary .....	4-1
4.1.1 Containment Vessel .....	4-1
4.1.2 Containment Penetrations .....	4-2
4.1.3 Seals and Welds .....	4-2
4.1.4 Closure .....	4-4
4.2 Requirements for Normal Conditions of Transport .....	4-5
4.2.1 Containment of Radioactive Material .....	4-5
4.2.2 Pressurization of Containment Vessel .....	4-10
4.2.3 Containment Criterion .....	4-11
4.3 Containment Requirements for Hypothetical Accident Conditions .....	4-13
4.3.1 Fission Gas Products .....	4-13
4.3.2 Containment of Radioactive Material .....	4-13
4.3.3 Containment Criterion .....	4-13
4.4 Special Requirements .....	4-16
4.5 References .....	4-17

### LIST OF TABLES

4-1	Radionuclide Inventory
4-2	Activity Concentration by Source
4-3	Determination of Effective $A_2$ by Source
4-4	Normal Transport and Hypothetical Accident Conditions Effective $A_2$ Values
4-5	Normal Transport and Hypothetical Accident Conditions Permissible Leakage Rates from the TN-68
4-6	Total Moles of Fission Gas by Fuel Type
4-7	Cask Gas Mixtures under Normal Transport and Hypothetical Accident Conditions

### LIST OF FIGURES

4-1	TN-68 Containment Boundary Components
4-2	Lid, Vent Port and Drain Port Metal Seals

## CHAPTER 4

### CONTAINMENT

#### 4.1 CONTAINMENT BOUNDARY

The containment boundary consists of the inner shell and bottom plate, shell flange, lid outer plate, lid bolts, penetration cover plate and bolts and the inner metallic O-rings of the lid seal and the two lid penetrations (vent and drain). The containment boundary is shown in Figure 4-1. The construction of the containment boundary is shown on drawings 972-71-2, 3 and 4 provided in Chapter 1. The containment vessel prevents leakage of radioactive material from the cask cavity. It also maintains an inert atmosphere (helium) in the cask cavity. Helium assists in heat removal and provides a non-reactive environment to protect fuel assemblies against fuel cladding degradation which might otherwise lead to gross rupture.

##### 4.1.1 Containment Vessel

The TN-68 containment vessel consists of: an inner shell which is a welded, carbon steel cylinder with an integrally-welded, carbon steel bottom closure; a welded flange forging; a flange and bolted carbon steel lid with bolts; and vent and drain covers with bolts. The overall containment vessel length is 189.0 in. with a wall thickness of 1.5 in. The cylindrical cask cavity has a diameter of 69.5 in. and a length of 178 in.

The containment shell and bottom closure materials are SA-203 Grade E and the shell flange is SA-350 Grade LF3. The containment lid material is SA-203 Grade E or SA-350 Grade LF3.

The cask design, fabrication and testing are performed under Transnuclear's Quality Assurance Program which conforms to the criteria in Subpart H of 10CFR71.

The materials of construction meet the requirements of Section III, Subsection NB-2000 and Section II, Material specifications or the corresponding ASTM Specifications. The containment vessel is designed to the ASME Code, Section III, Subsection NB, Article 3200. The containment vessel is fabricated and examined in accordance with NB-2500, NB-4000 and NB-5000. Also, weld materials conform to NB-2400 and the material specification requirements of Section II, Part C of ASME B&PV.

The containment vessel is hydrostatically tested in accordance with the requirements of the ASME B&PV Code, Section III, Article NB-6200 with the exception that the containment vessel is installed in the gamma shield shell during testing. The containment vessel is supported by the gamma shield during all design and accident events.

Even though the code is not strictly applicable to transport casks, it is the intent to follow Section III, Subsection NB of the Code as closely as possible for design and construction of the containment vessel. The casks may, however, be fabricated by other than N-stamp holders and materials may be supplied by other than ASME Certificate Holders. Thus the requirements of

NCA are not imposed. TN's quality assurance requirements, which are based on 10CFR71 Subpart H and NQA-1 are imposed in lieu of the requirements of NCA-3850. This SAR is prepared in place of the ASME design and stress reports. Surveillances are performed by TN and utility personnel rather than by an Authorized Nuclear Inspector (ANI).

The weld of the bottom inner plate to the containment shell is a Category C, Type 2 corner weld in accordance with Figure NB-4243-1 of the ASME Code. In accordance with NB-5231, Type 2 Category C full penetration corner welded joints require the fusion zone and the parent metal beneath the attachment surface to be ultrasonically examined after welding. If this weld is performed on the containment vessel after assembly with the outer shell, the UT inspection will be performed on a best efforts basis. It may not be possible to do a complete UT inspection, since the outer diameter of the shell is inaccessible. The joint will be examined by the radiographic method and either the liquid penetrant or magnetic particle methods in accordance with the ASME Code Subsection NB.

Paragraph NB-4213 requires the rolling process used to form the inner vessel be qualified to determine that the required impact properties of NB-2300 are met after straining by taking test specimens from three different heats. If the plates are made from less than three heats, each heat will be tested to verify the impact properties.

The materials of the TN-68 packaging will not result in any significant chemical, galvanic or other reaction as discussed in Chapter 2.

#### 4.1.2 Containment Penetrations

There are two penetrations through the containment vessel, both in the lid. One is the drain port and the other is the vent port. A double O-ring seal mechanical closure is provided for each penetration. Each penetration contains a quick disconnect coupling for ease of operation.

#### 4.1.3 Seals and Welds

The containment boundary welds consist of the circumferential welds attaching the bottom closure and the top flange to the vessel shell. Also, the longitudinal weld(s) on the rolled plate, closing the cylindrical vessel shell, and the circumferential weld(s) attaching the rolled shells together are containment welds.

Double metallic seals are utilized on the lid and the two lid penetrations. Helicoflex HND or equivalent seals may be used. The seals are shown in Figure 4-2. The Helicoflex metallic face seals of the lid and lid penetrations possess long-term stability and have high corrosion resistance. These high performance seals are comprised of two metal linings formed around a helically-wound spring. Additionally, all metallic seal seating areas are stainless steel overlaid for improved surface control. The overlay technique has been used for Transnuclear's storage and transport casks.

The metallic seals consist of an inner spring, a lining, and a jacket. The spring is Nimonic 90 or an equivalent material. The lining and jacket are stainless steel and aluminum, respectively.

The internal spring and lining maintain the necessary rigidity and sealing force, and provide some elastic recovery capability. The outer aluminum jacket provides a ductile material against the sealing surfaces. The jacket also provides a connecting sheet between the inner outer seals. Holes in this sheet allow for attachment screws and for communication between the OP transport cover and the space between the seals. This sheet, which is about 0.020 inch thick, has insufficient strength to transmit radial forces great enough to overcome the axial compressive forces on the seals, which are over 1000 lb/inch of seal length. The overpressure port seal is a single metallic seal of the same design, Helicoflex HN200 or equivalent.

All TN-68 surfaces which mate with the metallic seals are stainless steel.

The lid and penetration seals described above are contained in grooves. A high level of sealing over the storage period is assured by utilizing seals in a deformation-controlled design. The deformation of the seals is constant since bolt loads assure that the mating surfaces remain in contact. The seal deformation is set by the original diameter and the depth of the groove.

The nominal diameter of the lid seal is 6.6 mm, and the nominal groove depth is 5.6 mm. At 1 mm compression, the sealing force is 245 N/mm (1399 lb/inch)<sup>(1)</sup>. The total force of the double seal is 633,800 lb. The total preload of the 48 lid bolts is 6,490 kips, which is greater than the combined force of the seals, internal pressure, and normal conditions impact load 1,737 kips (Appendix 2.10.2).

The nominal diameter of the port seals is 4.1 mm, and the nominal groove depth is 3.2 mm. At 0.9 mm compression, the sealing force is 200 N/mm (1142 lb/inch). The total force of the double seal is 37,900 lb. The total preload of the 8 cover bolts is 64,000 lb, which is greater than the combined force of the seals and internal pressure, 40,000 lb.

The sealing force is maintained by the seal's internal spring. Due to creep, the sealing pressure decreases with increasing temperature as shown in the following table<sup>(11)</sup>. The ratios  $P_T/P_{20}$  compare the seal pressure temperature  $T$  °C to the seal pressure at 20°C. The long-term temperature limit is the point at which the sealing pressure becomes zero due to creep ( $P_{T_{max}} = 0$ ). The maximum normal temperature experienced by the seals in the TN-68 is 243 °F (Table 3-1).

Seal	$P_{119c}/P_{20c}$ (119 °C = 247 °F)	$P_{200c}/P_{20c}$ (200 °C = 392 °F)	Temperature limit
Lid, 6.6 mm	(439/670) = 66%	(250/670) = 37%	340 °C (644 °F)
Ports, 4 mm	(364/600) = 61%	(170/600) = 28%	280 °C (536 °F)

$P_{20c}$  and  $P_{200c}$  from Reference 1;  $P_{119c}$  by linear interpolation; sealing pressure  $P$  in  $N/mm^2$  (referred to as "intrinsic power  $P_u$ " in reference 1).

Helicoflex metallic seals are all capable of limiting leak rates to less than  $1 \times 10^{-7}$  ref  $cm^3/sec$ . After loading, all lid and cover seals are leak tested in accordance with ANSI N14.5. The acceptable total cask leakage (both inner and outer seals combined) is  $1 \times 10^{-5}$  ref  $cm^3/sec$ .

#### 4.1.4 Closure

The containment vessel contains an integrally-welded bottom closure and a bolted and flanged top closure (lid). The flanged lid plate is attached to the cask body with 48 bolts. The bolt torque required to seal the metallic seals located in the lid and maintain confinement under normal and accident conditions is provided in Drawing 972-71-2. The closure bolt analysis is presented in Appendix 2.10.2.

As previously mentioned, the lid contains two penetrations which are sealed by flanged covers fastened to the lid by 8 bolts each. The bolt torque required to seal the metallic seals in the penetration covers and maintain confinement under normal and accident conditions is provided in Drawing 972-71-2.

## 4.2 REQUIREMENTS FOR NORMAL CONDITIONS OF TRANSPORT

In accordance with 10 CFR 71.51, a Type B package must be designed, constructed and prepared for shipment so that "no loss or dispersal of radioactive contents, as demonstrated to a sensitivity of  $10^{-6}$  A<sub>2</sub> per hour" will occur under the tests specified in 10 CFR 71.71 for normal conditions of transport.

The guidelines of ANSI N14.5 were used to determine the leakage test criteria which demonstrate that the TN-68 meets the "no-loss" requirements of 10 CFR 71.51.

### 4.2.1 Containment of Radioactive Material

#### 4.2.1.1 Source Terms

Three sources are considered to determine the releasable airborne material from the TN-68 cask (Reference 4, NUREG/CR-6487).

- Residual activity on the cask interior surfaces as a result of loading operations (and, if applicable, previous shipments);
- Fission and activation-product activity associated with corrosion-deposited material (crud) on the fuel assembly surfaces, and
- Radionuclides within the individual fuel rods comprising the fuel assemblies.

The first source, residual contamination on the interior surfaces of the cask is neglected. Reference 4 indicates that this is negligible as compared to the crud deposition on the fuel rods.

The second source, crud, is basically the radioactive "flaky" material that is formed on the outside surface of the fuel rods due to the radioactive and corrosive environment of the BWR reactor. This material can be loosely bound to the fuel rod surface and may be dislodged during transportation and be available for release from the cask.

The third source is from the fuel itself. A breach in the fuel cladding may allow radionuclides to be released from the fuel to the interior of the cask. There are three types of releases associated with the breaches in the fuel rod cladding: gaseous radionuclides, volatiles and fuel fines.

As a conservative approach, to simplify calculations, it is assumed that crud spallation and cladding breaches occur instantaneously after fuel loading and closure operations. Therefore, all radioactivity is readily available for release if a leak occurs.

The containment analysis is based on the void volume within the TN-68 cask. The void volume is estimated below:

$$\text{Cavity Volume} = 675,273 \text{ in}^3$$

*Basket:*

Weight of Stainless Steel in Basket = 17,375 lbs  
Volume of Stainless Steel in Basket = 59,914 in<sup>3</sup>

Weight of Aluminum in Basket = 8,493 lbs  
Volume of Aluminum in Basket = 86,663 in<sup>3</sup>

Basket Volume = 59,914 in<sup>3</sup> + 86,663 in<sup>3</sup> = 146,577 in<sup>3</sup>

*Basket Holddown Ring:*

Weight of Holddown Ring = 1408 lbs  
Holddown Ring Volume = 4855 in<sup>3</sup>

*Volume of Fuel Assemblies:*

Fuel Assembly Volume = 2327 in<sup>3</sup>/assembly = 158,267 in<sup>3</sup> for 68 assemblies

*TN-68 Cask Void Volume:*

Cask Void Volume = 675,273 in<sup>3</sup> - 146,577 in<sup>3</sup> - 4855 in<sup>3</sup> - 158,267 in<sup>3</sup>  
= 365,574 in<sup>3</sup>  
= 6.0E+06 cm<sup>3</sup>

Source Activity from the Fuel

The fuel transported in the TN-68 transport packaging may have an initial enrichment of 3.3 wt% U-235, 40,000 MWD/MTU bundle average exposure and 10 year cooled provided the fuel acceptance criteria of Section 1.2.3 have been met. It is conservative to assume that 7x7 assemblies with these fuel parameters are loaded in the TN-68 cask transport packaging. (The 7x7 fuel assemblies have the largest initial uranium loading of all the BWR fuel types analyzed for the TN-68 and therefore the greatest source term.) The inventory is taken from Reference 5 which consists of activity from iodine, fission products that contribute greater than 0.1% of the design basis fuel activity and actinides that contribute greater than 0.01% of the design basis activity. Tritium is also included although it contributes slightly less than 0.1% of the design basis activity. The radionuclide inventory is presented in Table 4-1 (Reference 5).

*Source Activity from Release of Volatiles*

The source activity concentration inside the TN-68 due to the release of volatiles is calculated using the following equation (Reference 4).

$$C_{\text{volatiles}} = \{N_A f_B A_v f_v\} / V$$

where: N<sub>A</sub> = number of assemblies

$f_B$  = fraction of rods that develop cladding breaches  
 $A_V$  = specific activity of volatiles in the fuel assembly, Ci/assembly  
 $f_V$  = fraction of volatiles in a fuel rod released if a fuel rod develops a cladding breach  
 $V$  = void volume inside the containment vessel,  $\text{cm}^3$

Table 4-2 presents the results of this calculation.

#### *Source Activity from Release of Gaseous Isotopes*

The source activity concentration inside the TN-68 cask due to the release of gaseous isotopes is calculated using the following equation (Reference 4).

$$C_{\text{volatiles}} = \{N_A f_B A_V f_V\} / V$$

where:  $N_A$  = number of assemblies  
 $f_B$  = fraction of rod that develop cladding breaches  
 $A_G$  = specific activity of gases in the fuel assembly, Ci/assembly  
 $f_G$  = fraction of gases in a fuel rod released if a fuel rod develops a cladding breach  
 $V$  = void volume inside the containment vessel,  $\text{cm}^3$

Table 4-2 presents the results of this calculation.

#### *Source Activity from Release of Fuel Fines*

The source activity concentration inside the TN-68 due to the release of fuel fines is calculated using the following equation (Reference 4).

$$C_{\text{fines}} = \{N_A f_B A_F f_F\} / V$$

where:  $N_A$  = number of assemblies  
 $f_B$  = fraction of rod that develop cladding breaches  
 $A_F$  = specific activity of fuel fines in the assembly, Ci/assembly  
 $f_G$  = fraction of fuel fines released if a fuel rod develops a cladding breach  
 $V$  = void volume inside the containment vessel,  $\text{cm}^3$

Table 4-2 presents the calculated concentration of fuel fines inside the TN-68 for normal transport conditions.

#### Source Activity due to Crud Spallation

The fuel transported in the TN-68 transport packaging may be cooled a minimum of 10 years (provided the fuel acceptance criteria of Section 1.2.3 have been met). The activity density that results inside of the TN-68 as a result of crud spallation is calculated using the equation below (Reference 4).

$$C_{\text{crud}} = \{ f_C S_C N_R N_A S_{AR} \}$$

where

- $C_{\text{crud}}$  = activity density inside containment vessel as a result of crud spallation, Ci/cm<sup>3</sup>
- $f_C$  = crud spallation factor
- $V$  = free volume inside the containment vessel, cm<sup>3</sup>
- $S_C$  = crud surface activity, Ci/cm<sup>2</sup>
- $N_R$  = number of fuel rods per assembly
- $N_A$  = number of assemblies in the cask
- $d$  = rod outer diameter, cm
- $r$  = rod outer radius, cm
- $l$  = rod length, cm
- $S_{AR}$  = surface area per rod, cm<sup>2</sup>

The 10 x 10 fuel assembly is used to determine the maximum crud source since it has the largest overall surface area. (The presence of partial length fuel rods are conservatively neglected.) The surface area of the 10 x 10 fuel rods calculated for this containment analysis is presented below.

$$S_{AR} = (\pi d l) + \frac{1}{4}(2 \pi d^2)$$

where:

- $d$  = rod outer diameter = 0.404 in = 1.03 cm (from Table 5.2-1)
- $l$  = rod length = 160 in = 406.4 cm (from Table 5.2-1)

substituting and solving:

$$S_{AR} = 1317 \text{ cm}^2 / \text{rod}$$

#### 4.2.1.2 Determination of A<sub>2</sub> Values

The A<sub>2</sub> value of a mixture of radioactive nuclides is determined as follows:

$$A_{2 \text{ mixture}} = [ \sum (f_i / A_{2i}) ]^{-1}$$

- where:  $f_i$  is the fraction of total activity due to isotope i, and  
 $A_{2i}$  is the A<sub>2</sub> value for isotope i.

Using the methodology of 10 CFR 71 and Reference 4, the A<sub>2</sub> values are determined for each source (Table 4-3). The results provided in Tables 4-2 and 4-3 are combined to determine an effective A<sub>2</sub> for the TN-68 (Table 4-4).

#### 4.2.1.3 Determination of Permissible Leakage Rates

To determine the leakage rates, the four sources are combined to for the total source term:

$$C_{\text{total}} = C_{\text{crud}} + C_{\text{volatiles}} + C_{\text{gases}} + C_{\text{fines}}$$

From Reference 5, the permissible release rate, R, from the TN-68 is:

$$R = L \times C$$

where:

L = volumetric gas leakage rate ( $\text{cm}^3 / \text{s}$ )

C = curies per unit volume of the radioactive material that passes through the leak path.

R =  $A_2 \times 2.78 \times 10^{-10}$  /second for normal transport conditions

For normal conditions, the permissible leakage rate is  $2.47\text{E-}05$  cc/sec (Table 4-5). This value is converted to units of  $\text{ref-cm}^3/\text{sec}$  by first calculating equivalent hole size. From ANSI N14.5 (Reference 6):

$$L_u = (F_c + F_m)(P_u - P_d)(P_a/P_u) \text{ cc/sec at } T_u, P_u$$

Other definitions:

$L_u$  = upstream volumetric leakage rate, cc/sec =  $2.47\text{E-}05$  cc/sec

$F_c$  = coefficient of continuum flow conductance per unit pressure, cc/atm-sec

$F_m$  = coefficient of free molecular flow conductance per unit pressure, cc/atm-sec

$P_u$  = fluid upstream pressure, atm abs = 2.26 atm abs

$P_d$  = fluid downstream pressure, atm abs = 1.0 atm abs

D = leakage hole diameter, cm

a = leakage hole length, cm = 0.5 cm (assuming leak path length is on the order of the metal seal width)

$\mu$  = fluid viscosity, cP = 0.0257 cP

T = fluid absolute temperature,  $186^\circ\text{C} = 459$  K (average cavity gas temperature from Table 3-1)

M = molecular weight, g/mol = 4 g/mol (from ANSI N14.5, Table B.1)

$P_a$  = average stream pressure =  $\frac{1}{2}(P_u + P_d)$ , atm abs = 1.63 atm abs

$$L_u = (F_c + F_m)(P_u - P_d)(P_a/P_u) \text{ cc/sec}$$

where:

$$F_c = (2.49 \times 10^6 \times D^4) / (a\mu) \text{ cc/atm-sec}$$

$$F_m = \{3.81 \times 10^3 \times D^3 \times (T/M)^{0.5}\} / \{aP_a\} \text{ cc/atm-sec}$$

Substituting:

$$F_c = (2.49 \times 10^6 \times D^4) / (0.5 \times 0.0257) = 1.94\text{E}+08 D^4$$

$$F_m = \{3.81 \times 10^3 \times D^3 \times (459/4)^{0.5}\} / \{0.5 \times 1.63\} = 5.01\text{E}+04 D^3$$

$$\begin{aligned}
L_u &= (F_c + F_m)(P_u - P_d)(P_a/P_u) \text{ cc/sec} \\
2.47\text{E-}05 &= (F_c + F_m) (2.26 - 1.0) (1.63 / 2.26) \\
2.47\text{E-}05 &= (F_c + F_m) (0.91) \\
F_c + F_m &= 2.71\text{E-}05
\end{aligned}$$

Solving the equations above for D, yields a hole diameter of  $5.56 \times 10^{-4}$  cm.

This equivalent hole size, is then used to calculate the reference air rate at standard conditions. Assuming all upstream test conditions correspond to standard conditions:

$$L_u = (F_c + F_m)(P_u - P_d)(P_a/P_u) \text{ cc/sec}$$

where:

$$\begin{aligned}
F_c &= (2.49 \times 10^6 \times D^4) / (a\mu) \text{ cc/atm-sec} \\
F_m &= \{3.81 \times 10^3 \times D^3 \times (T/M)^{0.5}\} / \{aP_a\} \text{ cc/atm-sec}
\end{aligned}$$

Substituting:

$$F_c = \{2.49\text{E}+06 \times (5.56\text{E-}04)^4\} / (0.5 \times 0.0185) = 2.57\text{E-}05$$

$$F_m = \{3.81\text{E}+03 \times (5.56\text{E-}04)^3 \times (298/29.0)^{0.5}\} / \{0.5 \times 0.505\} = 8.31\text{E-}06$$

$$\begin{aligned}
L_{\text{std}} &= (F_c + F_m)(P_u - P_d)(P_a/P_u) \text{ cc/sec} \\
L_{\text{std}} &= (2.57\text{E-}05 + 8.31\text{E-}06)(1.0 - 0.01)(0.505 / 1.0) \\
L_{\text{std}} &= 1.70\text{E-}05 \text{ ref cm}^3 / \text{s}
\end{aligned}$$

#### 4.2.2 Pressurization of Containment Vessel

The TN-68 cask cavity is drained, dried and evacuated prior to backfilling with helium at the end of loading. If the TN-68 cask contains design basis fuel and has been in storage for a short period prior to shipment (i.e. thermal equilibrium is reached), the cask cavity temperature with 100°F ambient air and maximum solar load is 369°F. The maximum normal operating pressure during storage is 2.2 atm abs (Reference 5).

Similarly, during normal transport conditions, the maximum cavity gas temperature is 366°F (186°C) under hot environment conditions. The maximum initial pressure just prior to shipment (assuming no fuel rod failure) is also 2.2 atm abs. The operational procedure guidelines for conducting these activities are provided in Chapter 7.

#### *Cavity Gas Mixtures*

The determination of fission gases is based on the grams of fission gases from SAS2H / ORIGEN -S computer runs (from Reference 5 which utilizes fuel with 40,000 MWD/MTU bundle average exposure, 3.3 U-235 wt% initial bundle average enrichment and 10 year cooled). The gases which are considered following irradiation are: I, Kr, and Xe. The bulk of the fission gases remain trapped in the fuel pellet. The release fraction of 0.3 is applied to these gases. Table 4-6 presents the total moles of fission gas for the seven basic fuel types.

In addition to the fission gases, helium from rod pre pressurization and from cask backfilling operations are also included. The total moles of gas from these sources is also presented in Table 4-6.

The cavity gas mixture (assuming 3% fuel rod failure) is primarily 98.2% helium (from cask backfill operations and from rod pre-pressurization) with the balance consisting of xenon (1.6%), krypton (0.2%), iodine (0.1%), and possibly vaporized bromine. These results are presented in Table 4-7. This gas mixture is not explosive.

#### *Maximum Normal Operating Pressure*

The mechanism contributing to containment pressurization are ideal gas heating and release of fission gas from the fuel rods. The maximum normal operating pressure is calculated using the recommendation of NUREG-1617 (Reference 7) which uses the following conditions:

- 30% release rate of fission gas from fuel pellets into the gap between the fuel pellets and the cladding.
- 100% failure rate of fuel rod cladding.
- maximum cavity gas temperature of 366°F (186°C) under hot environment conditions.
- the gas volume (plenum and pellet to cladding volume) inside the fuel rods is conservatively neglected when calculating the cask free volume.

Based on Table 4-6, the General Electric 10x10 assembly contains the most free gas and is bounding. The pressures are calculated below

$$P_{100\% \text{ rod failure}} = (0.301 \text{ kg moles/cask} \times 0.08314 \times 459 \text{ K}) / (6.0 \text{ m}^3)$$
$$P_{100\% \text{ rod failure}} = 1.9 \text{ bars} = 1.9 \text{ atm abs}$$

$$\text{MNOP} = P_{\text{initial}} + P_{100\% \text{ rod failure}}$$
$$\text{MNOP} = 2.2 \text{ atm abs} + 1.9 \text{ atm abs} = 4.1 \text{ atm abs} = 60.3 \text{ psia}$$

Therefore, the maximum normal operating pressure for the TN-68 is 60.3 psia (45.6 psig). Casks designs with MNOP greater than 5.0 psig must be subjected to a structural pressure test in accordance with 10 CFR 71.85(b). The test pressure must be at least 1.5 times MNOP. The TN-68 will be subjected to a hydrostatic test at a pressure of 125 psig in accordance with ASME BP&V Code Section NB-6200. This test is described in Chapter 8.

#### 4.2.3 Containment Criterion

As will be demonstrated in Section 4.3.2, the reference leak rate for normal conditions,  $1.70\text{E-}05 \text{ ref cm}^3/\text{s}$ , is a significantly lower rate than the accident leakage rate. However, the acceptance criterion for fabrication verification and periodic verification leak test of the TN-68 containment

boundary shall be  $1.0 \times 10^{-5}$  ref  $\text{cm}^3/\text{sec}$ . This is conservative by 70% over the calculated value. The test must have a sensitivity of at least one half the acceptance criterion, or  $5 \times 10^{-6}$  ref  $\text{cm}^3/\text{s}$ .

### 4.3 CONTAINMENT REQUIREMENTS FOR HYPOTHETICAL ACCIDENT CONDITIONS

The containment requirement under hypothetical accident conditions specified by 10 CFR 71.51(a)(2). It states "there would be no escape of krypton-85 exceeding 10 A<sub>2</sub> in 1 week, no escape of other radioactive material exceeding a total amount A<sub>2</sub> in 1 week." It is assumed for purposes of the accident condition evaluation that 100% of the fuel rods fail thereby releasing all of the available fission gas in the fuel rod gas gap to the cask cavity.

Calculation of the fission gas inventory is discussed in Section 4.2.1.

#### 4.3.1 Fission Gas Products

Similar to normal transport conditions described in Section 4.2.1, the following equations from NUREG/CR-6487 (Reference 4) are used to determine the source term available for release.

$$\begin{aligned}
 C_{\text{volatiles}} &= \{N_A f_B A_V f_V\} / V \\
 C_{\text{gases}} &= \{N_A f_B A_F f_F\} / V \\
 C_{\text{fines}} &= \{N_A f_B A_F f_F\} / V \\
 C_{\text{crud}} &= \{f_C S_C N_R N_A S_{AR}\} \\
 C_{\text{total}} &= C_{\text{crud}} + C_{\text{volatiles}} + C_{\text{gases}} + C_{\text{fines}}
 \end{aligned}$$

Table 4-1 shows the free activity available for release from the fuel rods. Table 4-2 shows the activity concentration from each of the sources available for release from inside the TN-68. The release fractions for the radionuclides are taken from NUREG/CR-6487. Under hypothetical accident conditions, the cladding of 100% of the fuel rods is assumed to fail (f<sub>B</sub>=1.0).

#### 4.3.2 Containment of Radioactive Material

The TN-68 is designed to meet the hypothetical accident requirements of 10 CFR 71.51. The A<sub>2</sub> values are calculated using the methodology of 10 CFR 71.71 and NUREG/CR-6487. The A<sub>2</sub> values are provided in Tables 4-3 and 4-4.

#### 4.3.3 Containment Criterion

The allowable leak rates under hypothetical accident conditions are calculated using the methodology of NUREG/CR-6487 and previously presented in Section 4.2.3. The permissible leak rates under hypothetical accidents is 8.71E-03 cc/sec (Table 4-5). This value is converted to units of ref-cm<sup>3</sup>/sec by first calculating the equivalent hole size. The equations of ANSI 14.5 (also see section 4.2.1.3) are used:

$$L_u = (F_c + F_m)(P_u - P_d)(P_a/P_u) \text{ cc/sec at } T_u, P_u$$

where:

$$\begin{aligned}
 L_u &= 8.71E-03 \text{ cc/sec} \\
 P_u &= 4.2 \text{ atm abs}
 \end{aligned}$$

$$\begin{aligned}
P_d &= 1.0 \text{ atm abs} \\
a &= 0.5 \text{ cm} \\
\mu &= 0.0269 \text{ cP} \\
T &= 422^\circ\text{F} (= 217^\circ\text{C} = 490 \text{ K}) \\
M &= 4 \text{ g/mol (from ANSI N14.5, Table B.1)} \\
P_a &= 2.6 \text{ atm abs}
\end{aligned}$$

Substituting into the equations of ANSI N14.5:

$$\begin{aligned}
F_c &= (2.49 \times 10^6 \times D^4) / (0.5 \times 0.0269) = 1.85\text{E}+08 D^4 \\
F_m &= \{3.81 \times 10^3 \times D^3 \times (422/4)^{0.5}\} / \{0.5 \times 2.6\} = 3.01\text{E}+04 D^3 \\
L_u &= (F_c + F_m)(P_u - P_d)(P_a/P_u) \\
8.71\text{E}-03 &= (F_c + F_m)(4.2 - 1.0)(2.6 / 4.2) \\
F_c + F_m &= 4.39\text{E}-03
\end{aligned}$$

Solving the equations above for D, yields a hole diameter of  $2.167 \times 10^{-3}$  cm.

This equivalent hole size, is then used to calculate the reference air rate at standard conditions. Assuming all upstream test conditions correspond to standard conditions:

$$L_u = (F_c + F_m)(P_u - P_d)(P_a/P_u) \text{ cc/sec at } T_u, P_u$$

where:

$$\begin{aligned}
P_u &= 1.0 \text{ atm abs} \\
P_d &= 0.01 \text{ atm abs} \\
D &= 2.167\text{E}-03 \text{ cm} \\
a &= 0.5 \text{ cm} \\
\mu &= 0.0185 \text{ cP (from ANSI N14.5, Table B.1)} \\
T &= 298^\circ\text{K} \\
M &= 29.0 \text{ g/mol (from ANSI N14.5, Table B.1)} \\
P_a &= 0.505 \text{ atm abs}
\end{aligned}$$

$$L_u = (F_c + F_m)(P_u - P_d)(P_a/P_u) \text{ cc/sec}$$

$$\begin{aligned}
F_c &= \{2.49 \times 10^6 \times (2.167 \times 10^{-3})^4\} / (0.5 \times 0.0185) = 5.94\text{E}-03 \\
F_m &= \{3.81 \times 10^3 \times (2.167 \times 10^{-3})^3 \times (298/29.0)^{0.5}\} / \{0.5 \times 0.505\} = 4.92\text{E}-04
\end{aligned}$$

$$\begin{aligned}
L_{std} &= (F_c + F_m)(P_u - P_d)(P_a/P_u) \text{ cc/sec} \\
L_{std} &= (5.94\text{E}-03 + 4.92\text{E}-04)(1.0 - 0.01)(0.505 / 1.0) \\
L_{std} &= 3.21\text{E}-03 \text{ ref cm}^3 / \text{s}
\end{aligned}$$

Because the reference leak rate for normal conditions is lower than that for accident conditions, the leak test criterion developed in Section 4.2.3 demonstrates that the containment criteria for both normal and accident conditions are met. The structural and thermal consequences of

hypothetical accident loading conditions do not adversely affect the performance of the containment boundary structure or seals.

The impact limiters remain in place on the cask after the hypothetical accident as concluded in Chapter 2 for the limiting 15° oblique drop orientation. During the hypothetical accident the impact limiters provide insulation for the seals of the penetrations underneath them, including the lid seal, vent and drain ports, and the OP port.

Table 3-1 lists the maximum temperature of the seals during a hypothetical thermal accident (see Chapter 3). Temperatures are shown for those areas protected by the insulating effect of the impact limiters, and other areas exposed directly to the accident temperatures environment. None of these temperatures exceeds the seal limit of 536°F. The pressure inside the cask cavity also remains well below the design pressure of 100 psig as shown below. (Assuming 100% fuel rod failure.)

$$P_{HAC} = P_{initial} + P_{100\% \text{ rod failure}}$$

$$P_{initial} = (2.2 \text{ atm abs})(490 \text{ K} / 459 \text{ K}) = 2.3 \text{ atm abs}$$

$$P_{100\% \text{ rod failure}} = (0.301 \text{ kgmole/cask} \times 0.08314 \text{ bar}\cdot\text{m}^3/\text{kgmole K} \times 490 \text{ K}) / (6.0 \text{ m}^3)$$

$$P_{100\% \text{ rod failure}} = 2.0 \text{ bar} = 2.0 \text{ atm abs}$$

$$P_{HAC} = 2.2 + 2.0 = 4.2 \text{ atm abs} = 61.7 \text{ psia} = 47.0 \text{ psig}$$

In addition, the cavity gas mixture (assuming 100% fuel rod failure) consists of 62.7% helium (from cask backfill operations and from rod pre-pressurization), 32.5% xenon, 3.4% krypton, 1.4% iodine and possibly some vaporized bromine. The cavity gas mixture under accident conditions is presented in Table 4-7. This gas mixture is not explosive.

#### 4.4 SPECIAL REQUIREMENTS

Solid plutonium in the form of reactor elements is exempt from the double containment requirements of 10 CFR 71.63.

#### 4.5 REFERENCES

1. Helicoflex Catalog ET 507 E5930.
2. 10 CFR 71, "Packaging and Transportation of Radioactive Materials."
3. ASME Boiler and Pressure Vessel Code, 1995 Code with 1996 Addenda.
4. NUREG/CR-6487, "Containment Analysis for Type B Packages used to Transport Various Contents," Lawrence Livermore National Laboratory, 1996.
5. Transnuclear, Inc., "TN-68 Dry Storage Cask, Safety Analysis Report," Revision 4, May 1999.
6. ANSI N14.5-1997, "American National Standard for Radioactive Material – Leakage Tests on Packages for Shipment," February 1998.
7. NUREG-1617, "Standard Review Plan for Transportation Packages for Spent Nuclear Fuel," Draft Report for Comment, March 1998.

TABLE 4-1  
RADIONUCLIDE INVENTORY

	Ci/assembly <sup>1</sup>
<b>Volatiles</b>	
Sr 90	1.36E+04
Cs134	1.30E+03
Cs137	2.02E+04
Total – Volatiles	3.51E+04
<b>Gases</b>	
H 3	6.40E+01
Kr 85	1.03E+03
I129	7.62E-03
Total - Gases	1.09E+03
<b>Fines</b>	
Pu238	8.19E+02
Pu239	6.32E+01
Pu240	1.09E+02
Pu241	1.81E+04
Am241	4.06E+02
Cm244	6.25E+02
Y 90	1.36E+04
Ru106	1.15E+02
Sb125	1.32E+02
Pm147	2.10E+03
Sm151	7.57E+01
Eu154	1.32E+03
Eu155	4.61E+02
Total – Fines	3.79E+04

<sup>1</sup> Values are from Reference 5, based on a 7x7 fuel assembly (40,000 MWD/MTU burnup, 3.3 wt% U-235 initial bundle average enrichment, and 10 year cooled).

<sup>2</sup> Ba137m and Rh106 contribute 20.4% and 0.1%, respectively, to the total design basis activity. Ba137m and Rh106 are daughters of Cs137 and Ru106, respectively, with half lives of 2.6 min and 30 sec, respectively. In accordance with 10CFR71 Appendix A Note III, these radionuclides are evaluated with the parent nuclide.

TABLE 4-2

## ACTIVITY CONCENTRATION BY SOURCE

Source	Fraction available for release from the fuel rod <sup>(1)</sup> ( $f_V / f_G / f_F / f_C$ )	Fraction of rods that develop cladding breach <sup>(1)</sup>	Activity Concentration in TN-68 cask (Ci/cc) <sup>(2,3,4)</sup>
Normal Transport Conditions			
Volatiles	2E-04	0.03	2.39E-06
Gases	0.3	0.03	1.12E-04
Fines	3E-05	0.03	5.78E-07
Crud <sup>(5)</sup>	0.15	not applicable	6.97E-05
Hypothetical Accident Conditions			
Volatiles	2E-04	1.0	7.96E-05
Gases	0.3	1.0	2.18E-04
Gases - Kr-85 only	0.3	1.0	3.50E-03
Fines	3E-05	1.0	1.93E-05
Crud	1.0	not applicable	4.65E-04

1 Values taken from NUREG/CR-6487 (Reference 4).

2 68 assemblies per cask.

3 Cavity free volume is equal to  $6.0E+06 \text{ cm}^3$

4 Source term for the volatiles, gases and fines are based on the 7x7-49/0 fuel assembly. Source term for the crud is based on the 10x10-92/2 assembly (Fuel rod dimensions are provided in Chapter 5).

5 Crud source is based on a surface area of  $1.32E+03 \text{ cm}^2$  / rod and an initial surface activity of  $1254E-03 \text{ Ci/cm}^2$  at the time of discharge. At discharge, typically, fuel crud is composed of isotopes of cobalt, manganese, chromium and iron. After a 10 year cooling time, the only isotope of radiological significance is Co-60. A decay factor of 0.27 is included in the values listed above.

**TABLE 4-3  
DETERMINATION OF EFFECTIVE A<sub>2</sub> BY SOURCE**

Volatile Isotopes	Activity (Ci/Assembly)	Activity Fraction, FA	A <sub>2</sub> (Ci)	FA / A <sub>2</sub> (1 / Ci)
sr 90	1.36E+04	3.87E-01	2.7	1.44E-01
cs134	1.30E+03	3.70E-02	13.5	2.74E-03
cs137	2.02E+04	5.75E-01	13.5	4.26E-02
				1.89E-01 = 1 / A <sub>2</sub>
				A <sub>2</sub> , volatile, BWR = 5.29

**Normal Transport Conditions**

Gaseous Isotopes	Activity (Ci/Assembly)	Activity Fraction, FA	A <sub>2</sub> (Ci)	FA / A <sub>2</sub> (1 / Ci)
h 3	6.40E+01	5.85E-02	1080	5.42E-05
kr 85	1.03E+03	9.41E-01	270	3.49E-03
i129	7.62E-03	6.97E-06	Unlimited	0
				3.54E-03 = 1 / A <sub>2</sub>
				A <sub>2</sub> , gas, BWR = 282

**Hypothetical Accident Conditions**

Gaseous Isotopes	Activity (Ci/Assembly)	Activity Fraction, FA	A <sub>2</sub> (Ci)	FA / A <sub>2</sub> (1 / Ci)
h 3	6.40E+01	1.00E+00	1080	9.26E-04
i129	7.62E-03	1.19E-04	Unlimited	0
				9.26E-04 = 1 / A <sub>2</sub>
				A <sub>2</sub> , gas, BWR = 1080

Fines Isotopes	Activity (Ci/Assembly)	Activity Fraction, FA	A <sub>2</sub> (Ci)	FA / A <sub>2</sub> (1 / Ci)
pu238	8.19E+02	2.16E-02	5.41E-03	3.99E+00
pu239	6.32E+01	1.67E-03	5.41E-03	3.08E-01
pu240	1.09E+02	2.87E-03	5.41E-03	5.31E-01
pu241	1.81E+04	4.77E-01	0.270	1.77E+00
am241	4.06E+02	1.07E-02	5.41E-03	1.98E+00
cm244	6.25E+02	1.65E-02	1.08E-02	1.53E+00
y 90	1.36E+04	3.59E-01	5.41	6.63E-02
ru106	1.15E+02	3.03E-03	5.41	5.60E-04
sb125	1.32E+02	3.48E-03	24.30	1.43E-04
pm147	2.10E+03	5.54E-02	24.3	2.28E-03
sm151	7.57E+01	2.00E-03	108	1.85E-05
eu154	1.32E+03	3.48E-02	13.5	2.58E-03
eu155	4.61E+02	1.22E-02	54.1	2.25E-04
				1.02E+01 = 1 / A <sub>2</sub>
				A <sub>2</sub> , fine, BWR = 9.83E-02

Crud Isotopes	Activity (Ci/Assembly)	Activity Fraction, FA	A <sub>2</sub> (Ci)	FA / A <sub>2</sub> (1 / Ci)
Co-60	4.10E+01	1.00E+00	10.8	9.26E-02
				9.26E-02 = 1 / A <sub>2</sub>
				A <sub>2</sub> , crud, BWR = 10.80

**TABLE 4-4**  
**NORMAL TRANSPORT AND HYPOTHETICAL ACCIDENT CONDITIONS**  
**EFFECTIVE A<sub>2</sub> VALUES**

**NORMAL CONDITIONS**

Source	Releasable Activity (Ci/cc)	Fraction Activity FA	Effective A <sub>2</sub> (Ci)	FA/A <sub>2</sub> (1/Ci)
volatiles	2.39E-06	1.30E-02	5.29	2.45E-03
gases	1.12E-04	6.06E-01	282	2.15E-03
finest	3.87E-07	2.10E-03	9.83E-02	2.14E-02
crud	6.97E-05	3.79E-01	10.80	3.51E-02
Total	1.84E-04			6.10E-02 = 1/A <sub>2</sub>
				A <sub>2</sub> , BWR, NTC = 16.38

**ACCIDENT CONDITIONS**

Source	Releasable Activity (Ci/cc)	Fraction Activity FA	Effective A <sub>2</sub> (Ci)	FA/A <sub>2</sub> (1/Ci)
volatiles	7.96E-05	1.03E-01	5.29	1.94E-02
gases (w/o Kr-85)	2.18E-04	2.81E-01	1080	2.60E-04
finest	1.29E-05	1.66E-02	9.83E-02	1.69E-01
crud	4.65E-04	6.00E-01	10.80	5.55E-02
Total	7.75E-04			2.45E-01 = 1/A <sub>2</sub>
				A <sub>2</sub> , BWR, HAC = 4.09

TABLE 4-5  
 NORMAL TRANSPORT AND HYPOTHETICAL ACCIDENT CONDITIONS  
 PERMISSIBLE LEAKAGE RATES FROM THE TN-68

<u>Transport Conditions</u>	<u>Effective A2 (Ci)</u>	<u>Allowable Release Rate (Ci/sec)</u>	<u>Concentration (Ci/cc)</u>	<u>Permissible Leakage Rate (cc/sec)</u>	<u>Permissible Standard Leakage Rate (ref cc /sec)</u>
NTC	16.38	4.55E-09	1.84E-04	2.47E-05	1.70E-05
HAC - w/o Kr85	4.11	6.79E-06	7.81E-04	8.69E-03	3.21E-04
HAC - Kr85	270	4.46E-03	3.50E-03	1.27E+00	(1)

(1) Hypothetical accident condition without Kr-85 are bounding. This value not calculated.

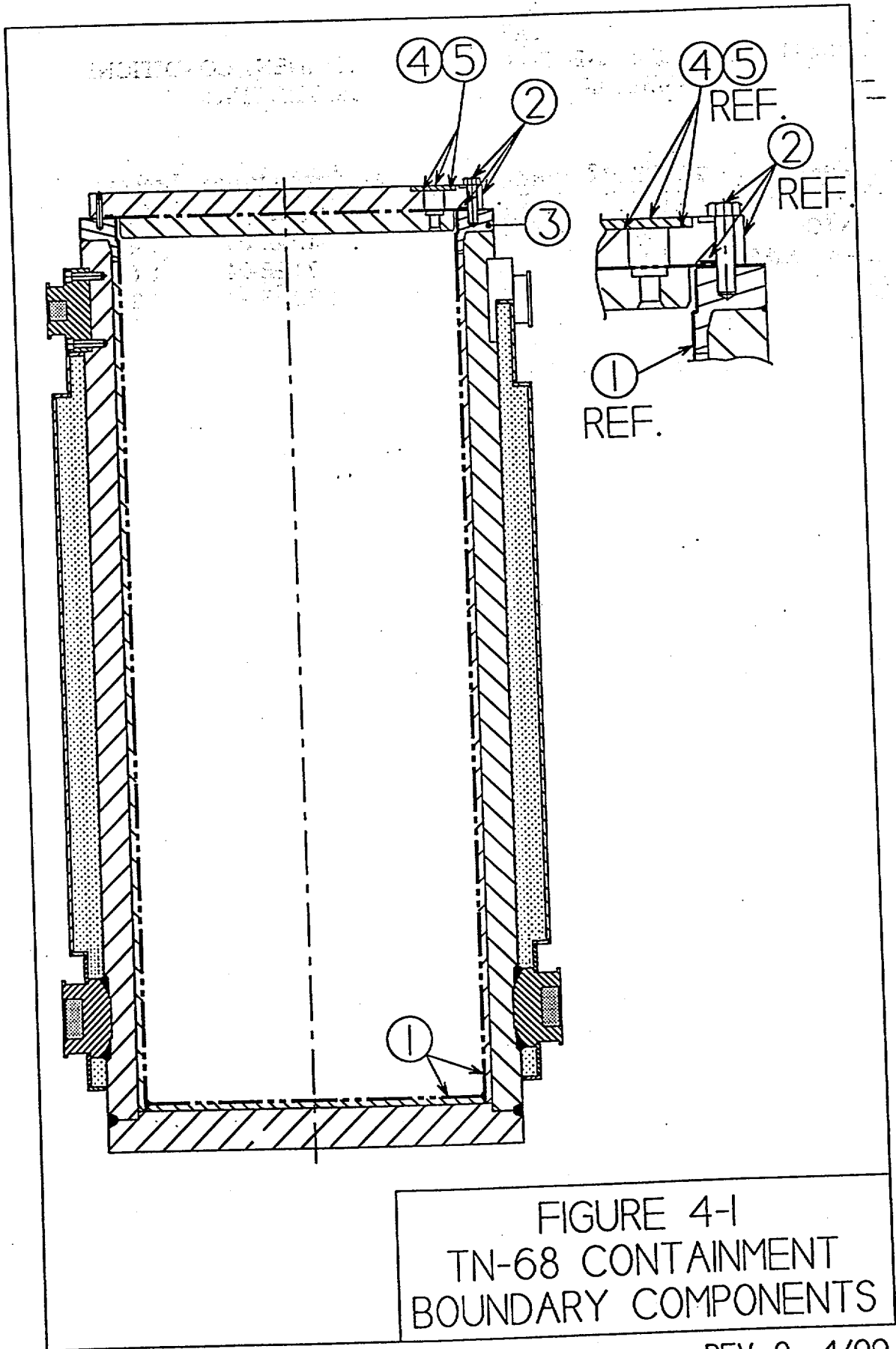
TABLE 4-6  
TOTAL MOLES OF FISSION GAS BY FUEL TYPE

	<u>7x7-49-0</u> (kgmole/cask)	<u>8x8-63-1</u> (kgmole/cask)	<u>8x8-62-2</u> (kgmole/cask)	<u>8x8-60-4</u> (kgmole/cask)	<u>8x8-60-1</u> (kgmole/cask)	<u>9x9-74-2</u> (kgmole/cask)	<u>10x10-92-2</u> (kgmole/cask)
<b>Fission Products<sup>1</sup></b>							
I	8.47E-03	8.05E-03	7.92E-03	7.79E-03	7.82E-03	7.52E-03	7.97E-03
Kr	1.98E-02	1.89E-02	1.88E-02	1.84E-02	1.85E-02	1.79E-02	1.89E-02
Xe	1.91E-01	1.82E-01	1.81E-01	1.78E-01	1.79E-01	1.72E-01	1.81E-01
<b>Rod Prepressurization<sup>2</sup></b>							
He	1.829E-02	1.646E-02	3.447E-02	3.336E-02	3.365E-02	9.058E-02	9.334E-02

- 1 Values are based on assembly bundle average burnup of 40,000 MWD/MTU, initial bundle average enrichment of 3.3 wt% U-235, and 10 year cooling.
- 2 Based on the fuel assembly data from Table 5.2-1.

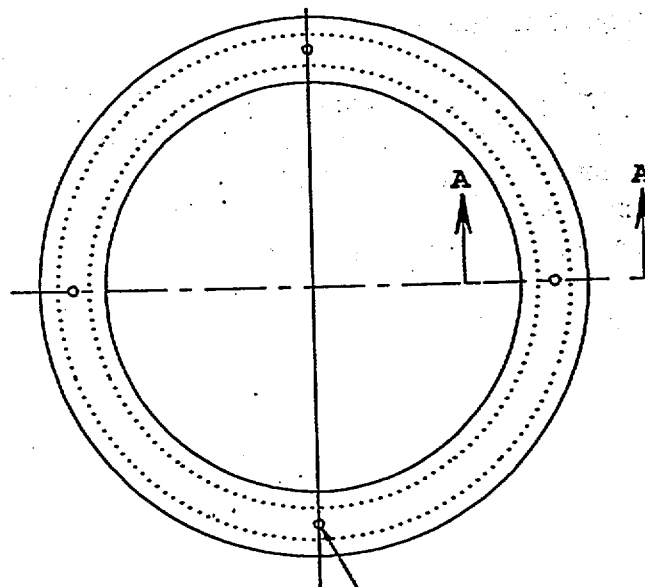
TABLE 4-7  
CASK GAS MIXTURES  
UNDER NORMAL TRANSPORT AND HYPOTHETICAL ACCIDENT CONDITIONS

	<u>Normal Transport Conditions (3% Fuel Rod Failure)</u>						
	<u>7x7-49-0</u> (kgmole/cask)	<u>8x8-63-1</u> (kgmole/cask)	<u>8x8-62-2</u> (kgmole/cask)	<u>8x8-60-4</u> (kgmole/cask)	<u>8x8-60-1</u> (kgmole/cask)	<u>9x9-74-2</u> (kgmole/cask)	<u>10x10-92-2</u> (kgmole/cask)
<b>Fission Products</b>							
I	2.54E-04	2.41E-04	2.38E-04	2.34E-04	2.35E-04	2.26E-04	2.39E-04
Kr	5.95E-04	5.67E-04	5.63E-04	5.52E-04	5.56E-04	5.38E-04	5.68E-04
Xe	5.73E-03	5.47E-03	5.43E-03	5.35E-03	5.38E-03	5.16E-03	5.42E-03
<b>Prepressurization</b>							
He	5.487E-04	4.938E-04	1.034E-03	1.001E-03	1.009E-03	2.717E-03	2.800E-03
<b>Helium Backfill</b>							
He	3.506E-01	3.506E-01	3.506E-01	3.506E-01	3.506E-01	3.506E-01	3.506E-01
<b>Total</b>	3.577E-01	3.574E-01	3.579E-01	3.577E-01	3.578E-01	3.592E-01	3.596E-01
	<u>Hypothetical Accident Conditions (100% Fuel Rod Failure)</u>						
	<u>7x7-49-0</u> (kgmole/cask)	<u>8x8-63-1</u> (kgmole/cask)	<u>8x8-62-2</u> (kgmole/cask)	<u>8x8-60-4</u> (kgmole/cask)	<u>8x8-60-1</u> (kgmole/cask)	<u>9x9-74-2</u> (kgmole/cask)	<u>10x10-92-2</u> (kgmole/cask)
<b>Fission Products</b>							
I	8.47E-03	8.05E-03	7.92E-03	7.79E-03	7.82E-03	7.52E-03	7.97E-03
Kr	1.98E-02	1.89E-02	1.88E-02	1.84E-02	1.85E-02	1.79E-02	1.89E-02
Xe	1.91E-01	1.82E-01	1.81E-01	1.78E-01	1.79E-01	1.72E-01	1.81E-01
<b>Prepressurization</b>							
He	1.829E-02	1.646E-02	3.447E-02	3.336E-02	3.365E-02	9.058E-02	9.334E-02
<b>Helium Backfill</b>							
He	3.506E-01	3.506E-01	3.506E-01	3.506E-01	3.506E-01	3.506E-01	3.506E-01
<b>Total</b>	5.881E-01	5.765E-01	5.926E-01	5.886E-01	5.899E-01	6.388E-01	6.515E-01

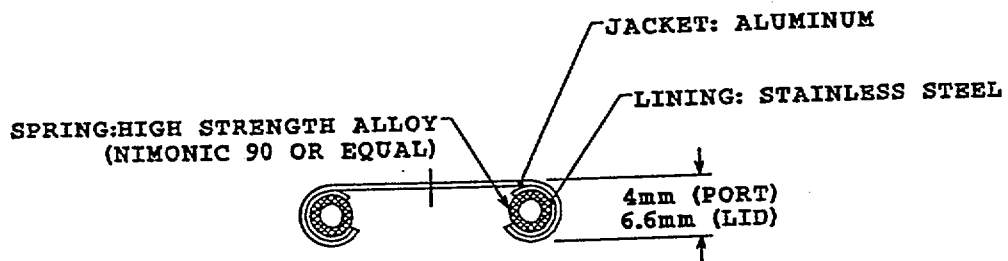


Notes:

1. Figure not to scale. Features exaggerated for clarity.
2. Phantom lines (— · · — · · — ) indicates containment boundary.
3. Containment boundary components are listed below:
  - 1 Cask body and inner shell.
  - 2 Lid assembly outer plate, closure bolts and inner o-rings.
  - 3 Bolting flange.
  - 4 Vent port cover plate, bolts and seals.
  - 5 Drain port cover plate, bolts and seals.



HOLES, AS REQ'D. FOR ATTACHMENT SCREWS & OVERPRESSURE PORT COMMUNICATION.



SECTION A-A

FIGURE 4-2  
LID. VENT PORT & DRAIN PORT  
METAL SEALS

## CHAPTER 6

### CRITICALITY EVALUATION

#### 6.1 Discussion and Results

Criticality control in the TN-68 is performed by the basket structural components, which maintain the relative position of the spent fuel assemblies under normal and accident conditions as demonstrated in Chapter 2, and by the neutron absorbing plates between the basket compartments.

The TN-68 contents are limited to the GE fuel designs listed in Chapter 1, with a maximum lattice-average enrichment of 3.7 wt % U235. Fuel assemblies with or without channels are acceptable. Any fuel channel thickness up to 0.120 inch is acceptable on any of the fuel designs. Criticality control does not require special loading patterns or special rotational orientation of the fuel assemblies. The TN-68 may be loaded with pool water at maximum density, i.e., at 4 °C.

The criticality evaluation is organized as follows:

- a) Determination of the most reactive lattice (Section 6.4.2A). All of the design basis fuels are evaluated with uniform enrichment to determine the most reactive geometry. The effect of water in the fuel pins and of fuel channels is also evaluated.
- b) Uniform enrichment model validation (Section 6.4.2B). The results using fuel lattice models with pin-by-pin enrichment variation are compared with results obtained using uniform enrichment models. Vanished lattices are also compared with the uniform enrichment models. If the uniform enrichment model underpredicts  $k_{eff}$ , the modeling bias will be determined and the Upper Subcritical Limit will be reduced by that amount.
- c) TN-68 single package evaluation (Section 6.4.2C). The uniform enrichment model of the most reactive fuel lattice is used for this evaluation. The TN-68 package is evaluated for the following conditions:
  - varied water density,
  - varied fuel compartment inside dimension and pitch between compartments,
  - off-center placement of fuel in the compartments.
  - combined effects: most reactive normal configuration
  - hypothetical accident condition.
- d) TN-68 package infinite array evaluation (Section 6.4.2D).
  - most reactive normal configuration bounds the hypothetical accident condition
- e) Benchmarking (Section 6.5). An upper subcritical limit (USL) is determined by subtracting from unity an administrative margin of 0.05, the bias determined from benchmark calculations and any modeling bias.

All calculations assume fresh fuel composition and ignore burnable poisons. Non-uniform flooding of the basket is not evaluated because all the spaces in the basket are interconnected, and therefore this is not a credible condition.

## Results

The maximum  $k_{\text{eff}}$  under all evaluated conditions is  $0.9250 \pm 0.0008$ . The upper subcritical limit (USL) is 0.9331. In all cases,  $k_{\text{eff}} + 2\sigma < \text{USL}$ .

### 6.2 Package Fuel Loading

The allowable contents are listed in Chapter 1. Fuel characteristics used in the criticality calculations are listed in Table 6.2-1. Because an infinite array of packages is evaluated for both normal and accident conditions, the transport index for criticality safety is zero.

Where fuel pins have variable axial enrichment, the average is calculated for each axial zone (lattice), and the lattice with the highest average enrichment is used to characterize the entire bundle for criticality purposes. The average enrichment is defined as the simple arithmetic average of pin enrichments:

$$E_{\text{avg}} = \sum_{i=1,n} E_i / n$$

Where  $E_i$  is the enrichment of pin  $i$ , and  $n$  is the number of fuel pins in the lattice. There is no averaging of the axial enrichment variation in this evaluation; "bundle average" enrichments, which are an average enrichment over the entire fuel bundle, including natural uranium blankets, are not used to qualify fuel for transport in the TN-68.

To maintain subcriticality, the maximum lattice-average enrichment of the fuel bundle must be less than or equal to 3.7 weight % U235.

The acceptable contents of the TN-68 do not include failed fuel other than fuel with hairline cracks or pinholes in the cladding. Fuel bundles from which fuel pins are missing are not allowable contents unless the missing pin is replaced.

### 6.3 Model Specification

#### 6.3.1 Description of Calculational Model

Infinite length fuel, basket, and packaging body are modeled by taking one "layer" of the basket, as shown in Figure 6.3-1, and applying periodic reflection to the top and bottom. Fuel pins are modeled individually. Water rods in the fuel are modeled explicitly, except for fuels where large water rods displace several fuel rods. In those cases, due to modeling constraints, the water rods are modeled as water cells, without the Zircaloy tube. The stainless steel basket compartment tubes, stainless steel bars, neutron poison plates, egg-crate gaps, and thermal expansion gaps are modeled explicitly as shown in Figures 6.3-2 through 6.3-8. The dimensions used for the neutron poison plates and the gaps are shown in Table 6.3-1, which compares the model dimensions with the design dimensions. The thermal expansion gaps and the vertical egg-crate

slots are wider in the model than in the TN-68 design, and the area of the neutron poison plate is correspondingly smaller.

The dimensional variations in the basket that can affect criticality are the thickness of the tube and plate materials, and the inside dimension of the tubes. Except as noted, all cases are run with the nominal compartment inside dimension, 6 inches. Section 6.4.2C demonstrates that  $k_{eff}$  decreases as the compartment size increases, and it also demonstrates criticality safety for the minimum compartment size, 5.97 inches. The tolerances on the plate and tube materials are very small (see Table 6.3-1). The undersize allowance is negligible from the criticality standpoint, and the oversize tolerance would decrease reactivity. Furthermore, in practice it is not possible to assemble the basket compartments and plates perfectly line to line as they are in the criticality model, so the compartments will be slightly further apart than the plate thicknesses alone would indicate. These considerations confirm that the material thicknesses used in the calculations are appropriate.

The aluminum basket rails, packaging body, and outer water reflector are included, and the outer neutron shield is neglected. The complete package model is shown in Figure 6.4-4. The following differences between the model and the design have been evaluated:

Model	Design
0.156 inch thick outer absorber plates	0.305 inch thick outer absorber plates
egg crate slots repeated at all compartment corners, including ends of plates	plates have thermal expansion gap up to 0.5 inch wide at the ends of each plate
aluminum basket rails all around	stainless steel rail at 4 axes of basket
4 outermost plates are 0.156 thick, borated	4 outermost plates are 0.156 inch thick, non-borated aluminum
Basket rail holes circular	Basket rail holes triangular

The first four changes are evaluated by the model shown in Figure 6.3-9. In this model,

- half thickness borated aluminum plates are added at the perimeter
- this added material is only half the compartment width; the volume of the plates still left out at the intersections is greater than the volume of neutron absorber that would be removed if the plates were cut 0.5 inch shorter at their ends
- stainless steel plates are inserted at the axes
- at the four axes, the outermost basket plate is replaced with non-borated aluminum

A comparison of this model with the baseline indicates that the model is equivalent to, or conservative with respect to the design:

baseline model:	$k_{eff} = 0.9151 \pm 0.0016$
design approximation model:	$k_{eff} = 0.9123 \pm 0.0016$ .

The triangular openings in the design basket rails have a larger cross sectional area than the cylindrical holes used in the criticality model. By reducing the amount of water at the basket perimeter, the moderation of reflected neutrons is reduced. This in turn reduces the effectiveness of the borated aluminum plate at the basket perimeter in capturing returning neutrons. Less water at the perimeter causes increasing reactivity, and therefore the model with the cylindrical holes is conservative.

The description above refers to the model used for the single package evaluation, Section 6.4.2 C. The models used for the most reactive fuel evaluation and the uniform enrichment validation are somewhat different. The differences are described in the respective calculation descriptions. For array evaluations, the cylindrical water reflector is replaced with a close fitting, water cuboid with mirror reflection on all sides.

### 6.3.2 Package Regional Densities

Materials are converted to atom densities by the Material Information Processor in the CSAS25 code sequence<sup>(1)</sup>. The mass densities supplied to the code are reported in Table 6.3-2.

Two materials are modeled for the poison plates. The first is an alloy of aluminum and about 1.7 wt% boron, the boron being enriched to about 95 wt % B10. Because this material is subjected to extensive acceptance testing as described in Chapter 8, the calculations take credit for 90% of the minimum specified boron 10 areal density. The density used in the calculation is 0.034 g B10/cm<sup>3</sup>, and the plate thickness is 0.792 cm. The corresponding areal density is  $0.034(0.792) = 0.0269$  gB10/cm<sup>2</sup>. The minimum specified boron content, using 90% credit is  $0.0269/0.9 = 0.030$  g B10/cm<sup>2</sup>.

The second material evaluated is a boron-carbide/aluminum metal matrix composite, consisting of about 15 volume % boron carbide particles and 85 % aluminum. This is subject to less rigorous acceptance testing as described in Chapter 8. In this case, the calculations take 75% credit for the B10, and the minimum specified boron content for this material is 0.036 g B10/cm<sup>2</sup>.

Studies have been conducted to show that neither of these materials will degrade significantly as both have excellent resistance to thermal and radiation alteration in the service environments of interest to this application. Both are solid, non-friable materials physically similar to their base aluminum alloys. Neither material includes any organic components or binders. They are held in place and protected from damage by the surrounding stainless steel bar and tube structure. The basket structure encloses the neutron absorber plates on all six sides.

## 6.4 Criticality Calculation

### 6.4.1 Calculational or Experimental Method

All calculations are performed using the CSAS25 sequence from the SCALE4.3 code system<sup>(1)</sup> with the SCALE 27-group ENDF/B-IV cross section library. Within this sequence, resonance correction based on the fuel pin cell description is performed by NITAWL using the Nordheim Integral method, and  $k_{\text{eff}}$  is determined by the KENOva code using the Monte Carlo technique. A sufficiently large number of neutron histories is run so that the standard deviation is below 0.0020 for all calculations.

### 6.4.2 Fuel Loading or Other Contents Loading Optimization

#### A. Determination Of The Most Reactive Fuel Lattice

## A. Determination Of The Most Reactive Fuel Lattice

All lattices listed in Table 6.2-1 are evaluated with the maximum TN-68 design basis lattice enrichment, 3.7%, in all pins. The lattices are analyzed with and without water in the fuel pellet-cladding annulus, and with and without fuel channels. All lattices are analyzed with the minimum and maximum fuel channel thicknesses, 0.065 and 0.120 inch thick, and one intermediate thickness. The lattices are centered in the fuel compartments.

The package model for this evaluation differs from the TN-68 design in the following ways:

- the boron 10 content in the poison plates is lower,
- the egg-crate (vertical) slots run the full height of the poison plate,
- the fuel, basket, and packaging body are infinite length (periodic reflection on "z" faces of model),
- the basket rails are a homogenized 50/50 volume % mixture of water and aluminum, and
- the stainless steel bars between compartments are modeled as carbon steel.

In all other respects, the model is the same as that described in Sections 6.3.1 and 6.3.2. The sole purpose of this model is to determine the *relative* reactivity of different lattices in a configuration similar to the TN-68. The model is shown in Figure 6.4-1.

A typical input file is included in Appendix 6.7. The results of these calculations are listed in Table 6.4-1. The most reactive fuel lattice evaluated for the TN-68 is the GE generation 12 lattice, 10x10 array, with water in the fuel rods and with the 0.065 inch thick fuel channel.

## B. Uniform Enrichment Model Validation

Except for the earliest fuels, BWR fuel lattices do not actually have the same enrichment fuel in each fuel pin. It is necessary to validate the use of fuel lattice models in which all fuel pins have the same enrichment, because the most reactive fuel evaluation and the TN-68 criticality use this model. To do this,  $k_{eff}$ 's of variable pin-enrichment lattice models and of equivalent uniform enrichment lattice models are calculated and compared. The variable enrichment pin models are all normalized so that the lattice average enrichment is 3.7 %. The pin enrichment patterns and the normalized equivalents are shown in Appendix 6.8. In all those patterns, the control blade corner is in the upper right, and the highest enrichment corner is in the lower left; they are oriented this way in the quarter-basket model so that the highest enrichment zones face the package longitudinal axis. The equivalent average enrichment for the uniform enrichment model is defined in Section 6.2.

The package model for this evaluation differs from the TN-68 design in the following ways:

- the boron 10 content in the poison plates is lower,
- the egg-crate (vertical) slots run the full height of the poison plate,
- the fuel, basket, and packaging body are infinite length (periodic reflection on "z" faces of model),
- the basket rails are a homogenized 50/50 volume % mixture of water and aluminum,
- the stainless steel bars between compartments are modeled as carbon steel, and

- the package is modeled with a square cross section and 64 fuel assemblies. This is a significant difference from the actual package, but again, the sole purpose of this model is to determine the *relative* reactivity of different fuel models in a configuration similar to the TN-68. The square cross section was used to simplify modeling the case where the highest enrichment zones of the variable pin enrichment fuel lattices are all rotated toward the package longitudinal (z) axis. This is done by modeling a quarter of the package cross section, and then using mirror reflection along the x and y axes. This orientation is more reactive than either random or uniform rotational orientation of the lattices. The model is shown in Figure 6.4-2.

The results of the calculation are listed in Table 6.4-2. The case designations may be correlated to the pin enrichment patterns by referring to Appendix 6.8. The last six cases in the table are vanished lattice cases corresponding to the six cases immediately before them. These are the lattices above the partial length fuel rods; the partial length rod has vanished, and is replaced by water, as shown in Figure 6.4-3. Because of the improved moderation, the vanished lattice can be more reactive than the complete lattice. Typical input files for the varied enrichment model of both the full and vanished lattices are included in Appendix 6.7.

Examination of the difference between  $k_{\text{eff}}$  calculated with the uniform enrichment model and  $k_{\text{eff}}$  calculated with the varied enrichment model indicates that the uniform enrichment model has an average positive (conservative) bias of  $0.0032 \pm 0.0037 \Delta k_{\text{eff}}$ . Subtracting  $2\sigma$  results in a negative bias of 0.0042 which will be applied in the determination of the Upper Subcritical Limit in Section 6.5.3.

### C. TN-68 Single Package Evaluation

This evaluates the TN-68 in a variety of configurations intended to bound all normal and accident conditions. The following conditions are evaluated for the three most reactive fuels as determined from Table 6.4-1: 10x10, 0.065 channel, 7x7(2, 2b), 0.120 channel, and 8x8(9, 9b, 10), 0.120 channel. All fuels are modeled with uniform pin enrichment. There is water in the fuel pellet-cladding annulus and inside the package.

- Baseline: Fuel centered in 6 inch compartments, 100% water density. TN-68 model and material densities per Sections 6.3.1 and 6.3.2.
- The inside dimension of the compartment is increased to 6.05 inches. All compartments move correspondingly further apart. This case verifies that the minimum compartment size is the most reactive dimensional configuration. By moving the compartments closer together, it reduces the neutron leakage, and by reducing the thickness of the water layer between the lattice and the compartment wall, it reduces the effectiveness of the neutron poison plates between the compartments.
- Variation of water density throughout: The water density in the fuel and the entire basket is varied from 1 to 100%, including water at the maximum density of  $1.000 \text{ g/cm}^3$ , which occurs at  $4 \text{ }^\circ\text{C}$ . The water reflector remains at full density ( $0.9982 \text{ g/cm}^2$ ) for all cases.
- Fuel lattices off-center in the compartments: Several channel thicknesses and a lattice with no channel are investigated. All lattices are shifted toward the longitudinal axis of the basket until the fuel channel or the outer pin cells of the lattice contact two compartment walls. This is not a credible configuration, but is intended to bound all cases of off-center fuel.

These evaluations confirm that

- optimum internal moderation occurs for full density water; the difference between  $1.00 \text{ g/cm}^3$  and  $0.9982 \text{ g/cm}^3$  is negligible.
- the most reactive fuel configuration is the fuel with a 0.120 inch thick channel shifted off the compartment center toward the package center, and
- a smaller basket compartment sizes results ins a more reactive basket configuration.

Based on these conclusions, the combination of optimum moderation, most reactive fuel configuration, and minimum compartment size, 5.97 inches, is evaluated for both the borated aluminum and the metal matrix composite neutron absorbers.

The results are reported in Table 6.4-3. The model for the combination of off-center fuel with minimum compartment size is shown in Figure 6.4-4, and sample input files are included in Appendix 6.7.

Lastly, the analysis considers the hypothetical drop accident, and the consequent accelerations experienced by the fuel assemblies. The evaluations in Chapter 2 demonstrate that the basket geometry is maintained in the hypothetical accident. Appendix 2.10.7 provides a structural analysis of the fuel under hypothetical accident conditions. Based on the conclusions of Appendix 2.10.7, the accident criticality analysis assumes that the fuel pins do not shear through, but the fuel pin spacer grids collapse, resulting in the fuel rods moving closer together. Therefore, reduced pin pitch is evaluated as the credible tipover accident configuration. The 7x7, 8x8, 9x9, and 10x10 lattices are modeled with pin pitch uniformly reduced. For the 7x7, 8x8, and 10x10 the baseline models above are used. For the 9x9, a similar baseline model is used, based on the most reactive 9x9 fuel in Table 6.4-1. The results, listed in Table 6.4-4, confirm that for all lattices,  $k_{\text{eff}}$  in the TN-68 basket decreases with decreasing pin pitch. Therefore, the hypothetical accident is bounded by the normal conditions evaluated above.

#### D. Package Array Evaluation

An infinite rectangular array of packages with optimum internal moderation and interspersed water is modeled to demonstrate criticality safety for both the normal and damaged package arrays.

The array evaluation uses the combined worst case contents configuration and optimum internal moderation from the single package normal conditions evaluation. Fuel assemblies are assumed to be intact, which is the most reactive condition as shown by the single package hypothetical accident evaluation. The same three fuel designs evaluated for the single package are evaluated for the array.

The input files from the single package evaluation are modified by changing the outer water cylinder to a water filled cuboid tangent to the outside of the packaging, and applying mirror neutron reflection to all faces. To find optimum interspersed moderation, the water density in the external cuboid (the space between the packages) is varied, while the internal moderator density is held constant at its optimum value.

The neutron shield and the impact limiters are neither modeled, nor considered in the spacing of packages in the array. The impact limiters in particular would have the effect of increasing the package spacing if they were included.

The results are presented in Table 6.4-5. As expected for a heavy-walled package, there is little difference between the single package and array results. Variation of the interspersed water density results in random variations in  $k_{\text{eff}}$ , with no discernable trend.

### 6.4.3 Criticality Results

The highest result for the single package, normal and accident conditions is  $k_{\text{eff}} = 0.9240 \pm 0.0008$ , which occurs for 10x10 fuel with 0.120 thick channels, intact fuel assemblies shifted toward package center, and 100% density water internal moderation.

The highest result for an infinite array of packages, normal and accident conditions is  $k_{\text{eff}} = 0.9250 \pm 0.0008$ , which occurs for 10x10 fuel with 0.120 thick channels, intact fuel assemblies shifted toward the package center, 100% density water internal moderation and 75% density water interspersed moderation.

## 6.5 Critical Benchmark Experiments

### 6.5.1 Benchmark Experiments and Applicability

The critical experiments and input files are taken from NUREG/CR-6361<sup>(5)</sup>. The input files are obtained from ORNL, and modified to change the cross section library to the SCALE 27 group library that is used in all the TN-68 criticality evaluations. Experiments which feature simple arrays, separator plates, steel reflector walls, water holes, and borated poison plates are selected. Experiments with features that are not characteristic of the TN-68 transport packaging are not used. Such features include soluble boron, poisons other than boron, poison rods, reflector walls other than steel, and flux traps. The 73 critical experiments chosen, and their descriptive characteristics are listed in Table 6.5-1.

### 6.5.2 Details of Benchmark Calculations

An upper subcritical limit (USL) is determined using Method 1, "confidence band with administrative margin", described in Section 4.1.1 of NUREG/CR-6361. The USLSTATS program, Version 1.3.4, distributed by Oak Ridge National Laboratory and described in NUREG/CR-6361 is used to perform the statistical analysis. The administrative margin is 0.05, and the confidence level  $1-\gamma_1$  will be 0.95. It is assumed that the actual value of  $k_{\text{eff}}$  in all the experiments is exactly 1.

The characteristics water/fuel volume, hydrogen to fissile atom ratio (H/X), fuel pin pitch, and enrichment are listed in Tables 2.1 and 3.5 of NUREG/CR-6361. One additional characteristic, boron 10 concentration in the separator plates, is calculated in Table 6.5-2. A comparison of the range of these characteristics in the experiments, and the corresponding values for the TN-68 and

its contents verifies that the TN-68 falls within the range covered by the critical experiments. See Table 6.5-4.

Criticality calculations and benchmarks were performed on the same platform, a Hewlett Packard 9000/715 Workstation.

### 6.5.3 Results of Benchmark Calculations

The quantitative characteristics of the critical experiments and results of the benchmark calculations are listed in Table 6.5-3.

Eight subsets of the results are analyzed to determine if there is a trend in the bias (calculated  $k_{eff}$  -1) as a function of an experimental variable. In all subsets, the data test normal, although the sample size for the boron density is too small for this determination to be conclusive. A least mean squares linear regression is performed to fit the data of  $k_{eff}$  as a function of each independent variable, and the Pearson correlation coefficient  $r$  is determined. A coefficient of zero indicates no correlation, and a coefficient of  $|1|$  indicates exact correlation. The results are listed in Table 6.5-4. The values of the correlation coefficient, as well as a visual examination of the data plots, indicate that there is very little correlation between the bias and any of the experimental variables, and therefore, no discernable trend. The best correlation between bias and an experimental variable occurs for enrichment. The data and the linear regression results for the ratio of water volume to fuel volume in the pin cell are plotted in Figure 6.5-1.

The minimum value of the USL from all the data sets is 0.9373, which occurs for pin cell water to fuel pellet volume ratio, as shown in Table 6.5-4.

There is no modeling bias due to the package model as discussed in Section 6.3.1. The modeling bias due to the use of a uniform pin enrichment model of the lattice is -0.0042, as discussed in Section 6.4.2B. This bias is added to the USL determined from the benchmark evaluation:

$$0.9373 - 0.0042 = 0.9331$$

This is the USL value used in the TN-68 criticality analysis.

## 6.6 References

1. SCALE-4.3, Modular Code System for Performing Standardized Computer Analyses for Licensing Evaluation for Workstations and Personal Computers, CCC-545, ORNL, March 1997.
2. ORNL/TM-10902, Physical Characteristics of GE BWR Fuel Assemblies, 1989.
3. GE Proprietary Data
  - a. Initial Core Fuel Design Summary for Peach Bottom Atomic Power Station Unit 3, NEDC-10816, March 1973
  - b. Peach Bottom 2 Reload 1 Nuclear Design Report, NEDE 21051, September 1975
  - c. Peach Bottom 3 Reload 2 Nuclear Design Report, NEDE 21759, December 1977
  - d. Peach Bottom 2 Reload 3 Nuclear Design Report, NEDE 23896, July 1978
  - e. Fuel Bundle Design Report GE8B-P8DQB321-11GZ-80M-4WR-150-T
  - f. Fuel Bundle Design Report GE8B-P8DQB319-9GZ-80M-4WR-150-T
  - g. Fuel Bundle Design Report GE9B-P8DWB310-11GZ-80M-150-T
  - h. Fuel Bundle Design Report GE9B-P8DWB324-10GZ-80M-150-T
  - i. Fuel Bundle Design Report GE9B-P8DWB320-10GZ-80M-150-T
  - j. Fuel Bundle Design Report GE9B-P8DWB324-10GZ1-80M-150-T
  - k. Fuel Bundle Design Report GE9B-P8DWB328-11GZ-80M-150-T
  - l. Fuel Bundle Design Report GE11-P9HUB307-5G5.0/4G4.0-100M-146-T-LTA
  - m. Fuel Bundle Design Report GE11-P9HUB334-10GZ1-100M-146-T
  - n. Fuel Bundle Design Report GE11-P9HUB367-11GZ-100M-146-T
  - o. Fuel Bundle Design Report GE11-P9HUB387-12GZ3-100T-146-T
  - p. Fuel Bundle Design Report GE11-P9HUB405-13GZ1-100T-146-T
  - q. Fuel Bundle Design Report GE13-P9DTB400-13GZ-100T-146-T
  - r. Fuel Bundle Design Report GE13-P9DTB397-13GZ-100T-146-T
  - s. Fuel Bundle Design Report GE13-P9DTB392-15GZ-100T-146-T
  - t. Fuel Bundle Design Report GE13-P9DTB39-13GZ-100T-146-T
  - u. Fuel Bundle Design Report 8DRB284-7G4.0-100M-150
  - v. Fuel Bundle Design Report 8DRB285-4G2.0-100M-150
  - w. Fuel Bundle Design Report 8DRB299-7G4.0-100M-150
  - x. Fuel Bundle Design Report P8DRB299-3G5.0/4G4.0-100M-150
4. Power Authority of the State of New York, Inquiry No. Q-02-1961 (RFQ for FitzPatrick Dry Spent Fuel Storage System)
5. NUREG/CR-6361, Criticality Benchmark Guide for Light-Water-Reactor Fuel in Transportation and Storage Packages, 1997
6. NAC UMS Safety Analysis Report, Rev. 0, EA790-SAR-001, Docket No. 71-9270.

# TN 68 TRANSPORT PACKAGING

## CHAPTER 7

### TABLE OF CONTENTS

	<u>Page</u>
7. OPERATING PROCEDURES	
7.1 Package Loading.....	7-1
7.1.1 Preparation for Loading.....	7-1
7.1.2 Loading.....	7-2
7.1.3 Preparation for Transport.....	7-3
7.2 Package Unloading.....	7-6
7.2.1 Receipt of Package from Carrier.....	7-6
7.2.2 Preparation for Unloading.....	7-6
7.2.3 Contents Removal.....	7-7
7.3 Preparation of Empty package for Transport.....	7-8
7.4 Other Procedures.....	7-11
7.4.1 Preparation of Cask Used in Storage for Transport.....	7-11
7.5 References.....	7-13

### LIST OF FIGURES

- 7-1 Torquing Pattern
- 7-2 Typical Setup for filling Cask with Water

This page intentionally blank

## CHAPTER 7

### OPERATING PROCEDURES

This chapter contains TN-68 loading and unloading procedures that are intended to show the general approach to cask operational activities. A separate Operations Manual (OM) will be prepared for the TN-68 to describe the operational steps in greater detail. The OM, along with the information in this chapter, will be used to prepare the site-specific procedures that will address the particular operational considerations related to the cask. The operations required to convert the cask from its storage configuration to its transport configuration are also described in here.

#### 7.1 PACKAGE LOADING

##### 7.1.1 Preparation for Loading

- 7.1.1.1 Upon arrival of the empty packaging, on its transport vehicle (rail or heavy haul trailer) and shipping frame, perform a receipt inspection to check for any damages or irregularities. Verify that the records for the packaging are complete and accurate.
- 7.1.1.2 Remove the security device, the impact limiter attachment bolts, tie-rods, and the associated hardware, as necessary.
- 7.1.1.3 Remove the front and the rear impact limiters, as well as the front spacer and the ancillary shield ring, using a suitable crane and a two-legged sling or an equivalent.
- 7.1.1.4 Remove the tie-down strap and trunnion support block caps.
- 7.1.1.5 Clean the external surfaces of the cask, if necessary, to get rid of the road dirt.
- 7.1.1.6 Attach the lift beam to the cask handling crane hook, and engage the lift beam to the two upper (top) trunnions.
- 7.1.1.7 Rotate the cask slowly from the horizontal to the vertical position.
- 7.1.1.8 Lift the cask from the transport/shipping frame and place it in the cask preparation area.
- 7.1.1.9 Disengage the lift beam from the cask
- 7.1.1.10 Remove the neutron shield pressure relief valve and install the plug in the neutron shield vent hole.
- 7.1.1.11 Remove the lid bolts and the lid.
- 7.1.1.12 Replace the lid seal using the retaining screws, and inspect the lid sealing surface. Check for defects in the seal contact areas that may prevent a proper seal. (This step may be performed at any time prior to installing the lid on the loaded cask).

- 7.1.1.13 Replace the seals in the vent, drain and transport covers, and inspect the sealing surfaces. Check for defects in the seal contact areas that may prevent a proper sealing. (This step may be performed at any time prior to installing covers on the loaded cask).
- 7.1.1.14 Visually inspect the lid bolts and the bolt hole threads to ensure that they do not have any laps, seams, cracks or damaged threads.
- 7.1.1.15 Remove the hold down ring from the cask cavity.
- 7.1.1.16 Verify that the basket is installed in the cask, with no evident signs of damage to either. Verify that there is no foreign material in the cask.
- 7.1.1.17 Move the cask to the cask loading area using the lift beam attached to the top trunnions.

## 7.1.2 Loading

Note: The term 'cask loading pool' is used to describe the area where the cask is to be loaded.

- 7.1.2.1 Lower the cask into the cask loading pool, while rinsing the exterior of the cask with demineralized water and filling the interior with demineralized or pool water.
- 7.1.2.2 Disengage the lift beam and move it aside.
- 7.1.2.3 Load the pre-selected spent fuel assemblies into the basket compartments. Procedures shall be developed to ensure that the fuel loaded into the cask meets the fuel specifications in chapter 1.2.3 of the SAR.
- 7.1.2.4 Verify the identity of the fuel assemblies loaded into the cask, and document the location of each fuel assembly on the cask loading report.
- 7.1.2.5 At least one lid penetration (drain or vent port) must be completely open (both cover and quick-disconnect fitting removed) prior to the installation of the lid. Using the lift beam and the lid lifting slings, lower the lid placing it on the cask body flange over the two alignment pins.
- 7.1.2.6 Engage the lift beam on the upper (top) trunnions, and lift the cask so that the top of the cask is above the water surface in the pool, and install some of the lid bolts. The lid bolts should be hand tight.

Note: Throughout this procedure, all bolt threads are to be coated with Nuclear Grade Neolube or equivalent.

- 7.1.2.8 Using the drain port in the lid, drain the water from the cask. The cask is drained by connecting one end of a drain hose to the Hansen coupling in the drain port and routing the other to a pump. This may be done either before or after lifting the cask out of the pool. While lifting the cask out of the pool, the exterior of the cask may be rinsed with clean deionized water to facilitate decontamination.

Note: In order to minimize internal hydrogen accumulation, the cask should be drained completely within 18 hours of the start of draining. If this period is exceeded, the cask cavity should be inerted by injecting nitrogen, argon or helium through the open lid penetration, while the draining continues. An initial gas flow rate of 0.6 m<sup>3</sup> per minute (21 cfm) will purge the cask cavity volume in about 10 minutes, after which the flow rate can be reduced to about 3 cfm until the draining is complete.

- 7.1.2.9 Disconnect the drain line.
- 7.1.2.10 Move the cask to the decontamination area and disengage the lift beam.

### 7.1.3 Preparation for Transport

Note: The maximum potential for worker exposure exists during the decontamination of the cask and other operations near the lid, after the water is pumped out of the cask. Worker exposure can be minimized by use of temporary shielding (lead "bean bags", plastic neutron shielding), and by minimizing the exposure time and maximizing the distance, as well as using any measures to facilitate decontamination.

- 7.1.3.1 Decontaminate the cask until acceptable surface contamination levels are obtained.
- 7.1.3.2 Install the remaining lid bolts and torque them to 200 ft-lbs. Follow the torquing sequence shown in Figure 7-1. Repeat the torquing process following the sequence of Figure 7-1. Torque to 600 ft-lbs in the second pass, 1000 ft-lbs in the third pass and between 2050 and 2100 ft-lbs in the final pass. A circular pattern of torquing may be used, to eliminate further bolt movement.
- 7.1.3.3 Remove the plug from the neutron shield vent, and reinstall the pressure relief valve, making sure that it is operable and set.
- 7.1.3.4 Evacuate the cask cavity using the Vacuum Drying System (VDS) to remove the remaining moisture, and verify the dryness as follows:
- a) Using a wand attached to the vacuum drying system, remove any excess water from the seal areas through the passageways at the overpressure drain and vent ports.
  - b) Remove the quick disconnect from the drain port, and install the drain port cover.

- c) With the quick disconnect removed to improve evacuation, connect the VDS to a flanged vacuum connector installed over the vent port. Purge or evacuate the helium supply lines and evacuate the cask to 4 millibar ( $4 \times 10^{-4}$  MPa) or less. Make provisions to prevent or correct any icing of the evacuation lines, if necessary.
- d) Isolate the vacuum pump. If, in a period of 30 minutes, the pressure does not exceed 4 millibar ( $4 \times 10^{-4}$  MPa), the cask is adequately dried. Otherwise, repeat the vacuum pumping until this criterion is met.
- e) Backfill the evacuated cask cavity with helium (minimum 99.99% purity), to slightly above atmospheric pressure. Then, remove the vacuum connector and immediately install the quick disconnect fitting.
- f) Attach the vacuum/backfill manifold to the vent port fitting, purge or evacuate the helium supply lines, and re-evacuate the cask to below 100 mbar.

7.1.3.5 Isolate the vacuum pump, and backfill the cask cavity to approximately 2.0 atm abs (14.7 psig) with helium (minimum 99.99% purity).

7.1.3.6 Leak test the inner lid, inner vent and drain port cover seals. The maximum acceptable cask seal leak rate is  $1 \times 10^{-5}$  ref  $\text{cm}^3/\text{sec}$ . The leak test shall be performed in accordance with ANSI N14.5<sup>(2)</sup>. For ports containing quick-disconnects, purge the cavity below the cover with helium, at a minimum flow rate of 80 cubic feet per hour for at least 20 seconds. Install the port cover. (A partial pressure of at least 50% helium will be obtained under the cover.) Install the vent and drain cover bolts and torque to 35 ft-lbs in the first pass and to 60 - 65 ft-lbs in the final pass following the torquing sequence shown in Figure 7-1 prior to leak testing.

7.1.3.7 If the cask does not pass the leak test, determine the source of the leak. If the leak is in a vent or drain cover, remove the cover and replace the seals. Also examine the sealing surface for any obvious indication of scratches or defects. Repeat the leak test after replacing the seals.

7.1.3.8 If the cask still does not pass the leak test, evaluate the test method or return the cask to the pool and replace the lid seals.

7.1.3.9 Install the overpressure transport cover. Torque the bolts to the value specified on drawing 972-71-2.

7.1.3.10 Re-engage the lift beam to the upper (top) trunnions of the cask.

7.1.3.11 Move the transport vehicle into the loading position.

7.1.3.12 Lift the cask off the decontamination pad, and place the rear trunnions on the rear trunnion supports of the transport frame.

7.1.3.13 Rotate the cask from the vertical to the horizontal position.

7.1.3.14 Install the lower (bottom) trunnion support caps and the tie-down strap.

- 7.1.3.15 Check if the surface dose rates and the surface contamination levels are within the regulatory limits. Install an optional shield ring adjacent to the top of neutron shield, if required, based on dose limits.
- 7.1.3.16 Install the spacer on the front end of the cask. Then remove the spacer lifting eye bolts.
- 7.1.3.17 Install the front and the rear impact limiters onto the cask. Lubricate the attachment bolts with Never-Seez or an equivalent and torque to 200 ft-lb, diametrically in the first pass, and to 250 - 300 ft-lb in the final pass.
- 7.1.3.18 Install thirteen impact limiter attachment tie-rods between the front and the rear impact limiters.
- 7.1.3.19 Render the impact limiter lifting lugs inoperable by covering the lifting holes or installing a bolt inside the holes to prevent their inadvertent use.
- 7.1.3.20 Install security seal on one tie-rod and lock sleeve.
- 7.1.3.21 Install a transportation enclosure.
- 7.1.3.22 Check the temperature on all accessible surfaces to make sure that it is <math><185^{\circ}\text{F}</math>.
- 7.1.3.23 Perform a final radiation and contamination survey to satisfy the shield test requirements and to assure compliance with 10CFR71.47 and 71.87.
- 7.1.3.24 Apply appropriate DOT labels and Placards in accordance with 49CFR172. Prepare the final shipping documentation.
- 7.1.3.25 Release the loaded cask for shipment.

## 7.2 PACKAGE UNLOADING

### 7.2.1 Receipt of Package from Carrier

- 7.2.1.1 Upon arrival of the loaded cask, perform a receipt inspection of the cask to check for any damage or irregularities. Verify that the security seal is intact, and perform a radiation survey.
- 7.2.1.2 Verify that the records for the packaging are complete and accurate.
- 7.2.1.2 Remove the security seal, the impact limiters, tie-rods, and the associated hardware.
- 7.2.1.3 Render the impact limiter lifting lugs operable by removing the covering on the lifting holes or the bolt inside the lifting holes, that prevented their inadvertent use.
- 7.2.1.4 Remove the front and rear impact limiters as well as the front spacer, using a suitable crane and a two-legged sling or an equivalent.
- 7.2.1.5 Remove the tie down strap and trunnion support block caps.
- 7.2.1.6 Attach the lift beam to the cask handling crane hook, and then engage the lift beam to the two upper (top) trunnions.
- 7.2.1.7 Rotate the cask slowly from the horizontal to the vertical position.
- 7.2.1.8 Lift the cask from the transport/shipping frame, and place it in the decontamination area.
- 7.2.1.9 Disengage the lift beam from the cask, and move the crane as well as the lift beam from the area.
- 7.2.1.10 Clean the external surfaces of the cask, if necessary, to get rid of the road dirt.
- 7.2.1.11 Remove the neutron shield pressure relief valve, and install the plug in the neutron shield vent hole.

### 7.2.2 Preparation for Unloading

- 7.2.2.1 Remove the vent cover.
- 7.2.2.2 Collect a cavity gas sample, through the vent port quick-disconnect coupling, if required
- 7.2.2.3 Analyze the gas sample for radioactive material, and add necessary precautions based on the cavity gas sample results.

Note: If degraded fuel is suspected, additional measures, appropriate for the specific conditions, are to be planned, reviewed, and approved by the appropriate

plant personnel, as well as implemented to minimize worker exposures and radiological releases to the environment. These additional measures may include provision of filters, as well as respiratory protection and other methods to control releases and exposures to ALARA.

- 7.2.2.4 In accordance with the site requirements, vent the cavity gas through the hose until atmospheric pressure is reached.
- 7.2.2.5 Remove the vent port quick-disconnect and the drain port cover. Attach the vent port adapter.
- 7.2.2.6 Loosen the lid bolts and remove all but six lid bolts, approximately equally spaced.
- 7.2.2.7 Attach the cask to the crane using lift beam. Attach the lid lifting equipment.
- 7.2.2.8 Attach the fill and drain lines to the drain quick-disconnect coupling and the vent port adapter.
- 7.2.2.9 Ensure that appropriate measures are in place for proper handling of steam. Both fill and drain lines should be designed for a minimum of 100 psig steam, to prevent steam burns and radiation exposures due to a possible line failure.
- 7.2.2.10 Lower the cask into the spent fuel pool cask pit, while spraying the exterior of the cask with demineralized water to minimize contamination. Lower the cask until the top surface is just above the water level. Note: The cask may be filled with some water before lowering the cask into the pool or while the cask is partially submerged in the spent fuel pool. Vent the cavity pressure, and then remove the drain port cover.

### 7.2.3 Contents Removal

Note: In BWR spent fuel pools, there may be significant amounts of fuel crud particulate material. Precautions should be taken to ensure that this particulate material does not become airborne or float on the surface of the water, becoming a radiation concern. Precautions may include enhanced filtering of the pool water during the loading and unloading operations, as well as increased ventilation and monitoring of airborne contamination during all spent fuel pool activities.

- 7.2.3.1 Begin pumping pool or demineralized water into the cask through the drain port, at a rate of 1 gpm, while continuously monitoring the exit-pressure (See Figure 7-2). Continue pumping the water at a rate of 1 gpm for at least eighty minutes. By this time, the water level in the cask will have reached the active fuel length.
- 7.2.3.2 The flow rate can then be gradually increased, while monitoring the pressure at the outlet. If the pressure gage reading exceeds 55.3 psig, close the inlet valve until the pressure falls below 50 psig. Re-flooding can then be resumed.

- 7.2.3.3 After verifying that a steady stream of water is coming from the vent line (by checking for bubbles or carefully lifting the hose out of the water), take a sample for chemical analysis.
- 7.2.3.4 When the cask is full of water, remove the hose from the drain port, and the hose and the vent port adapter from the vent port. Remove the remaining six lid bolts.
- 7.2.3.5 Lower the cask and place it on the bottom of the pool/pit while rinsing the lift beam with demineralized water.
- 7.2.3.6 Raise the lift beam from the cask, removing the cask lid.
- 7.2.3.7 Unload the spent fuel assemblies in accordance with the site procedures.
- 7.2.3.8 At least one lid penetration must be completely open (both cover and quick-disconnect fitting removed) prior to installation of the lid. Using the lift beam and lid lifting slings, lower the lid placing it on the cask body flange, over the two alignment pins.
- 7.2.3.9 Engage the lift beam on the upper (top) trunnions, and lift the cask out of the pool.
- 7.2.3.10 Using the drain port in the lid, drain the water from the cask in accordance with the procedures. This may be done either before or after lifting the cask out of the pool. While lifting the cask out of the pool, the exterior of the cask may be rinsed with clean deionized water to facilitate decontamination.

Note: In order to minimize internal hydrogen accumulation, the cask should be drained completely within 18 hours of the start of draining. If this period is exceeded, the cask cavity should be inerted by injecting nitrogen, argon, or helium through the open lid penetration while the draining proceeds. An initial inert gas flow rate of 0.6 m<sup>3</sup> per minute (21 cfm) will purge the cask cavity volume in about 10 minutes, after which the flow rate can be reduced to about 3 cfm until the draining is complete.

- 7.2.3.11 Disconnect the drain line from the quick-disconnect couplings.
- 7.2.3.12 Move the cask to the decontamination area, and disengage the lift beam.

### 7.3 PREPARATION OF EMPTY PACKAGE FOR TRANSPORT

- 7.3.1 Decontaminate the cask until acceptable surface contamination levels are obtained.
- 7.3.2 Lubricate and install the lid bolts and torque them to 200 ft-lbs. Follow the torquing sequence shown in Figure 7-1. Repeat the torquing process following the sequence of Figure 7-1. Torque to 400 ft-lbs in the second pass. A circular pattern of torquing may be used, to eliminate further bolt movement.
- 7.3.3 Remove the plug from the neutron shield vent, and reinstall the pressure relief valve, making sure that it is operable and set.
- 7.3.4 Evacuate the cask cavity using the Vacuum Drying System (VDS) to remove the remaining moisture, and verify the dryness as follows:
- Using a wand attached to the vacuum drying system, remove any excess water from the seal areas through the passageways at the overpressure drain and vent the ports.
  - Remove the quick disconnect from the drain port, and install the drain port cover.
  - With the quick-disconnect removed to improve evacuation, connect the VDS to a flanged vacuum connector installed over the vent port. Purge or evacuate the helium supply lines and evacuate the cask to 4 millibar ( $4 \times 10^{-4}$  MPa) or less. Make provision to prevent or correct icing of the evacuation lines.
  - Isolate the vacuum pump. If, in a period of 30 minutes, the pressure does not exceed 4 millibar ( $4 \times 10^{-4}$  MPa), the cask is adequately dried. Otherwise, repeat vacuum pumping until this criterion is met.
  - Backfill the evacuated cask cavity with helium (minimum 99.99% purity) to slightly above atmospheric pressure, remove the vacuum connector, and immediately install the quick disconnect fitting.
  - Attach the vacuum/backfill manifold to the vent port fitting, purge or evacuate the helium supply lines, and re-evacuate the cask to below 100 mbar.
- 7.3.5 Isolate the vacuum pump, and backfill the cask cavity with an inert gas.
- 7.3.6 Install the overpressure transport cover. Torque the bolts to the value specified on drawing 971-71-1.
- 7.3.7 Re-engage the lift beam to the upper (top) trunnions of the cask.
- 7.3.8 Move the transport vehicle into the loading position.
- 7.3.9 Lift the cask off the decontamination pad, and place the rear trunnions on the rear trunnion supports of the transport frame.
- 7.3.10 Rotate the cask from the vertical to the horizontal position.
- 7.3.11 Install the front and rear trunnion tie-downs, by torquing them to 100 ft-lb.

- 7.3.12 Check if the surface dose rates and the surface contamination levels are within the regulatory limits.
- 7.3.13 Install the spacer on the front end of the cask. Then remove the spacer lifting eye bolts.
- 7.3.14 Install the front and the rear impact limiters onto the cask. Lubricate the attachment bolts with Never-Seez or an equivalent, and torque to 200 ft-lbs, diametrically in the first pass, and to 400 ft-lbs in the final pass.
- 7.3.15 Install thirteen impact limiter attachment tie-rods between the front and the rear impact limiters.
- 7.3.16 Render the impact limiter lifting lugs inoperable, by covering the lifting holes or installing a bolt inside the holes to prevent their inadvertent use.
- 7.3.17 Perform a final radiation and contamination survey to satisfy the shield test requirements and to assure compliance with 10CFR71.47 and 71.87.
- 7.3.18 Install a transportation enclosure.
- 7.3.19 Apply appropriate DOT labels and Placards in accordance with 49CFR172, and prepare the final shipping documentation.
- 7.3.20 Release the empty cask for shipment.

## 7.4 OTHER PROCEDURES

### 7.4.1 Preparation of Cask Used in Storage for Transport

The TN-68 cask is designed for storage as well as transport. The following steps describe the steps required to convert the TN-68 from its storage configuration to the transport configuration. In some cases, the casks which have been used for storage may not have the transport regulatory plate or nameplate installed on them. These plates must be installed prior to transport. In addition, some casks that have been used for storage, may not have the impact limiter attachment lugs installed on them. The lugs must be welded to the outer shell, prior to using the cask for transport.

- 7.4.1.1 Review the loading records and ensure that the fuel within the storage cask meets the requirements for the transport.

Note: The following steps may be performed at the ISFSI site.

#### *A. Storage Area.*

- 7.4.1.2 Disconnect the overpressure system from the monitoring panel. Depressurize the overpressure tank and disconnect the tubing at the protective cover.

- 7.4.1.3 Position the cask transporter over the cask.

Note: The following 3 steps may not be necessary if preparation is done on the storage pad .

- 7.4.1.4 Engage the lifting arms and lift the cask to the designated lift height.

- 7.4.1.5 Move the cask to the loading area.

- 7.4.1.6 Lower the cask down onto the floor, disconnect the cask transporter and remove the transporter from the loading area.

#### *B. Loading Area.*

- 7.4.1.7 Remove the protective cover.

- 7.4.1.8 Tighten the lid bolts to 2050-2100 ft lb following the torquing sequence shown in Figure 7-1 using at least two passes.

- 7.4.1.9 Remove the overpressure tank assembly and the top neutron shield.

- 7.4.1.10 Inspect the sealing surface at the overpressure port. Check for defects in the seal contact area that may prevent proper sealing. Leak test the lid seals through the

overpressure port. The maximum acceptable cask seal leak rate is  $1 \times 10^{-5}$  ref cm<sup>3</sup>/sec. The leak test shall be performed in accordance with ANSI N14.5<sup>(2)</sup>.

- 7.4.1.11 Install the overpressure transport cover. The transport cover should have a new metallic seal. Torque the transport cover bolts to the value specified on Drawing 972-71-1.
- 7.4.1.12 Remove the storage shield ring if necessary.
- 7.4.1.13 Check the surface dose rates above the radial neutron shield.
- 7.4.1.14 Place the lower (bottom) trunnions on the rear trunnion supports of the transport frame.
- 7.4.1.15 Rotate the cask from the vertical to the horizontal position.
- 7.4.1.16 Install the lower (bottom) trunnion support caps and the tie-down strap, by torquing them to 100 ft-lb.
- 7.4.1.17 Check if the surface dose rates and the surface contamination levels are within the regulatory limits. Install an optional shield ring adjacent to the top of neutron shield, if required, based on dose limits.
- 7.4.1.18 Install the spacer on the front end of the cask. Then remove the spacer lifting eye bolts.
- 7.4.1.19 Install the front and the rear impact limiters onto the cask. Lubricate the attachment bolts with Never-Seez or an equivalent and torque to 200 ft-lb, diametrically in the first pass, and to 400 ft-lb in the final pass.
- 7.4.1.20 Install thirteen impact limiter attachment tie-rods between the front and the rear impact limiters.
- 7.4.1.21 Render the impact limiter lifting lugs inoperable by covering the lifting holes or installing a bolt inside the holes to prevent their inadvertent use.
- 7.4.1.22 Install security seal on one tie-rod and lock sleeve.
- 7.4.1.23 Install a transport enclosure.
- 7.4.1.24 Check the temperature on all accessible surfaces to make sure that it is <185 °F.
- 7.4.1.25 Perform a final radiation and contamination survey to satisfy the shield test requirements and to assure compliance with 10CFR71.47 and 71.87.
- 7.4.1.26 Apply appropriate DOT labels and Placards in accordance with 49CFR172. Prepare the final shipping documentation, and release the loaded cask for shipment.

## 7.5 REFERENCES

1. ANSI N14.6-1993, American National Standard for Radioactive Materials Special Lifting Devices for Shipping Containers Weighing 10,000 Pounds (4500 kg) or More
2. ANSI N14.5-1997, Leakage Tests on Packages for Shipment of Radioactive Materials
3. NUREG-0612, Control of Heavy Loads at Nuclear Power Plants, US Nuclear Regulatory Commission, July, 1980

## CHAPTER 8

### ACCEPTANCE TESTS AND MAINTENANCE PROGRAM

#### 8.1 Acceptance Tests

The following reviews, inspections, and tests shall be performed on the TN-68 packaging prior to initial transport. Many of these tests will be performed at the Fabricator's facility prior to delivery of the cask to the utility for use. Tests will be performed in accordance with written procedures approved by Transnuclear Inc.

##### 8.1.1 Visual Inspection

Visual inspections are performed at the Fabricator's facility to ensure that the packaging conforms to the drawings and specifications. The visual inspection includes verifying that all specified coatings are applied and the packaging is clean and free of cracks, pinholes, uncontrolled voids or other defects that could significantly reduce its effectiveness. Visual inspection is also performed to verify that the packaging has been fabricated and assembled in accordance with the drawings and other requirements specified in the SAR. Weld inspection is performed in accordance with the applicable ASME code sections. Dimensions and tolerances shown on the drawings provided in Chapter 1 are confirmed by measurements. Prior to shipping, the packaging will be inspected to ensure that it is in good physical condition. This inspection shall include verification that all accessible cask surfaces are free of grease, oil or other contaminants, and that all cask components are in an acceptable condition for use. The sealing surfaces on the flange, lid and covers are inspected to ensure that there are no gouges, cracks or scratches that could result in an unacceptable leakage.

##### 8.1.2 Structural and Pressure Tests

The structural analyses performed on the packaging are presented in Chapter 2. To ensure that the packaging can perform its design function, the structural materials are chemically and physically tested to confirm that the required properties are met. All welding is performed using qualified processes and qualified personnel, according to the ASME Boiler and the Pressure Vessel Code<sup>(1)</sup>. Base materials and welds are examined in accordance with the ASME Boiler and Pressure Vessel code requirements. NDE requirements for welds are specified on the drawings provided in Chapter 1. All NDE is performed in accordance with written and approved procedures. The inspection personnel are qualified in accordance with SNT-TC-1A<sup>(2)</sup>.

The confinement welds are designed, fabricated, tested and inspected, in accordance with ASME B&PV Code Subsection NB. Exceptions to the code taken regarding the containment vessel are described in Chapter 2, Section 2.11. The basket is designed, fabricated, and inspected in accordance with the ASME B&PV Code Subsection NG. Exceptions to the code taken regarding the basket are described in Section 2.1.2.2. Welds of the noncontainment structure are inspected as per the NDE acceptance criteria of ASME B&PV Code, Subsection NF.

## Pressure Tests

A pressure test is performed on the packaging assembly (containment vessel installed in the gamma shield shell) at a pressure of 125 psig. This is well above 1.5 times the maximum normal operating pressure of 18.5 psig. The test pressure is held for a minimum of 10 minutes. The test is performed in accordance with ASME B&PV Code, Section III, Subsection NB, Paragraph NB-6200 or NB-6300. The containment vessel is installed in the gamma shield shell during testing. All visible joints/surfaces are visually examined for possible leakage after application of the pressure. Temporary gaskets and seals may be used in place of the metallic seals during the test.

In addition, a bubble leak test is performed at a pressure equal to or greater than 4.5 psig, on the resin enclosure. The purpose of this test is to identify any potential leak passages in the enclosure welds. The bubble leak test pressure is set at 1.5 times the relief valve set pressure.

## Load Tests

The lifting trunnions are fabricated and tested in accordance with ANSI N14.6<sup>(3)</sup> and are designed for nonredundant (single failure proof) lifting. A load test of three times the design lift load is applied to the trunnions for a period of ten minutes, to ensure that the trunnions can perform satisfactorily.

A force equal to 1.5 times the impact limiter weight will be applied to the lifting lugs of each limiter for a period of ten (10) minutes. At the conclusion of the test, the impact limiter lifting lugs (including welds) will be:

- a) Visually examined for defects and permanent deformations.
- b) Examined by the magnetic particle method for defects. Acceptance Standards will be in accordance with Article NF-5340 of Section III of the ASME Boiler and Pressure Vessel Code.

### 8.1.3 Leak Tests

Leakage tests are performed on the containment seals at the Fabricator's facility. These tests are usually performed using the helium mass spectrometer method. Alternative methods are acceptable, provided that the required sensitivity is achieved. The leak test is performed in accordance with ANSI N14.5<sup>(4)</sup>. The personnel performing the leakage test are qualified in accordance with SNT-TC-1A<sup>(2)</sup>.

The permissible leakage rate for the containment boundary is less than or equal to  $1 \times 10^{-5}$  ref  $\text{cm}^3/\text{sec}$ . The sensitivity of the leakage test procedure is at least  $5 \times 10^{-6}$  ref  $\text{cm}^3/\text{sec}$ .